POLITECNICO DI MILANO

Facoltà di Ingegneria Industriale e dell'Informazione

Corso di Laurea in
Ingegneria Energetica

Modelling and Evaluation of Solar Process Heat Integration on Supply Level

Relatore: Prof. Mario MOTTA

Co-relatore: Ing. Marcello APRILE

Tesi di Laurea di:

Nicolò CATTANIA   Matr. 783618

Anno Accademico 2013 - 2014

Acknowledgement

I would like to express my gratitude to the people who help me during the months I expended in Freiburg writing this thesis. In particular I thank:

- My supervisor at Fraunhofer ISE Annabell Helmke, who offered me guidance in the daily work and corrected patiently this paper

- Stefan Heß and Michael Schmid of the Prozesswärme Team in Fraunhofer ISE, for their precious advice and collaboration

- My colleagues at Fraunhofer, for the friendly atmosphere in the office as well as the help they offered me in the first months with ColSim

- All the friends I met in the these months and made living in Freiburg pleasant and special

- Mario Motta, Marcello Aprile and Antoine Frein of Politecnico di Milano for their support from Italy.

I take this opportunity also to thank who was close to me during these years of study, in particular my family for the moral and financial support and my fellows at Politecnico di Milano for the mutual assistance and the great time we had together.

Table of contest

List of Figures

List of Tables

Sommario

Un quarto del consumo energetico europeo è calore richiesto da processi industriali, il così detto calore di processo [1]. Al giorno d'oggi la maggior parte di questo calore viene prodotto bruciando combustibili fossili [2].

L'utilizzo di fonti di energia rinnovabile per soddisfare questa domanda energetica ha un enorme potenziale quantitativo in termini di riduzione della nostra dipendenza dai combustibili fossili.

In tal senso, una possibilità interessante è lo sfruttamento dell'energia solare per fornire calore a processi industriali.

Lo scopo di questa tesi è modellare e valutare l'integrazione di sistemi solari termici in impianti industriali.

Come prima cosa è stato sviluppato un modello di un impianto termico industriale, che consiste in una caldaia che produce vapore ad alta pressione e un sistema di distribuzione che fornisce il vapore ai processi industriali.

Sono stati sviluppati modelli di vari sistemi solari termici integrati con il preesistente impianto industriale. Per ogni configurazione sono state fatte simulazioni annuali variando il sito e le dimensioni dell'impianto solare termico, con lo scopo di trovare le integrazioni più promettenti.

I risultati sono stati analizzati da un punto di vista energetico, confrontando le prestazioni di ogni configurazione in termini di frazione solare, energia solare utile e risparmio di combustibile. Questi risultati sono stati poi rielaborati, svolgendo una prima analisi sulla fattibilità economica delle configurazioni proposte.

Dall'analisi dei risultati emerge che le due integrazioni più interessanti sono il preriscaldamento di acqua di rete e la produzione di vapore. Nel primo caso l'energia solare è sfruttata efficientemente ma è possibile trasferire solo limitate quantità di calore (2,58% della domanda totale); per questo è conveniente solo per impianti con grande domanda energetica e considerevoli portate di acqua di rete. La produzione di vapore può raggiungere frazioni solari molte più alte ma ha un rendimento più basso, a causa del mancato sfruttamento della radiazione diffusa e della mancanza di un sistema di stoccaggio del calore. Per questo è fattibile solo se c'è un'elevata DNI.

Parole chiave: solare termico, calore di processo, modellazione

Abstract

Heat consumed by industries, the so called process heat, amounts to around one fourth of the total European energy demand [1]. Currently the most of this heat is supplied burning fossil fuels [2].
The conversion of process heat to renewable energy sources has therefore a huge quantitative potential in terms of reduction of our dependence on fossil fuels.
In this sense, one interesting option is to provide heat to industries exploiting solar energy, the so called solar process heat.

The aim of this master thesis is the modelling and evaluation of the integration of solar process heat in industrial heat supply systems.
At first it has been developed a model of a conventional industrial heat supply system, which consists of a boiler producing high pressure steam and a distribution net delivering the steam to the industrial processes.
In order to find the most promising integrations of such a system with solar process heat, different configurations of solar thermal systems have been modelled. Several annual simulations have been accomplished, varying the location and the dimension of the solar thermal system.
The results have been analysed from an energetic point of view, comparing the benefit of each configuration in terms of solar fraction and solar energy gain. It has been then performed an economic evaluation about the feasibility of the suggested integrations.

The conclusion is that the two most promising integration points are pre heating of make-up water (using a storage) and direct steam generation.
Make-up water pre heating exploits solar energy efficiently but can only supply a limited amount of heat (2,58% of the total heat demand). For this reason this integration is profitable only for supply networks with high make-up water mass flows, otherwise the solar thermal system is small and it specific costs are high.
Direct steam generation instead can obtain a much higher solar fraction than make-up water pre heating but has lower efficiency due to minor diffuse radiation acceptance and no storage in the solar system. Therefore direct steam generation is profitable only if there is a large availability of DNI.

Keywords: solar process heat, supply level, steam network, modelling

Chapter 1

Introduction

1.1 Motivation

The energy system of the most of the industrialized countries is currently based on fossil fuels [3]. The preponderance of this energy source is due to its low cost, reliability and flexibility.

However, the exploitation of fossil fuels compels to face several problems: limited amount of available resources, raise of geopolitical conflicts caused by unequal distribution of the resources, environmental and health risks linked to emission of air pollutants, global climate change due to the massive production of CO_2 and other greenhouse gas.

For this reason in the last decades there has been a strong impulse toward a change of the actual situation.

These efforts have been directed at two different goals: the reduction of the energy demand improving the energy efficiency of the consumers and the change of the way electricity and heat are generated. One of the most promising solutions is the exploitation of renewable energies sources, that can solve all the problems mentioned above without having dangerous secondary effects.

In order to foster Europe to become a "highly energy-efficient, low carbon economy" [4], in March 2007 the European Union has set three targets, known as "20-20-20" targets, to be reached within 2020. These targets are [4]:

- A 20% reduction in EU greenhouse gas emissions from 1990 levels;
- Raising the share of EU energy consumption produced from renewable resources to 20%;
- A 20% improvement in the EU's energy efficiency.

According to recent studies [1], in 2011 industrial process heat amounted to around 26% of the total energy consumption in the EU. However, nowadays process heat is almost only generated burning fossil fuels [2].

For this reason the use of renewable energy sources to provide heat to industrial processes has a huge potential to fulfill the targets mentioned above.

In this context it has been showed that solar thermal plants in Europe could provide 3,8% of the industrial heat demand [5]. Notwithstanding, solar process heat is nowadays scarcely diffused due to high costs and lack of reliability when compared with traditional gas-powered plants. These obstacles can be overcome by research.

One of the most used systems to supply process heat is the steam network, a centralized heat generation plant using steam as heat transfer fluid. Such a system covers for example around 40% of the total energy demand in industrial process in the US [6]. The integration of such a system with solar thermal systems is a current research topic at the research institute Fraunhofer ISE.

1.2   Aim of the thesis

The purpose of this thesis is the modelling of a steam network and of its integrations with solar thermal systems.
The models will be used to perform annual simulations in order to find the most promising configurations and understand the economic feasibility of the chosen integrations.

1.3   Methodology

The modeling of the steam network and of its integrations with solar thermal systems is based on a literature review about these topics. Particular attention has been given to the components and possible energy efficiency measures of industrial steam networks.
The choice and design of the most suitable integrations between such a system and solar thermal plants has been done according to the work conduct by Fraunhofer ISE and Universität Kassel, summarized in [7].
This literature review will be described in chapter 2.

The models have been developed in ColSim, a simulation tool developed at Fraunhofer ISE. A description of the models, their components and assumptions will be described in chapter 3.
The pressure and temperature levels of the steam network, as well as the time variant heat demand that it supplies to the industrial processes, has been chosen according to representative values of a middle sized energy efficient German laundry. These values have been researched by Michael Schmid within his master thesis at Fraunhofer ISE [8] and have been adapted in order to represent a steam network with standard energy efficiency.

The models have been then validated and used to perform annual simulations: the results have been then post-processed in excel, in order to make an economic analysis of the modeled integrations. These results will be presented in chapter 4.

Eventually the results of the economic analysis have been compared with reference values, in order to evaluate the economic feasibility of the modeled configurations. These evaluations will be discussed in chapter 5.

Chapter 2

Solar thermal energy and its potential for process heat applications

This chapter is a review on solar thermal process heat.
The first section describes solar thermal systems: the fields of application and their potential will be discussed.
In the second part process heat generation and distribution will be described, focusing on systems that use steam as heat transfer medium. Eventually the possibility of integration of such a system with a solar thermal system will be investigated.

2.1 Solar thermal energy

Solar energy is radiant energy released by nuclear fusion into the sun. The little amount of this radiation that reaches the earth exceeds by far the human energy consumption. Compared with fossil fuels, solar energy has the advantages to be costless, renewable and environmentally friendly. On the other hand its exploitation as energy source is made complex by several factors: it is dilute on a large surface, requiring plants extended on vast areas; moreover its availability depends on the time of the day, the season and on the weather conditions, so that its exploitation is not highly predictable and cannot always cover the entire energy demand if there is no storage system.

Solar energy can be directly harnessed in two ways: with photovoltaic (PV) or solar thermal plants. Photovoltaic cells convert solar irradiation directly into electrical energy thanks to the photoelectric effect [9].
Solar thermal systems instead provide thermal energy: a solar collector absorbs solar irradiation converting it into thermal energy which is transferred into a fluid. The thermal energy carried by the fluid can be used directly or alternatively can charge a thermal storage, which can supply heat also when there is no availability of solar energy.

The performance of a solar thermal system depends on the conversion of solar radiant energy into heat in the collector and on the distribution of the heat. The distribution system consists essentially in pipes that connect the collector with the process that requires heat, the so called load. The heat transfer fluid heated in the collector reaches temperatures higher than the ambient temperature;

therefore part of the gained heat is lost to the surrounding environment, reducing the efficiency of the solar thermal system.

Several components and configurations have been developed in order to improve the performance of the system, adapting it to different environmental conditions such as ambient temperature or available irradiation and most of all to the requirements of the load, in terms of the needed temperature and operating times.

2.1.1 Solar radiation and solar angles

This chapter gives definitions related with solar radiation and solar angles, necessary for the comprehension of the next chapter. [9] has been used as a reference.

When solar radiation arrives to the earth it passes at first through the atmosphere. A part of the radiation is scattered, changing its direction, while the rest continues on the same trajectory until it reaches a surface:

- Diffuse radiation: radiation deviated by scattering by the atmosphere

- Direct radiation: radiation not deviated by scattering by the atmosphere

- Global radiation: sum of diffuse and direct radiation.

The energy associated to the radiation incident on a surface can be described as:

- Irradiance (*G*), [W/m²] is the rate at which radiant energy is incident on a surface per unit area

- Irradiation (*H*), [J/m²] is the incident energy per unit area on a surface, found by integration of the irradiance

G depends on the relative position of the surface compared with the direct radiation, described by the angle of incidence (showed in Figure 2.1):

- Angle of incidence or incidence angle (θ) is the angle between the beam radiation and the normal to the surface in question; it depends therefore on the orientation of the surface and the direction of the direct radiation.

Equation (2.1) and Figure 2.1 show how the same amount of energy is more diluted if θ increases.

In particular, using the subscript *N* for surfaces normal to the direct radiation and *T* for tilted surfaces, it is possible to describe the irradiance as a function of *θ*, as showed in equation (2.1).

$$G_T = G_N \cos \theta \qquad\qquad (2.1)$$
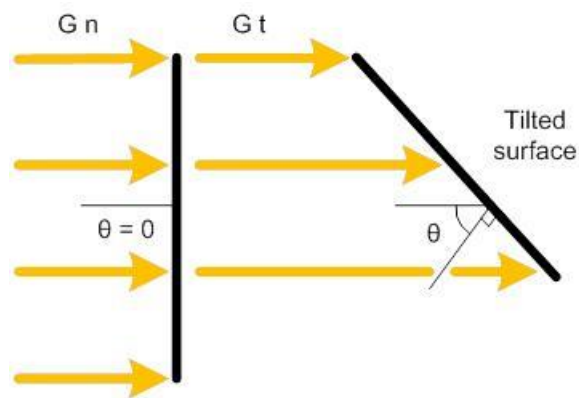
Figure 2.1. angle of incidence and irradiance on tilted surface

Figure 2.2 shows the angles necessary to describe the angle θ between the solar direct radiation and a generic surface.
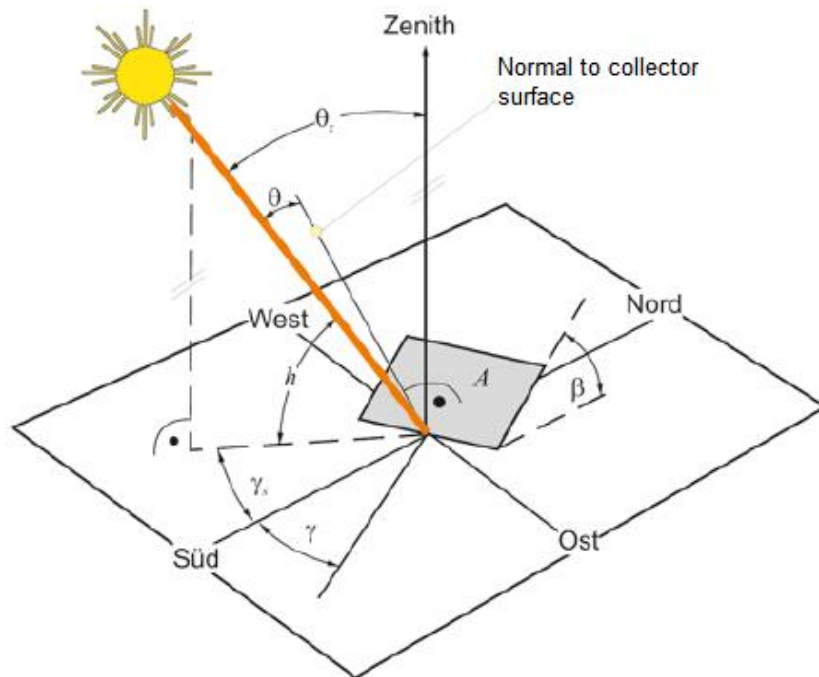
Figure 2.2. representation of solar angles [10]

- Zenith angle (θ_z) is the angle between the vertical to the ground and the direct radiation, therefore is the angle of incidence on a horizontal surface.

- Solar altitude angle (h) is the complement of the zenith angle.

- Solar azimuth angle (γ_s) is the angle between the south and the projection of the direct radiation on the horizontal surface.

- Slope (β) is the angle between the plane of the surface and the horizontal surface.

- Surface azimuth angle (γ) is the angle between the south and the projection of the normal to the surface on the horizontal surface.

θ_z and γ_s describe the direction of the direct radiation, while β and γ describe the position of the surface in question; θ can be therefore described as a function of these four angles, as shown in equation (2.2):

$$\theta = \cos\theta_z \cos\beta + \sin\theta_z \sin\beta \cos(\gamma_s - \gamma) \qquad (2.2)$$

Knowing these angles and G_N, it can be calculated the available irradiance on a tilted surface G_T, as in equation (2.1).

In order to maximize G_T and exploit conveniently the solar energy, θ should be minimized changing γ and β.
It can be done a distinction between two different kind of solar collectors: stationary and tracked collectors.

- Stationary collectors have fixed γ and β.
  These angles are chosen in order to maximize the solar energy supplied to the process during a whole year.
  The azimuth γ is usually oriented at south. The slope β that maximizes G_T changes with the season, since in winter the sun has higher zenith than in summer and therefore the collector have better performance with a high slope angle. Moreover, if the process has a variable energy demand during the year, the optimal slope β that maximizes the solar energy supplied to the process depends also on the process energy demand. For example space heating requires heat mostly in winter, therefore an integration with a solar thermal system should maximizes the energy available in winter and therefore prefer high β.
  In order to find the optimal β it is helpful to perform annual simulation with different collectors slope to find which maximizes the solar energy supplied to the process.

- Tracked collectors use motors to change their position and consequentially γ and/or β. Tracking can be done on one or two axis.

As it will become clear in the next chapter describing linear collectors, it can be necessary to consider the projections of θ on two planes: θ_l is the projection on the longitudinal plane that contains the axis of the linear collector; θ_t is the projection on the transversal plane, perpendicular to the axis of the collector, as shown in Figure 2.3.
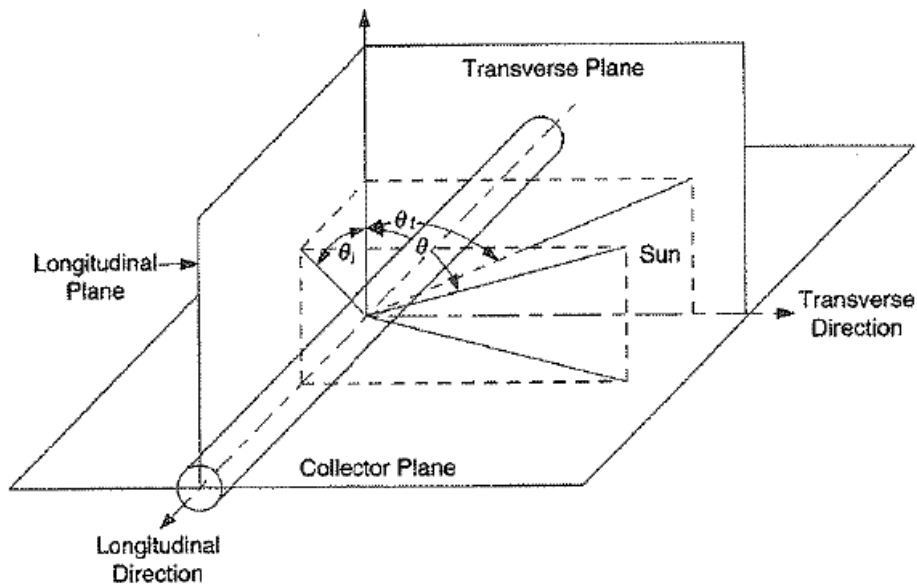
Figure 2.3. the planes of the evacuated tube incidence angle modifiers [9]

2.1.2 Solar thermal collectors

A solar thermal collector is a heat exchanger that absorbs solar irradiation on a dark surface, called absorber, and then transfers it to a fluid. The performance of solar collectors is determined by both optical losses and thermal losses.

The optical losses are the amount of incidence solar irradiation that is not transferred to the fluid.
Each material can reflect, transmit or absorb radiation. In a collector the incidence solar radiation is supposed to be reflected by mirrors, pass through glasses and be absorbed by the absorber: each of them is therefore designed to maximize the amount of radiation respectively reflected ρ, transmitted τ and absorbed α. Nevertheless just a share $\tau\alpha$ of the total incidence irradiation is exploited [9].
$\tau\alpha$ is a function of the incidence angle θ between the direct solar radiation and the normal to the collector surface, that means the optical losses changes with θ. Nevertheless the collector performance is represented by a collector characteristic efficiency equation (2.7), assuming a $\tau\alpha$ ($\theta = 0°$). This result must be corrected afterwards by a coefficient $K_{\tau\alpha}$ (θ) called incidence angle modifier, described in equation (2.3).

$$K_{\tau\alpha}\left(\theta\right) = \frac{\tau\alpha\left(\theta\right)}{\tau\alpha\left(\theta\,=\,0°\right)} \qquad (2.3)$$

It has to be remarked that $K_{\tau\alpha}$ *(θ)* doesn't take in account the reduction of available irradiation due to *θ≠0*, shown in equation (2.1). These two effect together form the IAM (incidence angle modifier).

The thermal losses are caused by heat exchange of the collector with the environment and therefore they increase along with the temperature difference between the absorber and the ambient temperature, reducing the efficiency of the collector as shown in Figure 2.4.

The efficiency of a collector can be described as [11]:

$$\eta = \frac{\dot{q}_u}{G_T} \qquad (2.4)$$

where $\dot{q}_u$ [W/m²] is the useful heat gained by the collector and G_T [W/m²] is the global irradiance on collector surface. The useful heat depends on the available irradiance, the optical properties of the collector and the heat losses:

$$\dot{q}_u = \left(G_T * \tau\alpha\right) - \dot{q}_l \qquad (2.5)$$

where $\tau\alpha$ is the solar energy absorbed dived by the incidence solar energy and $\dot{q}_l$ [W/m²] are the thermal heat losses, depending on the temperature difference between absorber and ambience.
According to equation (2.4), the efficiency of a collector can be described as:

$$\eta = \frac{\dot{q}_u}{G_T} = \left(\tau\alpha\right) - \frac{\dot{q}_l}{G_T} = \eta_0 - \frac{\dot{q}_l}{G_T} \qquad (2.6)$$

η_0 is called optical efficiency and depends on the incidence angle θ. Each collector is characterized by the parameter $\eta_{0,\,\theta\,=\,0}$, which is the optical efficiency for null incidence angle, and by the function $K_{\tau\alpha}\left(\theta\right)$.

An expression of η as a function of the difference of temperature ΔT between the absorber and the environment and the global irradiance on collector surface G_T is [11]:

$$\eta = \eta_0 - \left[a_1 * \frac{\Delta T}{G_T} + a_2 * \left(\frac{\Delta T}{G_T} \right)^2 \right]$$ (2.7)

where a_1 and a_2 are heat losses coefficients. Figure 2.4 shows that, as written in equation (2.7), the theoretical minimal collector losses are reached for $\Delta T = 0$, so that only the optical losses must be considered. The higher ΔT the higher the thermal losses, while the lower G_T the higher the thermal losses in comparison with the absorbed energy: therefore high ΔT and low G_T cause a reduction of the collector efficiency.
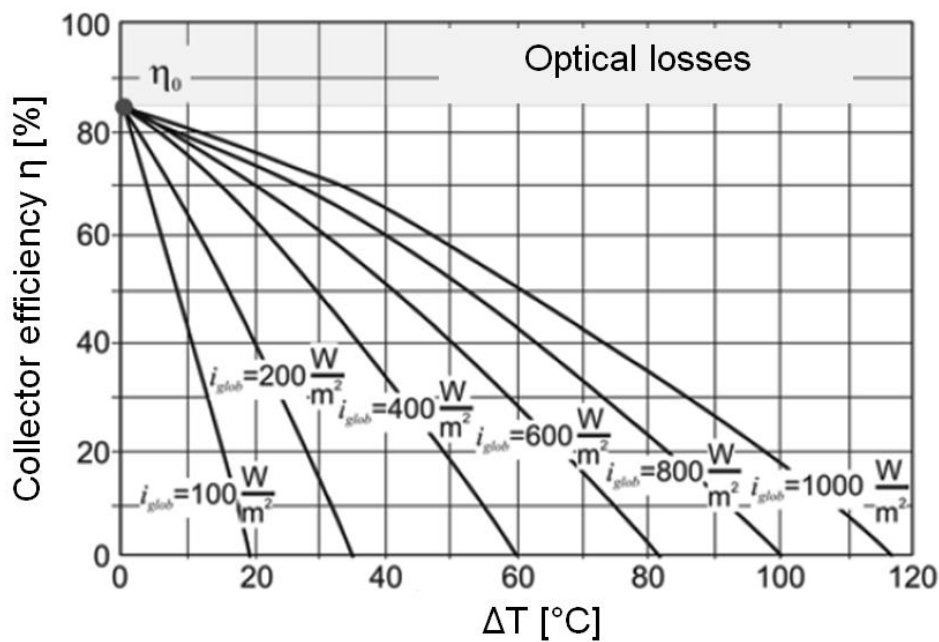
Figure 2.4. efficiency of a solar flat-plate collector as a function of ΔT and G_T [10]

There are several kind of collectors, characterized by different way of reducing optical and thermal losses:

-   Unglazed collectors [11], showed in Figure 2.5, are stationary collectors composed of an absorber plate made of plastic material or stainless steel, that converts the incident radiation in heat, and pipes where the working

fluid can pass in order to gain thermal energy from the absorber. Since there is no glazing, these collectors are simple, economical and have low optical losses, being the radiation in direct contact with the absorber; on the other hand, they have high thermal losses, particularly when there is wind and there is a considerable temperature difference between absorber and ambient. For this reason they are suited for low temperature applications such as swimming pool heating in summer.
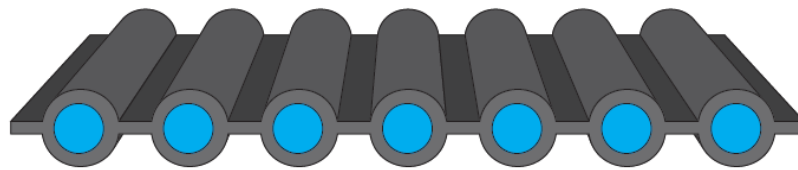
Figure 2.5. unglazed collector [11]

- Flat-plate collectors, showed in Figure 2.6, are stationary collectors composed of pipes in which the heat transfer liquid flows, covered by an absorber usually coated with blackened surface in order to increase the energy gain [12] and a glass cover with a transmission coefficient up to more than 0,9 [13].
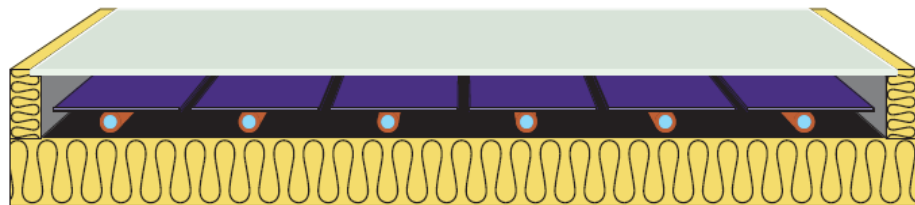
Figure 2.6. flat-plate collector [11]

The presence of this glass cover increases the optical losses but reduces natural convection and therefore the heat losses: for that reason these collector reaches a higher performance at higher absorber temperatures than an unglazed collector.
Heat losses are also reduced by insulating the back side of the collector, in order to reduce conduction losses.
The common temperature range of flat plate collector applications is between 30 and 80°C [14], even if they can reach higher temperatures, as shown in Figure 2.10.

Figure 2.7 shows an example of the energy fluxes of a typical flat-plate collector: the optical efficiency is more than 80%, while the collector efficiency is 60% and depends on the operative conditions.
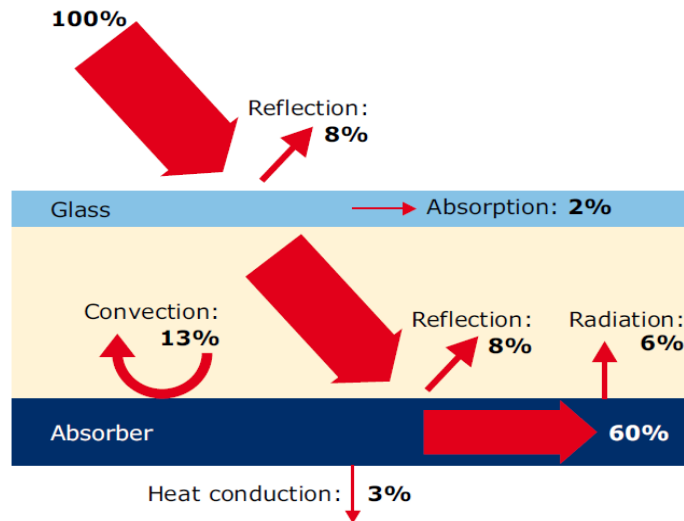
Figure 2.7. main losses of a flat-plate collector [7]

- Evacuated tube collectors, showed in Figure 2.8, are stationary collectors consisting of a number of glazed tubes with vacuum between the absorber and the glass, in order to reduce the convective heat losses to the ambience.
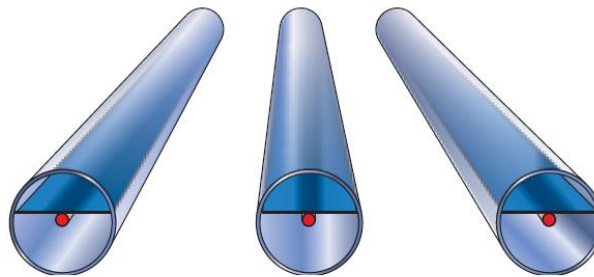
Figure 2.8. evacuated tube collectors [11]

These collectors can reach higher temperatures range than a flat-plate collector, keeping good efficiency also when the difference between absorber and ambient temperature is over 100°C; the temperature range of application is between 50 and 200°C [14].

Because of their tubular shape, these collectors need a biaxial incidence modifier $K_{\tau\alpha}$ that depends on the two projections of the incidence angle on the transversal plane θ_t and longitudinal plane θ_l, as shown in Figure 2.3.

According to [9] the incidence angle modifier is calculated as:

$$K_{\tau\alpha} = (K_{\tau\alpha})_t * (K_{\tau\alpha})_l \qquad\qquad (2.8)$$

where $(K_{\tau\alpha})_t$ is function of θ_t and $(K_{\tau\alpha})_l$ is function of θ_l.

- Linear concentrating collectors, such as parabolic through and Fresnel collectors showed in Figure 2.9, are one axis tracked collectors that use mirrors to focus the radiation on a tubular absorber, whose surface is considerably smaller than the aperture area, defined as the opening through which the solar radiation enters the concentrator [9]; consequentially the heat losses are strongly reduced, being the convective heat exchange directly proportional to the absorber area [9]:

$$\dot{q}_l = A_c * U * \Delta T \qquad\qquad (2.9)$$

Where $\dot{q}_l$ [W/m²] are the heat losses, A_c [m²] is the absorber area, U [W/m²*K] the overall heat transfer coefficient and ΔT [K] the difference of temperature between the absorber and the environment.
The ratio between aperture and absorber area is called concentration ratio, and indicates how the absorber area is reduced having the same available irradiation.
Concentrating collectors need a sun tracking system to receive always the radiation with the correct angle in order to focus it on the receiver; linear concentrating collectors track the sun rotating the mirrors on one axis, usually with north-south orientation in order to follow the daily movement of the sun from east to west. If the solar energy available exceeds the energy demand and no storage is available, it is possible to operate the solar field at partial load by defocusing part of the mirrors so that part of the radiation misses the absorber. The presence of a tracking system leads to more complex and expensive collector designs than stationary collectors such as flat-plate and evacuated tube collectors.
Tracked collectors can exploit almost exclusively direct radiation, because they redirect the sun beams towards the absorber. Since they cannot utilise the most of the diffuse light, they have less available solar

energy per aperture area than non-concentrating collector. Moreover the presence of a mirror that reflects only a fraction ρ of the incidence irradiation increases the optical losses, which are considerably higher than for non-concentrating collectors leading to an optical efficiency slightly superior to 60%.

For these reasons concentrating collectors are more expensive, have worse optical performances but better thermal performances than stationary collectors, so that they are suitable for applications having high temperature range, for example power generation.
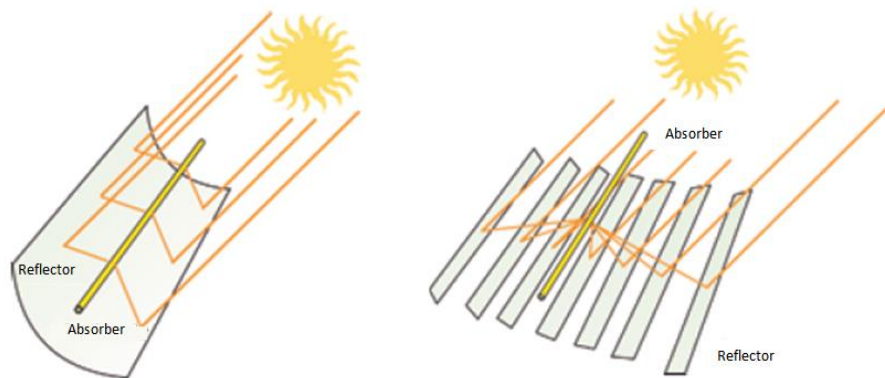
Figure 2.9. Parabolic through and Fresnel collectors [11]

As for evacuated tube collector, also Fresnel and parabolic collector have $K_{\tau\alpha}$ depending on the two components θ_t and θ_l of the incidence angle θ, as in equation (2.8)

-   Central-receiver systems concentrate the direct solar radiation of a large surface in one point, obtaining a higher concentration ratio than linear concentrating collectors and consequentially reaching higher temperature ranges, ideal for power generation. These systems need two axis tracking of the sun, in order to focus always the direct radiation into the central receiver.
    An example of central-receiver system is the solar power tower, which uses a field of heliostats to concentrate the radiation on a receiver, located at the top of the tower.

In Figure 2.10 are shown the performances and applications of several collectors.
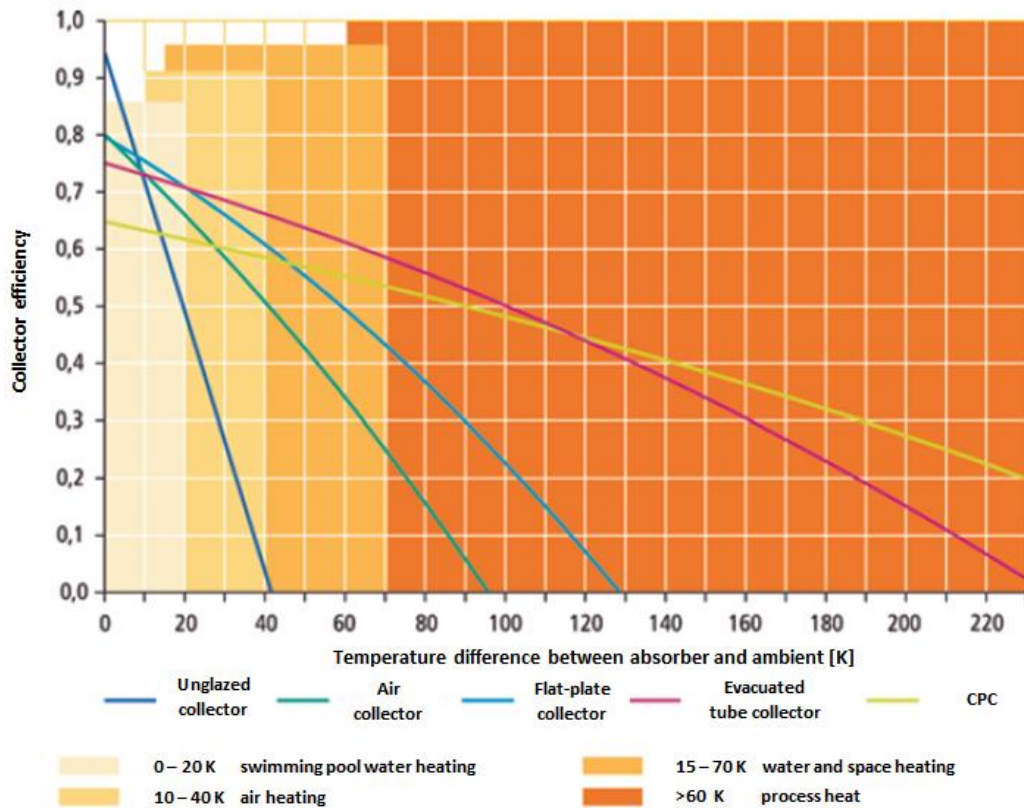
Figure 2.10. efficiency of several collectors and field of application [11]

2.1.3   Thermal storage

A problem related to the exploitation of solar energy is that its availability is not controllable, as it is with fuels, which can be burned when required. For this reason the solar energy gained often has a surplus or a deficit compared to the energy demand. This leads to a waste of energy in the first case and the necessity to have an auxiliary energy source to cover the gap between availability and demand in the second case.

To avoid this situation, one solution is to store solar energy in a buffer storage, which can be discharged when there is an energy demand: for example a surplus of solar energy during the day can be stored and used to satisfy the demand during the night, when no solar energy is available.
In other words, storages lead to a more efficient use of the available solar energy, since much more solar energy can be used if it can be temporarily

stored. On the other hand the presence of a storage increases the cost of the plant. Therefore the design of a storage is matter of an economic optimization.

The presence of a storage is particularly interesting for solar thermal systems because usually heat generation is done in stand-alone plant, unlike with electricity, and therefore there is mostly no possibility to sell a surplus of thermal energy to other consumers. Moreover, thermal storages are cheap and efficient.

The most common solar thermal storage is a water tank that stores the heat gained by the collector over a couple of hours (usually), until a process demands heat and the storage is discharged.

A limit of common thermal storages such as water tank is that they cannot accumulate energy during one season to use it in another, with the consequence that plants are usually oversized during summer, gaining more energy than it is required, and undersized in winter, requiring an auxiliary heater to cover all the demand. A good example is space heating, which needs large amount of energy in winter, while solar energy is available mostly in summer.

2.1.4 Application of solar thermal systems

Solar thermal technology can be used to satisfy heat demands of several processes: offices and houses need sanitary hot water and space heating at low temperature, below 100°C, that can be reached with flat-plate collector.

Solar thermal energy can be converted into electricity in solar thermal power plants, expanding in a turbine high temperature pressurized fluid, usually steam, heated by concentrating collectors.

Industrial and agricultural applications require large amount of thermal energy, the so called process heat, being one of the main energy consumers: according to [7], in Europe process heat accounts for 27% of the total final energy demand. According to [15], 30% of the industrial heat demand requires temperatures below 100°C and 27% between 100°C and 400°C, temperature ranges reachable with solar thermal systems. These data are shown in Figure 2.11.

The most interesting industrial branches for solar process heat are food, paper & pulp, textile, chemical and machinery industries [11, 15].
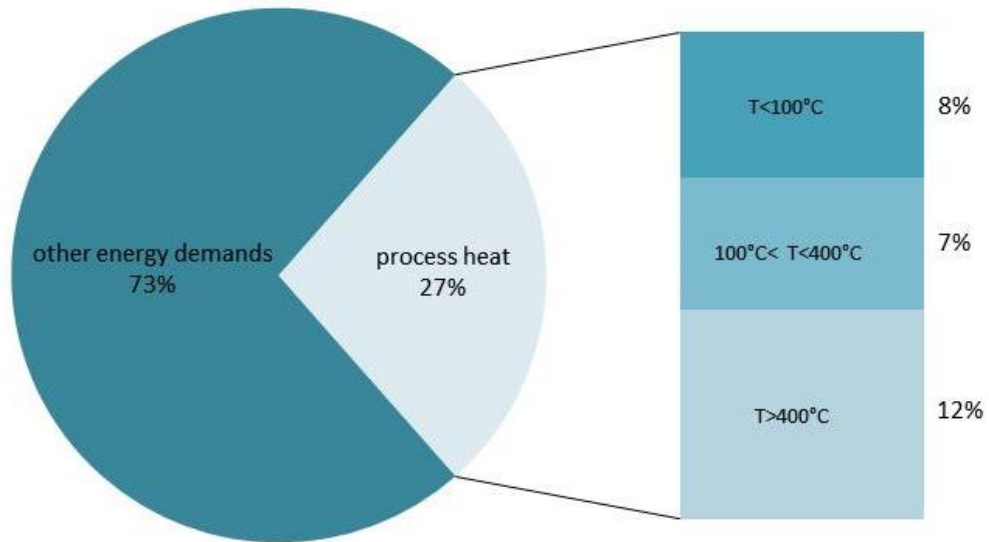
Figure 2.11. process heat share of the overall energy demand in Europe [16]

The use of solar thermal technologies for process applications has moreover a potentially constant load in all the seasons, which allows exploiting solar energy also in summer, unlike with space heating that is most necessary in winter, when there is a deficiency of solar energy.

Despite this considerable potential, nowadays solar thermal process heat is not widespread due to high capital cost for solar thermal technology compared with the low present energy market price, low intensity of solar energy that forces to the occupation of large areas, lack of competent workers in this field [17, 18]; moreover this technology is seen as not enough reliable to substitute conventional energy sources in industrial processes.

Other applications of solar thermal technology are water desalination, which allow the production of fresh water from sea water, and solar cooling, that uses thermal energy to power an absorption refrigerator, using conveniently the large availability of solar energy during the hot months [14].

According to [16], in 2011 the installed solar thermal capacity in 56 countries representing a share of 95% of the solar thermal market worldwide was 234,6 GW_{th}, corresponding to a total 335,1 million square meter of collector area; most of this capacity is installed in China (64,9%), followed by Europe (16,7%)

Asia excluding China: India, Japan, Korea South, Taiwan, Thailand
Latin America: Brazil, Chile, Mexico, Uruguay
Europe: EU 27, Albania, Macedonia, Norway, Switzerland, Turkey
MENA Region: Israel, Jordan, Lebanon, Morocco, Tunisia
Sub-Sahara Africa: Mozambique, Namibia, South Africa, Zimbabwe
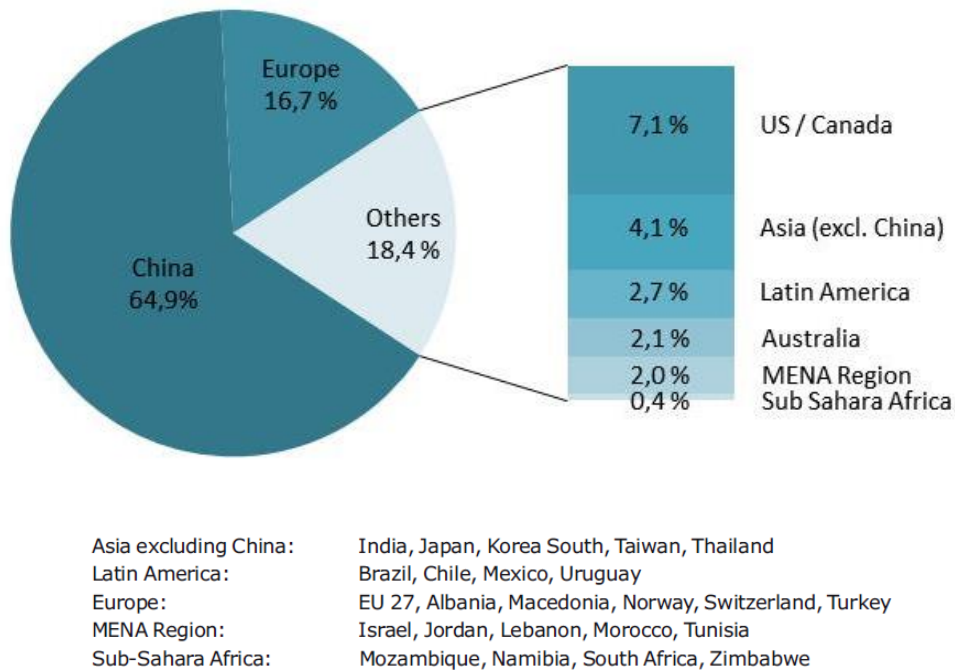
Figure 2.12. share of the total solar thermal installed capacity in operation (2011) [16]

Thanks to this existing plant there were energy savings of 20,87 million t $_{oe}$/y and CO_2 reduction of 64,82 million t $_{co2}$/y.

Considering just industrial applications, according to [5] the potential of solar process heat in the EU has been estimated as 3,8% of the overall industrial heat demand, equal to 72 TWh per year.

2.2 Process Heat

In this chapter process heat generation and distribution will be described, focusing on systems that use steam as heat transfer medium; moreover the possibility of energy efficiency measures will be investigated.

2.2.1 Description of a steam network

To analyse the potential of solar thermal technology in process heat applications is necessary to know how industrial plants manage heat generation and distribution. Many factories have centralized heat generation, with a boiler that burns fuel transferring heat to a fluid such as water, oil or steam, and a distribution system that delivers the thermal energy where it is needed;

otherwise is possible to generate heat where it is required, using electricity or burning fuel.

Centralized heat generation using steam as heat transfer fluid is one of the most used systems, covering for example around 40% of the total energy demand in industrial process in the US [6]: the diffusion of steam is due to several factors such as high heat capacity thanks to latent heat, high efficiency of heat exchange during condensation, no need of a pump, flexibility of the system, low toxicity, low cost of water, all features that make steam a good heat carrier fluid [19]; moreover many industrial processes have a direct use of steam, for example chemical processes that use it to control pressure and temperature.
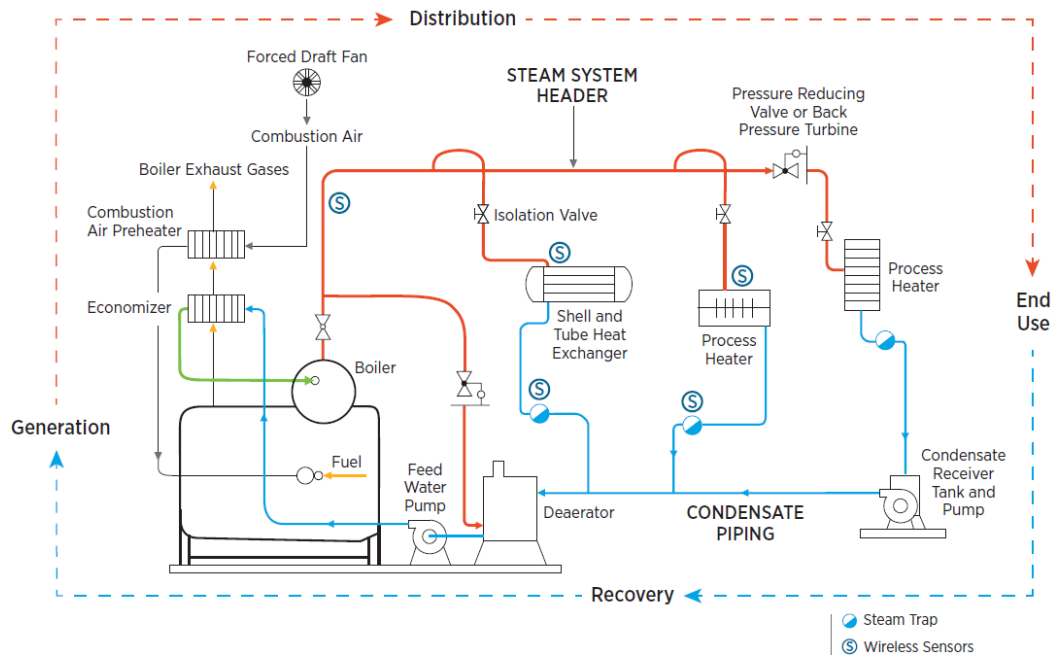
Figure 2.13. scheme of a steam network [6]

A steam network is a centralized heat generation plant that produces steam and delivers it to industrial processes. Following the life-cycle of the steam, the plant can be divided in four main areas shown in Figure 2.13: generation, distribution, end use and recovery.

- In the steam generation area water is gathered in a tank, called feed water tank (number 2 in Figure 2.14), and mixed with steam, in order to warm the water almost up to saturated condition and to strip incondensable gas before sending the water to a boiler. In the boiler (number 1 in Figure 2.14) pressurized saturated steam is generated: water coming from the feed water tank enters in a fixed volume and is

heated until it starts to evaporate, generating steam. Since the volume is constant, but steam has a lower density than water and therefore occupies more space, the pressure inside the boiler raises and consequently also the temperature increases, being the fluid in a two phase state. When the required pressure and temperature are reached, saturated steam can be extracted and sent to the load.

Many efficient plants have also an economizer, that cool down the flue gas at the outlet of the boiler heating the incoming boiler feed water, sparing around 5% of the fuel consumed in the boiler [20] (a more accurate description can be found in chapter 2.2.2).

Figure 2.14. steam generation system [21]

1. Steam generator
2. Feed water tank
3. Boiler feed pump
4. Water softening
5. Chimney
6. Blow down valve
7. Mixer- cooler
8. Cooling tank
9. Boiler control cabinet
10. Condensate tank
11. Hardness control
12. O2 and pH metering
13. Programmable Logic Controller
14. Sample cooler
15. Conductivity metering
16. Dosage of chemicals
17. Turbidity metering

- A distribution net is required to let the steam flow from the boiler to the load, flow caused by the pressure increase given by the boiler. This system consists fundamentally of a net of pipes, even if other auxiliary devices are required: the heat losses in the pipes lead to partial condensation of the saturated steam, producing water that gives problems of water hammering, considering the high steam speed (between 25 and 35 m/s for steam pressure between 5 and 10 bar [21]); for this reason the condensate has to be separated using steam traps.

Figure 2.15. steam trap and condensate management [22]

After the separation, the water is mixed with the condensate in the return line, as shown in   Figure 2.15.

Other devices that are present in steam lines are throttles that reduce the pressure of the system: this can be necessary both to feed heat at different temperatures depending on the load requirements and to regulate the pressure beyond the range permitted by the boiler, since often is more convenient to produce steam at high pressure and expand it than to make the boiler work at off-design conditions, reducing he boiler efficiency.

-   Once the saturated steam arrives at the end users, it can be used either directly in a process or it can condensate in a heat exchanger, supplying heat to the process, as shown in Figure 2.16. In the first case the process is called open process, in the second closed process.
    The discharged condensate at the outlet of closed process can recirculate to the feed water tank; the steam used in an open process instead is lost from the network and needs to be reintegrated.
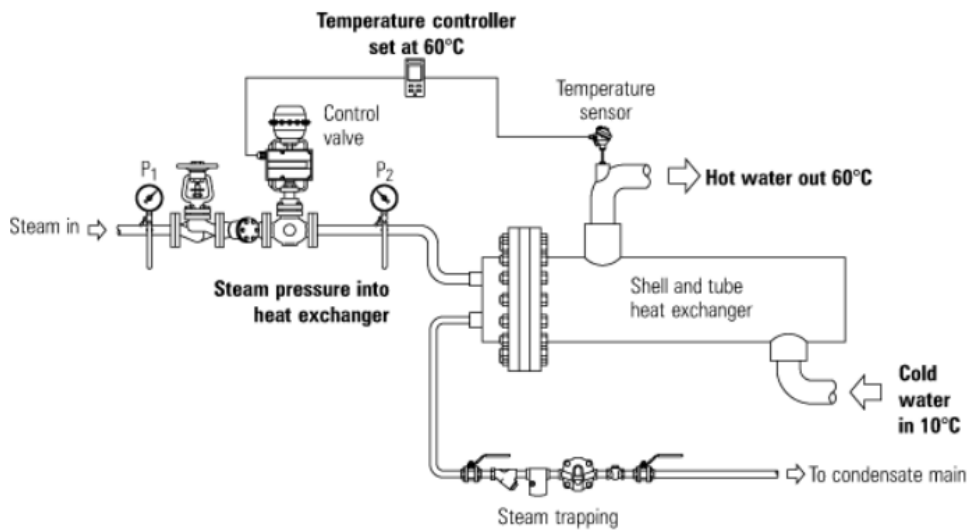
Figure 2.16. steam-water heat exchanger [22]

- If possible, the condensed steam is recovered after the load, saving water, energy and chemicals necessary for fresh water treatment. Before recirculating the condensate through a return line from the closed load to the feed water tank, it is necessary to bring the condensate to ambient pressure, since the feed water tank is not pressurized. This flashing operation, showed in Figure 2.17, produces water at 1 bar and steam, called flash steam, which can be recycle to feed heat to low temperature loads (a more accurate description can be found in chapter 2.2.2). The same operation can be done with the condensate coming from the steam trap on the steam line.
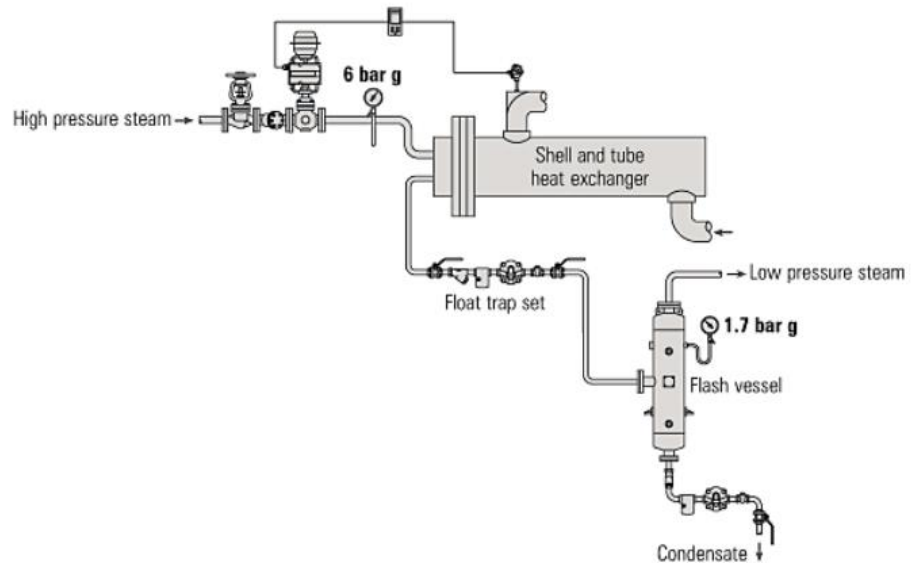
Figure 2.17. flash of the condensate after a closed load [22]

If the steam has been used directly in the process it cannot be flashed or recirculated, because it has been mixed with other fluid or chemicals. Therefore it is lost for the network. In order to keep a constant mass flow it is therefore necessary to compensate for the lost mass flow with fresh water, the so called make-up water, coming from the water supply net directly to the feed water tank.

2.2.2 Energy efficiency in steam networks

Energy saving systems are used to reduce the fuel consumption of a plant. In steam networks heat recovery is an important and common energy saving measure. Heat recovery systems are usually economical because they don't require the installation of an additional heat supply system, as it happens with solar thermal integration; therefore they have a short payback period, for example 1 or 2 years in the laundry sector [23]. Moreover, heat recovery from waste flows, such as flue gas out of the boiler and water out of the industrial process, raises the temperature level and reduces the temperature gap in which heat has to be provided to the system, limiting the potential of solar thermal integration.

A first measure to save energy is to improve the efficiency of the combustion and heat transfer in the boiler, which can be done by simply monitoring and controlling the combustion. In this way the primary energy consumption decreases without changing the heat demand of the plant.

Usually an industrial boiler reaches an efficiency of at least 80% [20]; the remaining part of the energy is wasted because of heat losses at the wall of the boiler or is contained in the flue gas. As shown in Figure 2.18, an economiser can recover part of the energy present in the flue gas, using it to warm the boiler feed water, consenting to spare up to 5% of the fuel.

Looking at Figure 2.18, it appears clear that energy recovery systems are competitors of solar thermal: the economiser reduces the temperature gap between the boiler feed water and the boiler, reducing the amount of energy suppliable with a solar thermal system. Moreover, if a solar thermal system would be installed, it should supply heat a higher temperature because of the presence of the economiser. This would reduce the collector efficiency.
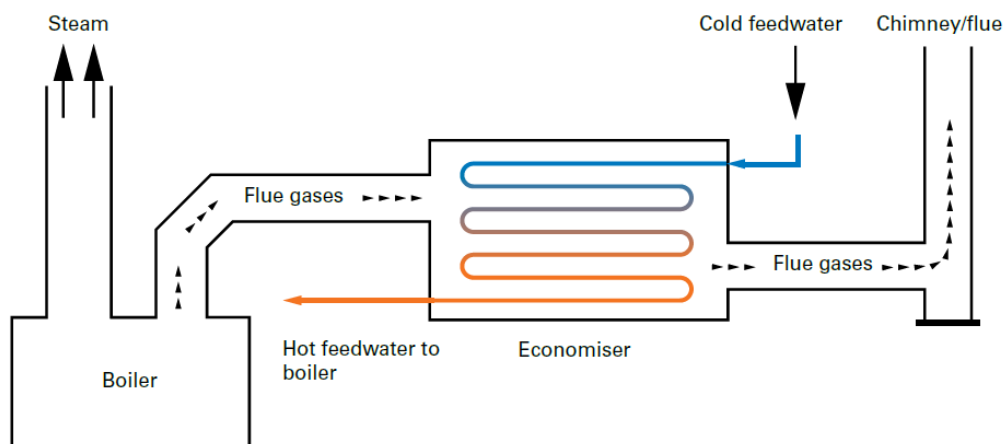
Figure 2.18. economiser [20]

The other way to spare fuel is to reduce the energy demand of the plant, which means the amount of steam generated.

The steam produced in the boiler flows through a distribution system until it reaches the loads. The energy contained in the steam is partially lost because of heat losses in the pipes of the distribution system, partially used in the process (useful energy) while a part is wasted after the process, remaining contained in the outlet mass flows.

In order to reduce the overall energy demand of the plant, that is the sum of these three energy flows, it is possible to insulate the distribution system, limiting the heat losses, to improve the efficiency of the processes or to recover the heat contained in the outlet mass flows:

A boiler produces pressurized steam, which is condensed delivering heat to a process. Usually the return line and the feed water tank are kept at almost ambient pressure, so that it is necessary to flash the condensate; this operation

causes the evaporation of a fraction of the condensate, the so called flash steam (as shown in Figure 2.19), which can be used to feed low-temperature processes.
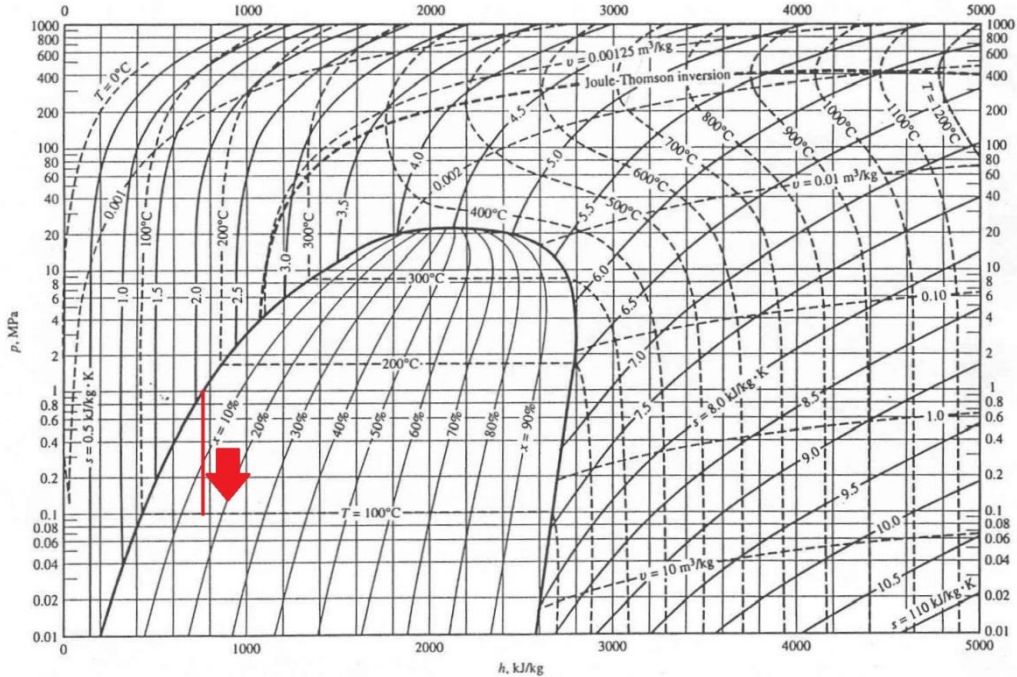
Figure 2.19. isenthalpic expansion of H$_2$O in the two phases region from 10 to 1 bar

The fraction of the condensate that remains at saturated liquid conditions after the expansion can be recirculated saving the energy still contained inside it and avoiding water treatment necessary for make-up water. The condensate is at saturated conditions, which means its enthalpy depends on the lower pressure of the system; pressurized condensate lines consent to keep the feed water tank warmer, but are more expensive, so that it is common to operate with condensate at almost ambient pressure.

If the steam is used in an open process, the outlet condensate can't be flashed or recirculated so that its energy would be lost. Nevertheless it is possible to recover the heat contained in this mass flow to warm the make-up water.

2.3   Integrations of solar thermal systems in steam network

The most common use of solar thermal integration in industrial process is water heating, that is simple and cost effective [24], using stationary collectors. Temperatures higher than 100°C can be reached with pressurized systems and concentrating collectors.

Solar thermal technology can also be used to generate steam: this application has higher temperature ranges, reachable with parabolic trough collectors or

Fresnel collectors. Steam can be generated directly (two phases in the collectors), flashing pressurized hot water or using oil as heat transfer fluid in the collector and then generating steam in an oil-water heat exchanger.

Another use of solar energy in industrial applications is air heating using air collectors, in order to pre heat the air that goes to the boiler.

2.3.1   Supply and process level

The integration of solar thermal technology in an industrial plant can be done in several sites, called integration points, characterized by different temperature range, pressure level and time depending energy demand. A first distinction can be done between integration on process or supply level: in the first case solar heat is provided directly to the process, for example heating a bath as shown in **Fehler! Verweisquelle konnte nicht gefunden werden.**. The features of a solar integration on process level depend on the process itself [25].
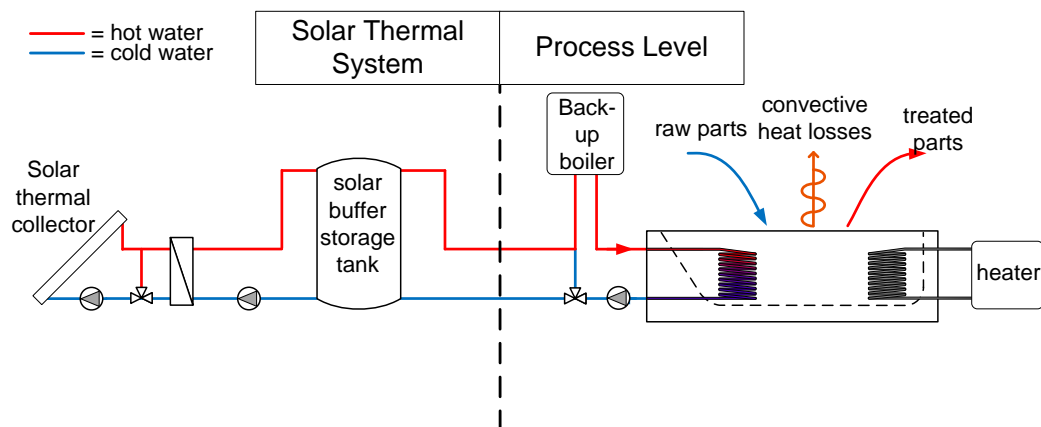
Figure 2.20. example of integration on process level: solar heating of an industrial bath [7]

Otherwise, if an industrial plant has centralized heat generation, it is possible to integrate it with solar thermal technology, for example generating steam or preheating water, as shown in Figure 2.21: this is the so called integration on supply level.

Within this master thesis has been investigated only this second opportunity.
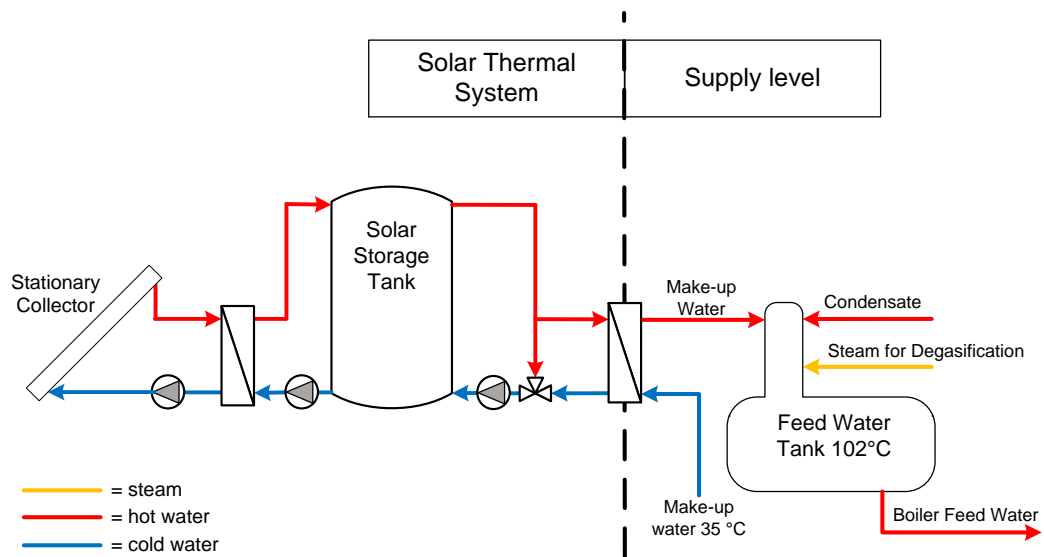
Figure 2.21. example of integration on supply level: solar heating of make-up water [7]

2.3.2   Integration points on supply level

Several integration points on supply level have been identified, as shown in Figure 2.22. To be successfully integrated with solar thermal technology, an integration point has to satisfy some criteria [26]:

- low temperature level
- constant load profile (daily, weekly, annually)
- high thermal energy demand
- low effort to make the integration
- low sensitivity to changes
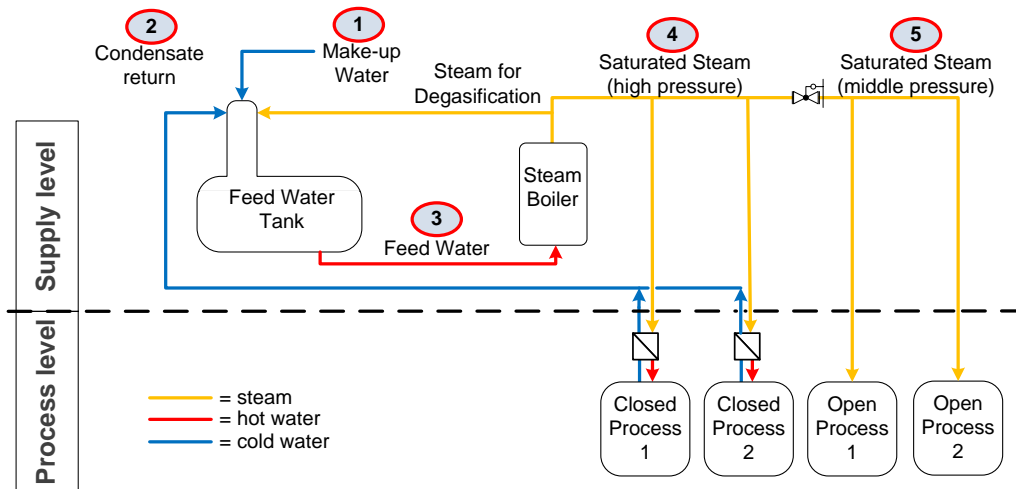
Figure 2.22. integration points in a steam network

1. Pre heating of make-up water: if steam is used directly in open processes it is necessary to reintegrate the lost mass flow with fresh water called make-up water. This water has low temperature, since it is taken from the water supply network; therefore it can be conveniently pre-heated almost up to saturation temperature (usually under 100°C since it is at ambient pressure). An advantage of this integration is that it doesn't have major effect on the control and operations of the conventional plants [25]; moreover the low temperature range allows to use flat-plate collector, cheaper than evacuated tube or concentrating collectors.
   This integration is worthy if the make-up water mass flow is considerable [25], that means if the industrial processes use directly large amount of steam, and if the temperature of the make-up water is low.
   For this reason, efficiency measures that recover heat from the lost steam to increase the temperature of the make-up water, also reduces inevitably the potential of this solar thermal integration point.

2. Pre heating of condensate: when steam is used in closed processes, delivering energy through a heat exchanger, it is possible to recirculate the condensate produced; usually this condensate is at ambient pressure and temperature around 90°C, so that is possible to heat this flow up to saturated conditions (100°C). This integration is not very promising since the amount of energy required is low [8], being the temperature difference around 10°C (also lower if energy efficiency measures are implemented); moreover the temperature range is higher than with make-up water, that means more expensive collector are required.

3. Boiler feed water: the water that flows to the boiler comes from a tank where is kept at around atmospheric pressure and 100°C. It is possible to pressurize this water before the boiler and heating heat to saturated conditions up to 150°C [25]. This integration has the advantage of warming the entire mass flow going to the boiler, which means both the condensate and the make-up water; but on the other hand it requires evacuated tube or concentrating collectors to reach higher temperatures. Moreover it is not convenient if an economizer is installed, since it can bring the boiler feed water up to around 135°C reducing the temperature difference achievable with a solar integration [8].

4. Steam generation: it is possible to generate steam with solar collectors in parallel with the boiler.

Table 2.1. enthalpy of make-up water, feed water and saturated steam [27]

	P [bar]	T [°C]	q [-]	h [kJ/kg]
make-up water	1	20	0	84,01
feed water	1,2	102	0	427,55
saturated steam	12	188	1	2783,87

$$\frac{\Delta h_{\text{steam generation}}}{\Delta h_{\text{total}}} = \frac{h_{\text{saturated steam}} - h_{\text{feed water}}}{h_{\text{saturated steam}} - h_{\text{make-up water}}} = 87,28\% \qquad (2.10)$$

Equation (2.10) shows that the most of the energy required by the steam network is used to generate steam, assuming the temperatures showed in Table 2.1. For that reason solar powered steam generation is the integration that can potentially supply the greater amount of heat to the steam network. Moreover it isn't affected by the installation of heat recovery systems as it happens with the integrations previously described.
This integration requires concentrating collectors and therefore it is successful only if large amounts of direct irradiation are available.

5. Low-pressure steam generation: if the processes fed by a steam network have different temperature levels, it is possible to generate steam at low pressure to supply heat just to the processes with lower temperature; the advantage of this integration is that the collector efficiency increases,

since the temperature are lower, but on the other hand the potential in terms of amount of heat required is lower, heating just a part of the mass flow and having a lower enthalpy difference.

Chapter 3

Model of solar thermal integration in the steam network of a commercial laundry

To evaluate the potential of solar process heat integration on supply level, a steam network has been modelled in ColSim, a simulation tool for solar thermal systems developed and used in Fraunhofer ISE.

The parameters characterizing the steam network model, such as steam mass flow and temperature, have been chosen taking as a reference the heat supply system of a typical German commercial laundry, investigated by Fraunhofer ISE within the project SoProW, particularly within the Master Thesis of Michael Schmid.

Eventually four integrations have been modelled adding solar thermal systems at the previous steam network model.

3.1 The simulation tool ColSim

ColSim is a simulation tool developed at Fraunhofer ISE to model HVAC and solar thermal systems. ColSim is written in the programming language C and can be operated on a LINUX system.

ColSim uses a graphical user interface (GUI), the vector graphic tool XFIG, to represents in a user-friendly way the modelled system.

As shown in Figure 3.1, the XFIG model is composed of pictures and lines: the pictures are called "Types" and represent the component of the plant. Every type has a corresponding file written in C-code that describes the behaviour of the real component. The lines or "Polylines" are used to link different types in the same way as the components are connected with hydraulic and electronic circuits in the real plant.
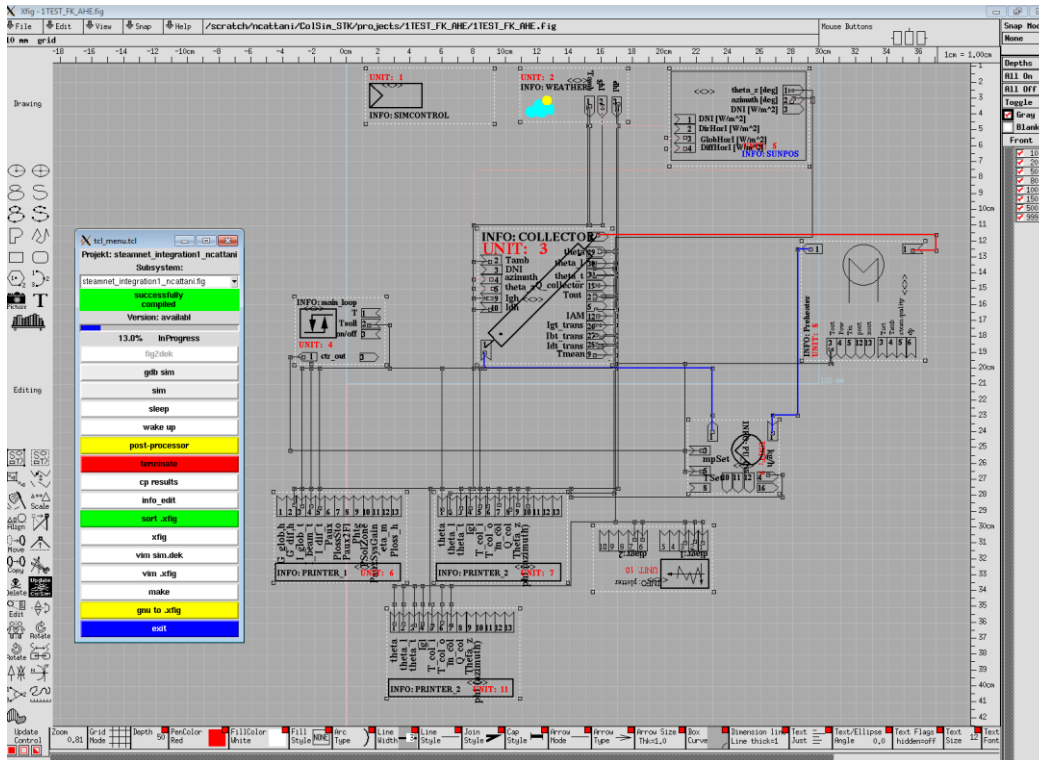
Figure 3.1. XFIG of a simple model in ColSim

The aim of a ColSim model is to predict how a real plant performs, that means how it interacts with the fluid circulating in the system.

In order to do that, the properties of the fluid are written in a struct[1] called "Plug", shown in Figure 3.2.

When the simulation starts, a Plug is generated by the pump, which is for default the first type to be considered, and then follows the connections drawn in the XFIG, reaching the inlet of a new type. When the C-code of the type is read, the fluid properties written in the Plug are modified, generating an outlet Plug that can be sent to the next type. At the end the Plug comes back to the pump, closing the loop.

---

[1] A struct is a C-code data type, that contains different variables

```
struct plugstructure
{
  double Q;  /**< [Ws] enthalpy total m_dry,msteam,m_water */
  double T;  /**< temperature */
  double h;  /**< timestep [s] used in Get_MixedPlug_Fluid() */
  double p;  /**< pressure [bar] */
  int    ident; /**< character table */

  double init_energy; /**< [Ws] plug initial energy/enthalpy */
  double qdot_in_sum; /**< [Ws] cumulated energy at input of plug*/
  double qdot_out_sum;/**< */
  double qdot_loss_sum;/**< */

  double x;     /**< [-] steam quality */
  double m;     /**< delta_m [kg] */
  double m_ad;  /**< mass of e.g. salinity [kg] */

  double cp;    /**< spec heat [kWs/kgK] */
  double U;     /**< U-value to ambient [W/K] */

  double TnextPlug;/**< ambient plug temp for ideal stratification;
                      following plug temperature */
  double Sf;       /**<Strong stratification factor,
                      provides ideal shifting thru direct flow */
  int    i_node;  /**< node index */
};
```

Figure 3.2. Plug struct in C [28]

The Plug struct describing the fluid contains information about pressure, temperature, mass and enthalpy; these properties in this chapter will be indicated using the nomenclature typical of ColSim, shown in Figure 3.2.

m_{plug} is the mass that flows during a period of time Δt, called time step h, through the polyline linking two types, while ΔQ_{plug} is the enthalpy associated to this mass:

$$m_{\text{plug}} = \dot{m} * h \tag{3.1}$$

$$\Delta Q_{\text{plug}} = \dot{m} * c_p * \left(T_{\text{plug}} - T_{\text{reference}}\right) * h \tag{3.2}$$

In ColSim in every type the inlet mass has to be equal to the outlet mass, so that mass cannot be accumulated, making the modelling of some components like storages with flexible filling level impossible.

In each time step the enthalpy is recalculated in each component. In particular the code of several types contains differential equations that describe the enthalpy balance on a control volume. These equations are simplified under several assumptions (one-dimensionality, constant density and pressure, absence

of diffusion) and then are solved by a finite difference method, discretizing the 1D space in segment called "Nodes". For each node is made a balance of the enthalpy that enters (ΔQ_{plugIn}), the one that exits ($\Delta Q_{\text{plugOut}}$), is accumulated ($m_n * c_p * \Delta T$) and exchanged during one time step:

$$c_p m_{n,h} \left(T_{n,h} - T_{n,h-1} \right) = \Delta Q_{plug,in} - \Delta Q_{plug,out} + Q_{Q/S} \tag{3.3}$$

where m_n is the mass of the node, $T_{n,h}$ is the node temperature at the time step h and $Q_{Q/S}$ is the enthalpy exchanges, seen as a source term.

Figure 3.3 shows how the energy balance is realized in ColSim:
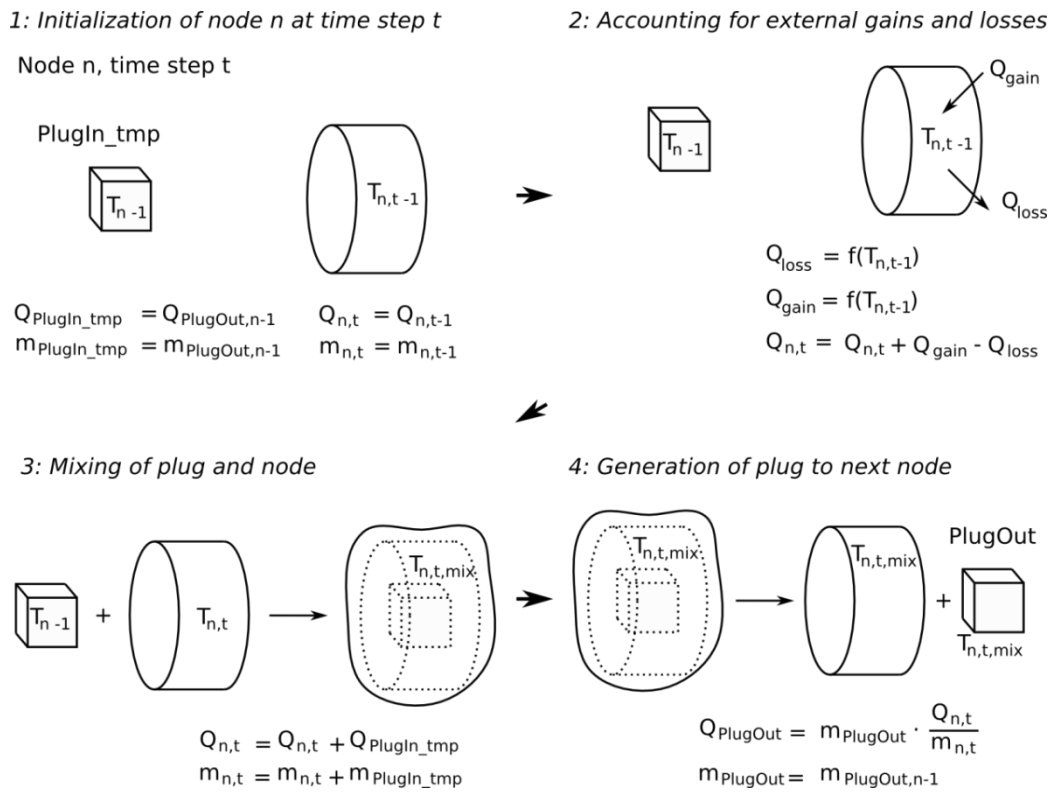
Figure 3.3. Plug Flow model in ColSim [28]

3.2 The laundry model

Load profile and temperature level required by a typical German commercial laundry have been used in order to characterize the heat demand of the steam network model.

These data are based on industrial sector study done within the project SoProW (coordinated by Fraunhofer ISE), which investigates the potential for solar process heat in laundries in Germany. In particular within the Master Thesis of Michael Schmidt typical dimensions and load profiles were investigated and a representative laundry model was set up.

Commercial laundries are an interesting sector of application for solar thermal technology since they have a large consume of heat at low-medium temperature (under 180°C), in average 1,3 kWh/kg $_{dry\ clothes}$, representing 88% of the total energy consumption of the plant [23]. Typically laundries use steam. Steam can be used directly, for example mixed with fresh water obtaining hot water necessary for the washing processes, or can be employed to heat another fluid via an heat exchanger. In laundries specifically air is heated, to be used for the dryer and the mangle.

For what concern this thesis, the laundries have been treated as heat consumer, without focusing on how the processes of a laundry actually work (for more information about it see [8]).

The necessary load profile and temperature level have been selected from real plants, elaborated to create a laundry model within Michael Schmid master thesis [8] and again modified for the purposes of this thesis.

It follows a description of Michael Schmid's laundry model. The final model is described in chapter 3.3.1.

Figure 3.4 shows the model of the steam network of a laundry created by Michael Schmid [8]: the idea behind this model is to find representative values characteristic of middle sized laundries that have already put in practise advanced energy savings measures.
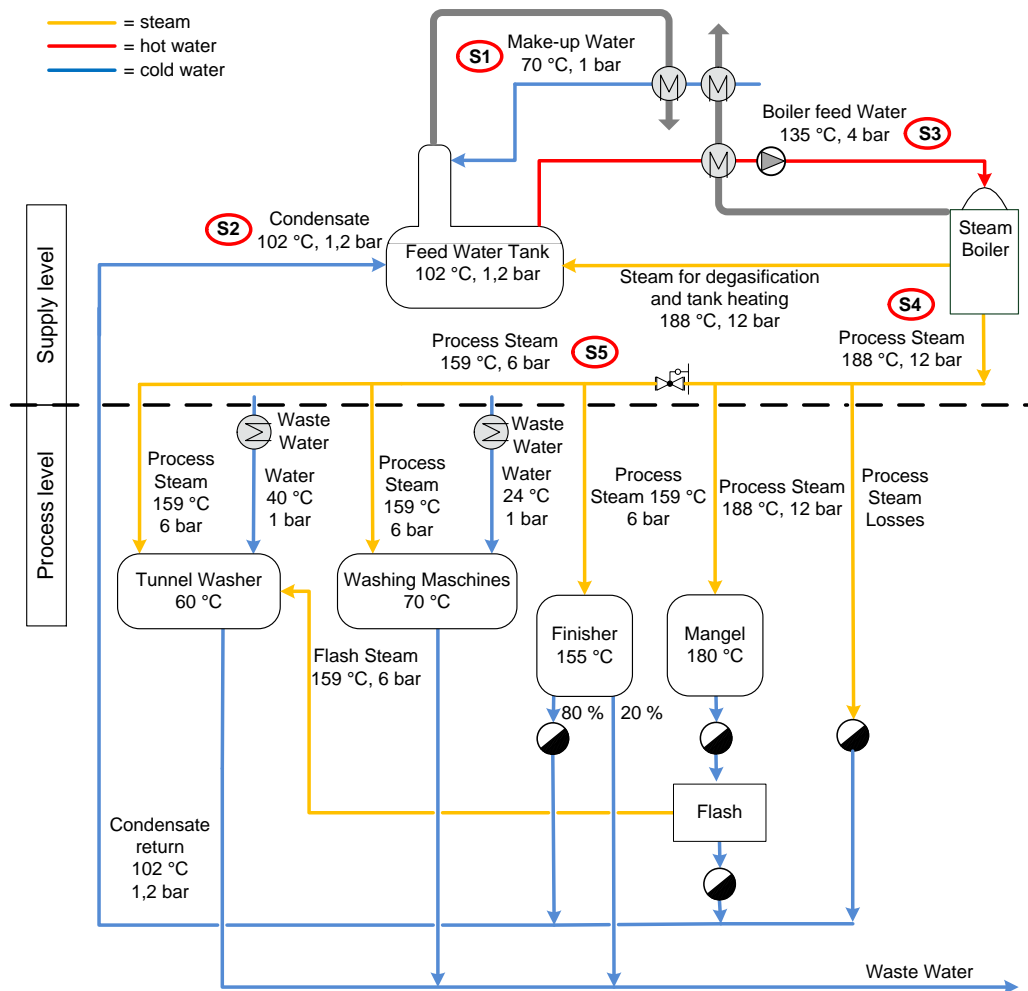
Figure 3.4. Michael Schmid's model of the steam network of a laundry. Integration points on supply level: 1 = heating of make-up water, 2 = heating of condensate, 3 = heating of boiler feed water, 4 = steam generation at high pressure, 5 = steam generation at low pressure.

In this model, the maximum steam temperature required by the processes is between 188°C, corresponding to 12 bar at saturated conditions; therefore steam is generated in a boiler at this temperature and pressure.

The larger share of steam is sent to heat exchangers to feed high temperature closed processes (mangle, finisher and dryer); after that the condensate is sent to a throttle, generating flash steam and low pressure condensate.

The other part of the steam generated in the boiler is directly used in washing processes; since it requires lower temperature and pressure it has to be expanded and de-superheated to 6 bar and 159°C. The water at the outlet of the process cannot be recirculated, so that it has to be reintegrated with make-up water;

nevertheless the energy in this outlet flow is recovered to pre heat the fresh water incoming into the open processes.

Also other efficiency measures are applied: the boiler feed water is pre heated in an economizer up to 135 °C, cooling the flue gas of the boiler; the make-up water is pre-heated up to 70°C recovering heat from the degasification steam and the flue gas from the boiler; the condensate is insulated so that the condensate returns at 102°C.

The laundry works from 6 pm to 16 pm for 5 days per week, 52 weeks per year. The steam production in the boiler depends on the overall heat demand of the laundry.

In Figure 3.5 is showed the profile of the generated steam, both with real data provided by a laundry and with a simplified load profile designed by Michael Schmid for its model. The specific behaviors of the real plant have been removed from the simplified profile, for example no steam generation after 16 pm has been considered because usually middle sized laundries stop their operations at this time.
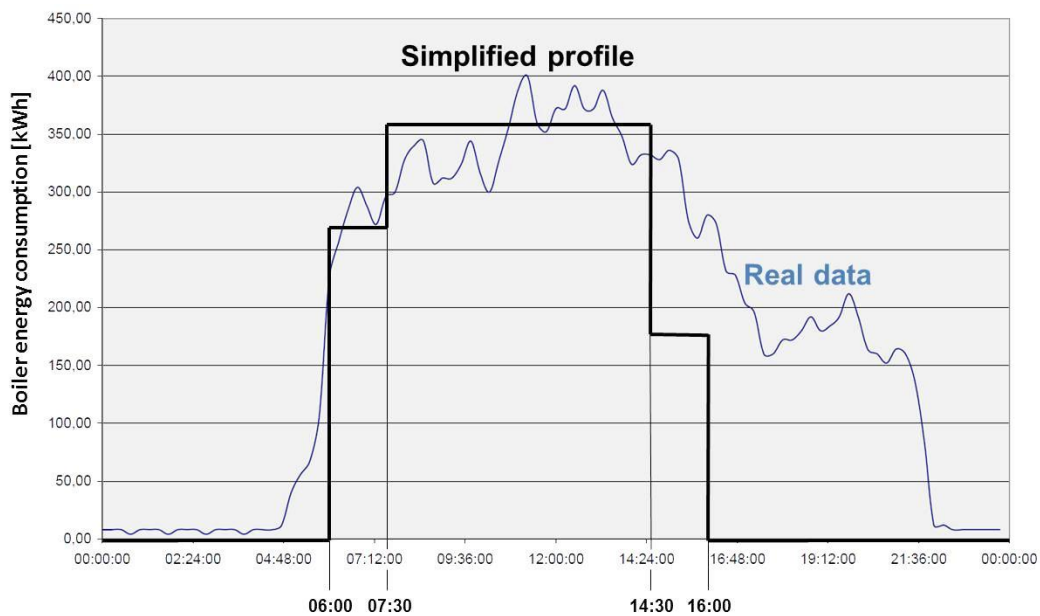
Figure 3.5. hourly profiles of steam generation

The mass flow of the make-up water is shown in Figure 3.6. The make-up water pump is switched on when the feed water tank level is too low and switched off when it is full.
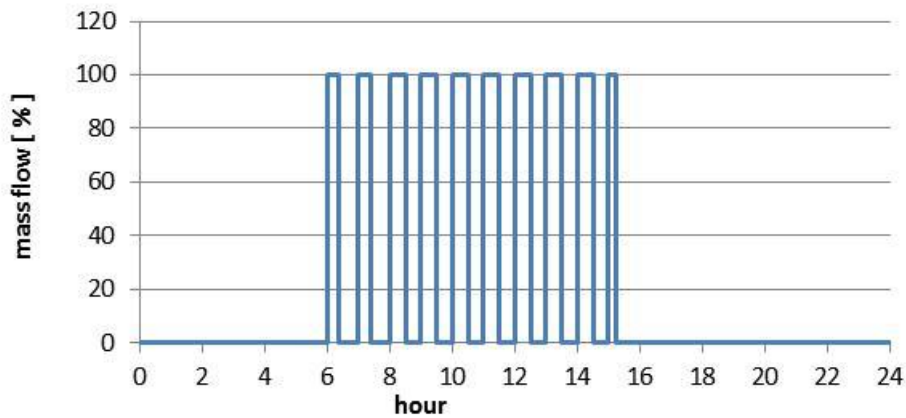
Figure 3.6. make-up water mass flow

3.3 Modelling of the steam network of a laundry in ColSim

The first configuration modelled in ColSim is a conventional steam network of a laundry. In order to do that pre-existing types have been adapted.
The model of a laundry shown in Figure 3.4 has been simplified and adapted, becoming a new model shown in Figure 3.7.
It follows a description of the model, its components, control strategy and parameters.

3.3.1 Description of the model

The aim of this model is to simulate the steam generation and distribution network necessary to supply heat to the processes of a middle sized laundry with standard energy saving measures.

Figure 3.7 shows the idea behind the model; a more complete and realistic description of the model in ColSim can be found in the Appendices.
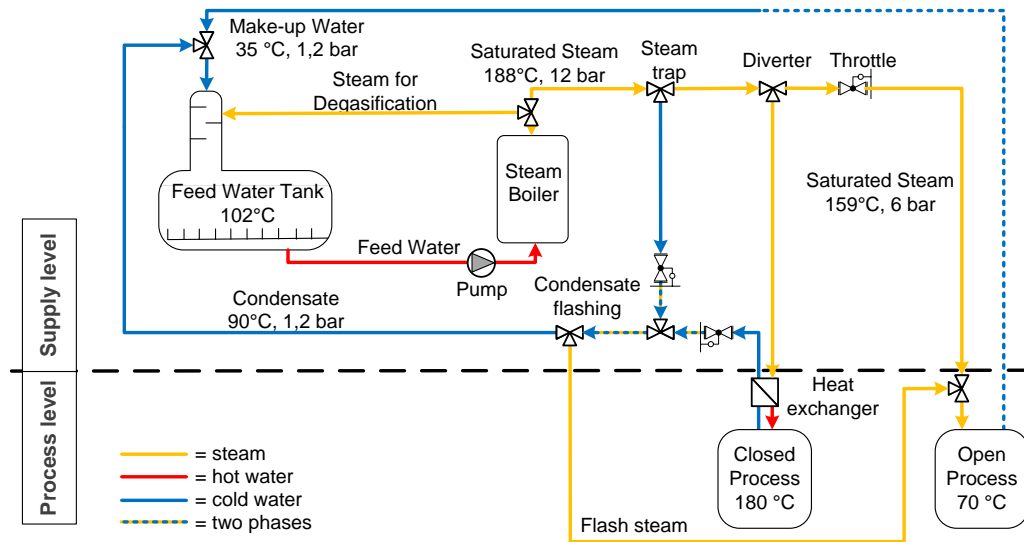
Figure 3.7. model of steam network

As shown in Figure 3.7, the model of a laundry presented in chapter 3.2 has been changed. All the processes of the model laundry shown in Figure 3.4 have been gathered in one closed and one open process, in order to simplify the model and reduce the calculation time. For both closed and open process has been considered the same load profile shown in Figure 3.5, neglecting particular behaviour of the single processes.

The closed process require a hot secondary fluid: high pressure saturated steam is condensed and sub cooled, heating the secondary fluid from 35°C to 180°C with a heat exchanger. 35°C is higher than the normal ambient temperature because the fresh air is pre-heated with the waste air flowing out from the process. This temperature has been assumed for this model, since the laundry model doesn't provide information on this temperature.
Eventually the process then absorbs energy from the secondary fluid and discharges it.
As shown in Figure 3.8, the closed process has been modelled as a cooler, which reduce the air temperature back to 35°C, so that it can be recycled as fresh air: this last passage is represented by the dotted line, which is not present in the real plant, that doesn't recycle the discharged air, but is necessary for the simulation since every hydraulic circuit in ColSim has to be closed.
In the real plant the condenser and sub cooler are two separated components, each with a fixed length and volume. This distinction has been kept also in the model. The outlet temperature of the condensate, on supply level, is a result of the simulation and depends on the heat exchanger features.
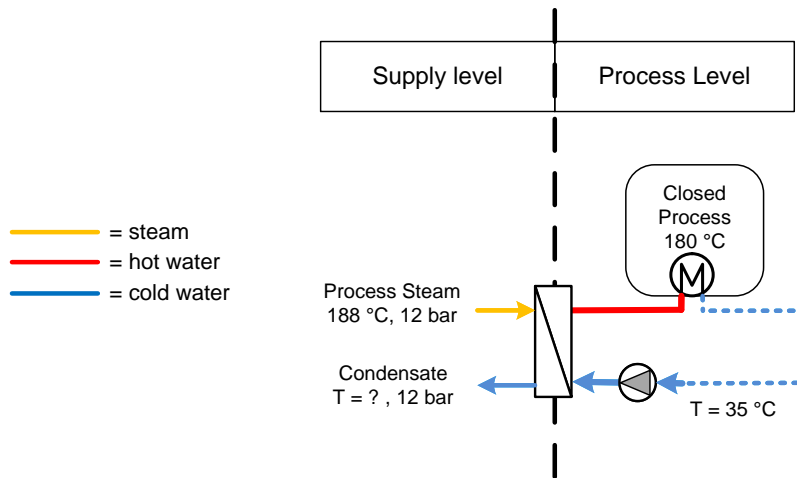
Figure 3.8. model of closed process

The open process use directly saturated steam at low pressure, mixing it with fresh water at 35°C in order to have hot water at 70°C; then the process absorbs the energy form the hot water and discharges it. 35°C has been assumed as inlet temperature of the fresh water of the open processes showed in Figure 3.4.

As shown in Figure 3.9, in the model steam and fresh water are mixed to get hot water; then the waste water is split by a diverter in two branches: one is recycled as fresh water, the other as make-up water that has to be reintegrated to compensate the steam losses. As with closed processes, in real plants there is no recycling of the waste water but this has to be modelled in ColSim since each hydraulic circuit has to be closed. This means that the make-up water mass flow shown in Figure 3.6 has been replaced with the load profile shown in Figure 3.5.
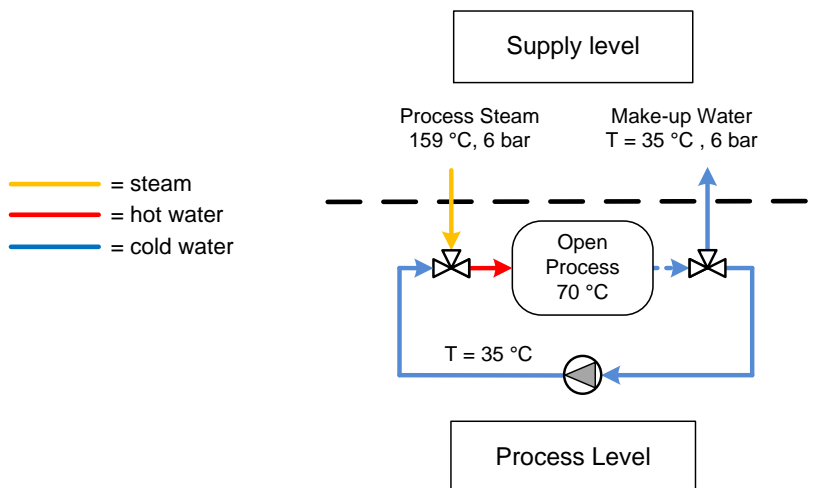
Figure 3.9. model of open process

Once modelled the process level, the goal is to model a supply level that can provide the demanded amount of heat to each load reaching the required target temperature. In order to do that, the process temperature is constantly measured. A signal is sent to a PID controller, which compares it with the target temperature in order to regulate the steam mass flow and consequentially the heat delivered. For instance, if the steam mass flow is reduced, less heat can be transferred to the process, which consequently can reduce its temperature. In this way the controller calculates the required amount of steam that has to be supplied to each process.

The supply level can be divided in generation, distribution and return parts.

The steam generation part is shown in Figure 3.10. It consists of a tank, that gathers the condensate at 90°C and the make-up water at 35°C, mixes them with steam in order to keep the top tank temperature at 102°C and degasify the make-up water; in order to do this the temperature is measured and sent to a PID controller, which regulates the steam mass flow.
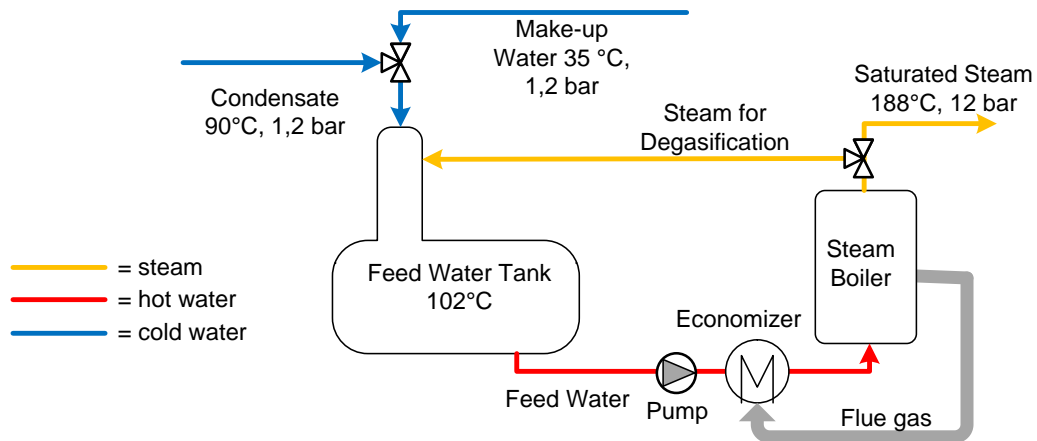
Figure 3.10. model of steam generation block

The condensate and make-up water temperatures are different from the temperatures of the laundry model presented in chapter 3.2. The reason behind this choice is that the laundry model was meant to represent an efficient plant, having advanced energy saving measures, while the model of the steam network developed for this thesis is meant to represent a realistic laundry, with average energy efficiency. Therefore the condensate lose around 10°C before coming to the feed water tank and the make-up water is pre heated from ambient temperature to 35°C. These assumptions have an influence on the integration of a solar thermal plant, for example increasing the temperature range for the

integration of make-up water. Therefore the results provided by this model are valid just for steam network with a similar energy efficiency level.

The tank modelled in ColSim has some differences from the one of a real plant: in reality it has a variable mass, because the incoming make-up water has an discontinuous mass flow as shown in picture Figure 3.6, while the outlet mass flow is more constant, as shown in picture Figure 3.5; in ColSim this cannot be simulated, therefore the make-up water mass flow is the same of the tank outlet mass flow, shown in picture Figure 3.5. Moreover, the degasification is not considered in ColSim.

After the tank the feed water is pumped, pre heated by an economizer recovering heat form the boiler flue gas. It is then sent to a boiler, where it evaporates. The feed water pump is regulated by PID controllers in order to generate the amount of steam that covers the energy demand, to maintain the temperature of 102 °C of the feed water tank, as described in chapter 3.3.2.

Moreover in this model the feed water pump increases the pressure from 1,2 to 12 bar between the feed water tank and the boiler inlet, while in reality the water reaches 5 bar in the pump, in order to have liquid in the economizer, and the boiler brings it to 12 bar, as described in chapter 3.3.2.

At the outlet of the boiler a diverter splits the steam required by the feed water tank for degasification, from the one that flows to the processes.
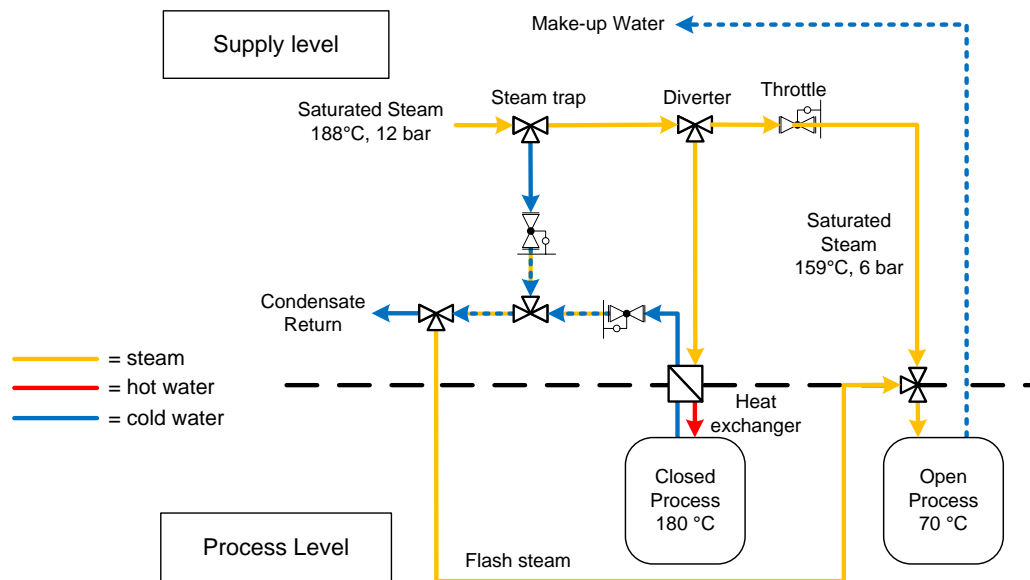
Figure 3.11. model of steam distribution and return lines

The distribution system, shown in Figure 3.11, delivers the steam to the processes. The steam is lead from the boiler to the processes through a network

of pipes. Even if the pipes are insulated, there are heat losses; since the boiler produces saturated steam, heat losses in the pipes cause condensation. For that reason steam traps are required to separate the condensate from the steam and send it to the condensate return lines.

The processes are supplied by the main steam line on different pressure levels. While the closed process is supplied at 12 bars, the open process is supplied at 6 bars; therefore is necessary a throttle that expands the steam at 6 bars for the open process.

Moreover, PID controllers regulate a diverter in order to split between the processes the mass flow of the main steam line.

After supplying the closed process, the condensate is brought to ambient pressure, generating flash steam. This steam is used to supply additional heat to the open load, as shown in Figure 3.12.
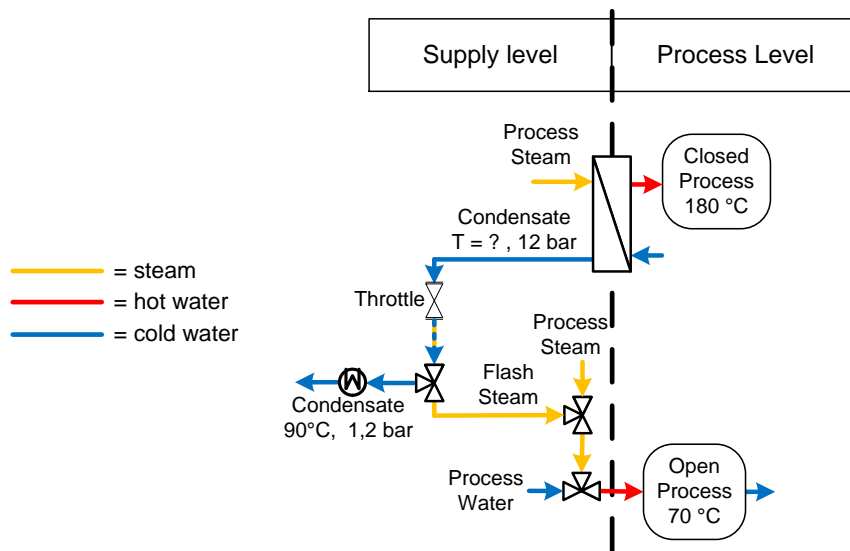
Figure 3.12. model of condensate flashing

The return lines close the cycle: the condensate at the outlet of the closed process is lead to the feed water tank. The water at the outlet of the open process is recirculated as make up-water at 35 °C; since this flow is not real but is necessary to run the simulation in ColSim, it is drawn with a dotted line in Figure 3.11.

3.3.2 Description of the components

Every ColSim type has a C-code file that modifies the properties of the fluid, written in the Plug, simulating how the real component interacts with the fluid.

In this section all the types used are described, explaining theirs operation, how they differ from the real components and what parameters have been adopted.

LOAD:

The load type reads a .txt file containing time variant data so it can be used by another type as an input.
In the steam network model the simplified load profile showed in Figure 3.5 is written in a .txt file as % of the maximal load, so that it has three values: 0.75 between 06:00 and 07:30, 1 between 07:30 and 14:30 and 0.5 between 14:30 and 16:00. This information is then sent to the pump on process level, so that the process has the correct mass flow and consequentially the energy demand shown before.

PUMP:

The pump is the first type of a circuit that is considered when the simulation starts in every time-step. At first the pump initializes the simulation generating a mass flow; when the simulation of a time step is done, the flow comes back to the pump. Since within ColSim is not possible to accumulate mass, the mass flow coming back to the pump has to be exactly the same as it was generated by the pump at the beginning of the time step.
In the system there are three pumps. The main pump before the boiler has to generate a mass flow that provides the right amount of energy to the feed water tank and the processes. To do that 3 PID controllers monitor the process temperatures and produce control signals called $ctrl_{cp}$ for the closed process, $ctrl_{op}$ for the open process and $ctrl_{tank}$ for the feed water tank. These signals are added in $ctrl_{tot}$, which is sent to the pump to generate the right mass flow.

$$\dot{m}_{\text{feed water}} = \dot{m}_{\text{set,pump}} * ctrl_{\text{tot}} \qquad (3.4)$$

$$ctrl_{\text{tot}} = ctrl_{\text{cp}} + ctrl_{\text{op}} + ctrl_{\text{tank}} \qquad (3.5)$$

where $\dot{m}_{\text{set,pump}}$ is a parameter of the pump.
Moreover each process has a pump, which generates a mass flow $\dot{m}_{\text{load}}$

$$\dot{m}_{\text{load}} = \dot{m}_{\text{max load}} * ctrl_{\text{load type}} \tag{3.6}$$

where $\dot{m}_{\text{max load}}$ is the maximal process mass flow, set as parameter in the pump, and $ctrl_{\text{load type}}$ is the control coming from the load type.

The mass flow of each load is calculated in the following way: knowing the average energy demand as well as the temperature difference of the process, it is possible to calculate the medium mass flow of a process:

$$\overline{\dot{m}_{\text{load}}} = \frac{\overline{\dot{Q}_{\text{load}}}}{c_p \, \Delta T_{\text{load}}} \tag{3.7}$$

$$m_{\text{load}} = \overline{\dot{m}_{\text{load}}} * h_{\text{day}} \tag{3.8}$$

Where m_{load} is the overall mass used from the process in a day and h_{day} are the working hours per day.
m_{load} can be calculated also as:

$$m_{\text{load}} = \sum^{3} (\dot{m}_{\text{load}} * h_{\text{load}}) \tag{3.9}$$

Where $\dot{m}_{\text{load}}$ is given by (3.6) and h_{load} are the hours in which the load type read a constant signal $ctrl_{\text{load type}}$. Since (3.8) must be equal to (3.9), the only unknown variable is $\dot{m}_{\text{max load}}$ in (3.6), that can be found solving the equation: the maximal mass flow of the open load 5242,1 kg/h and the one of the closed load is 4243,3 kg/h.

Another function of the pump is to increase the fluid pressure, which is set by an input; in the model the pressure at the outlet of the main pump is 12 bar.

PIPES

The pipe type, called header type in ColSim, models a pipeline with its pressure drops and heat losses. This type is divided in n "nodes", where n is set with a

parameter, so that the change of fluid temperature along the pipe is considered. In every node the heat losses with the environment are calculated as:

$$Q_{\text{loss}} = UA * (T_{\text{node}} - T_{\text{amb}}) * h \qquad (3.10)$$

where U [W/m²*K] is the overall heat transfer coefficient, the surface of the pipe A [m²], h [s] the time step and T_{amb} [°C] the ambient temperature.

THROTTLE

The throttle is a type that decreases the pressure of the fluid. The outlet pressure has to be assigned as parameter; the new fluid properties are then calculated from the set outlet fluid pressure and the inlet enthalpy, considering an isenthalpic expansion of the fluid.
This type doesn't have any node, which means it doesn't calculate the enthalpy balance on a control volume, but simply changes instantaneously the fluid properties.
In the model the throttle is used to lower the pressure level of the steam supplied to the open processes, which need steam at 159 °C and 6 bar. Moreover during the heat transfer with the closed process the steam is condensed and sub cooled. Before the condensate is pumped back to the feed water tank, it must be conditioned to ambient pressure in order to meet the requirements of the not pressurized tank. Reducing the pressure, the condensate is expanded and turns partly into steam. This steam, called flash steam can be still utilised in low temperature processes.
In ColSim the condensate is kept at 1,2 bar instead than at ambient pressure because the feed water tank has to be pressurized to free the gas after the degasification, and this can't be done if the incoming condensate is not under pressure.

HEATER

The heater type adds or takes enthalpy from the fluid and consequentially changes its temperature or its steam quality if there are two phases. It is possible to set the outlet steam quality or temperature, so that the simulation calculates the heat required, or vice versa to give the heat flux as input obtaining as result the outlet conditions of the fluid. Is it possible to add and remove enthalpy, so that this type simulates both a heater and a cooler.
The heater type doesn't have any heat capacity nor node, which means it doesn't calculate the enthalpy balance on a control volume (as for example the header pipe), but simply changes instantaneously the fluid properties. This feature

makes this type not suitable for a dynamic simulation with short time step, in which the realistic feature of the component have a strong influence on the not stationary behaviour of the type.

In the steam network model the heater type is used to simulate the boiler and the loads. A real boiler should increase both enthalpy and pressure, thanks to the density difference between steam and water; in ColSim instead the pressure difference between the steam at 12 bar and the feed water at 1,2 bar is given by the pump while the boiler brings the fluid to saturated steam conditions (12 bar, 188°C).

The load instead has to absorb energy and therefore the heater type that models it works represent a cooler. Since in ColSim it is mandatory to close the hydraulic loops, the outlet of the process is used as fresh fluid that flows back to the process, as shown in Figure 3.8 and Figure 3.9; therefore the cooler brings the fluid to 35°C.

DIVERTER:

The diverter splits one mass flow in two, according to a signal that can be given as constant parameter or input calculated with a controller. The fluid properties are kept constant and no energy balance on a control volume (with nodes) is calculated.

STEAM TRAP:

Another type similar to the diverter is the moisture separator, which divides a two phases flow in saturated gas and steam. This component is used in the steam lines to model a steam trap that extracts the condensate produced in the pipes caused by heat losses, and after the flash at the outlet of the closed process. In this case the flash steam is separated from the condensate and sent to supply heat to the open process, where is mixed with the process water and other steam coming from the boiler. The condensate instead is cooled to 90°C and sent back to the feed water tank, as shown in Figure 3.12.

MIXER:

In ColSim every diverter needs a mixer to close the hydraulic loop. A mixer simply merges the incoming flows, adding mass and enthalpy and calculating the corresponding outlet conditions. It is also possible to generate a signal, that describes the ratio between the two mass flows, and to use it to control a diverter that splits the mass flows exactly as they were before the mixer. This option is used for example for the open load, where the fresh water and steam are mixed and then separated with a diverter.

HEAT EXCHANGER:

As shown in Figure 3.13, the heat exchanger is modelled discretizing the two mass flows in n nodes and making an enthalpy balance for each flow in each node (the dotted cell in Figure 3.13), where the energy source term is the exchanged enthalpy calculated as shown in equation (3.11):

$$Q_{\text{exchanged,node}} = UA_{\text{node}} * \left(T_{\text{node,hot fluid}} - T_{\text{node,cold fluid}}\right) * h \qquad (3.11)$$

U is the overall heat transfer coefficient [W/(m²*K)], A is the node area, equal to the total area divided by *n*.
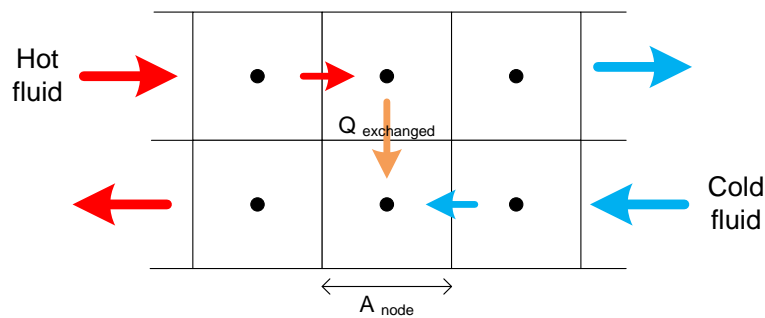
Figure 3.13. model of a counter flow heat exchanger

This type changes the enthalpy of the fluid, as also the heater type does; for that reason it could be possible to simulate an heat exchanger with an heater on the cold fluid and a cooler on the hot fluid, that respectively add and take the same amount of energy; the difference in using an heat exchanger type is that the outlet conditions, as well as the amount of heat exchanged, are result of the simulation depending on the features of the component (*U*, *A*, thermal capacity, heat losses), while in the heater type the outlet conditions are set before the simulation, that therefore gives obvious results.

This type has been used to simulate the counter flow heat exchanger that provides energy to the closed process. In reality such a heat exchanger consists of two components, a condenser and a sub cooler, both with a defined length and volume. In ColSim the condenser is modelled with a heater type, while the sub cooler is modelled with a proper heat exchanger, which calculates the outlet temperature of the condensate.

STORAGE:

As shown in Figure 3.14, the storage type is modelled discretizing a volume in *n* horizontal layers, each at a uniform temperature. For each of them an enthalpy balance is calculated. This energy balance takes in account several heat transfer mechanism, such as inlet and outlet mass flows, effects of internal heat exchangers, as well as convection and conduction between consecutive layers and heat losses to the environment. The results of the calculation are the temperature of the nodes, the outlet temperature of the flows and the heat losses.
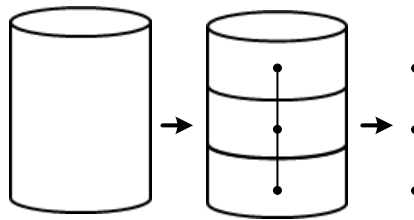
Figure 3.14. storage discretization

CONTROLLER:

As shown in the box in Figure 3.15, the controller type gets one or more input signals, usually physical properties of the fluid. The controller elaborates this information to get an output control signal, used to regulate other types. How the type calculates the output is defined in the program code and is set by the programmer to obtain a suitable control signal.
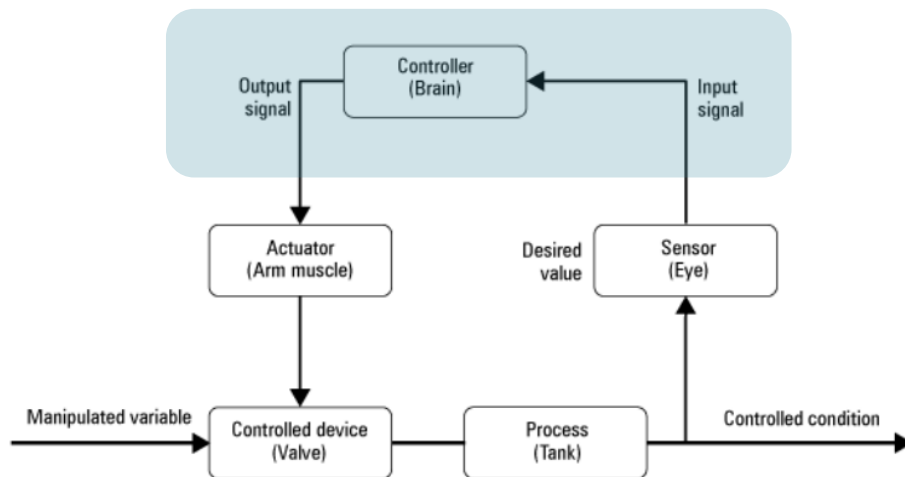
Figure 3.15. operations of a real automatic control: a sensor measure a physical property and send it as input to the controller, which elaborates it and to regulate a

In the steam network model, PID controllers are used to regulate the generated steam mass flow. A PID controller compares a measured property with a target one, creating an error signal called *e*:

$$e = T_{\text{target}} - T_{\text{measured}} \qquad (3.12)$$

This signal is used to produce a control signal ctrl, using three terms: one is proportional to *e*, one is an integration of *e* in the time and another one is the temporal derivative of *e* (for that reason PID); each of them has a coefficient *K* that can be set to adjust the control signal:

$$ctrl = K_p * e + K_i * \int e * dt + K_d * \frac{\mathrm{d}e}{\mathrm{d}t} \qquad (3.13)$$

This signal can be used to control a component, in this model it is used to regulate the steam generation and distribution according to the load temperature: the temperature in each load and in the tank is measured and compared with the target one, so that the bigger the error signal is, the lower is the temperature of the fluid and therefore more steam is required. The control signal is therefore used to control the amount of steam generated in the boiler by changing the mass flow of the main pump.

The proportional term compensates the deviation from the target value. In this case it will increase the amount of steam generated and send to a load if the process temperature is too low. Nevertheless, once the target is reached and the error signal is null, a steam mass flow is still required to keep the target temperature, but this wouldn't be done by the proportional term that would be null too. Therefore an integral term is required, keeping the control signal positive also when the error is almost zero.

A good control has to achieve the goal, in this case the target temperature, in short time and without oscillation. In order to do that is necessary to tune the controller, that means to set the K coefficients; there are several methods to do that, the one choose is manual tuning, making different simulations in order to find a good tuning.

3.4   Modelling of solar heating of make-up water in ColSim

The second configuration modelled in ColSim is the integration of the steam network presented in the chapter 3.3 with a solar thermal system that heats the make-up water. It follows a description of the model, its components, control strategy and parameters.

3.4.1   Description of the model: configuration without a storage

The make-up water is fresh water that is injected into the system to compensate for the steam losses in the open processes. In reality the water comes from the water supply net, which usually has low temperature, around 10°C. Such low temperatures offer a high pre-heating potential. One possibility is to pre-heat the incoming cold water recovering heat from the open process waste water. In this model a make-up water temperature of 35°C has been considered, assuming a pre-heating from 10°C using heat recovery.

The integration with a solar thermal system consist in just a water-water sensible heat exchanger, that increases the make-up water temperature up to 100°C; higher temperatures are not desired because there would be steam generation, that could be problematic in pipes dimensioned for water.

The solar thermal system has two configurations: with and without storage.
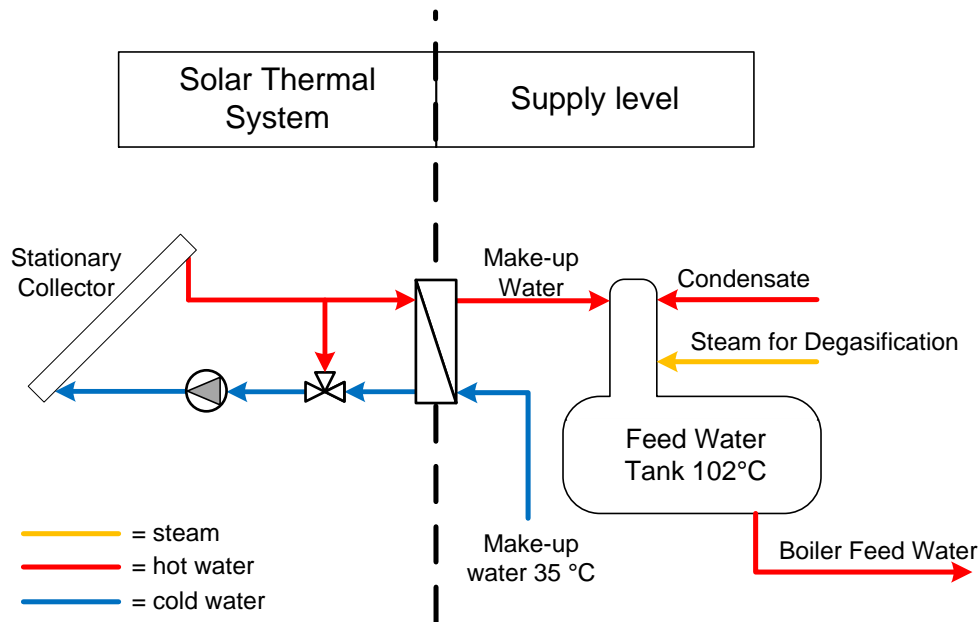
Figure 3.16. pre heating of make-up water, solar thermal system without a storage

As shown in Figure 3.16, water is pumped in stationary collectors, where it absorbs solar energy; if no storage is installed, the water flows directly to the heat exchanger, which supplies energy to the make-up water, and then comes back to the pump, closing the loop. Since the make-up water cannot get hotter than 102 °C, a by-pass allows reducing the mass flows that goes from the collector to the heat exchanger, in order to control the make-up water temperature.

In this configuration the solar pump can work just when the make-up water is needed, so that all the solar energy available when there is no instantaneous energy demand from the processes is not exploited.

Moreover such a configuration is technically feasible only if is available a continuous make-up water mass flow, such as the one chosen. The real make-up water mass flow shown in Figure 3.6 is actually too discontinuous, causing too much stagnation hours that could reduce drastically the service life of the collector and its energy gains. A configuration without a storage would not be feasible with the load profile of Figure 3.6.

It is instead feasible with the make-up water mass flow used for this simulation, resulting less complex and expensive of a configuration with the storage.

3.4.2   Description of the model: configuration with a storage

The presence of a solar thermal storage allows uncoupling the exploitation of solar energy from its use to supply heat to the steam network.
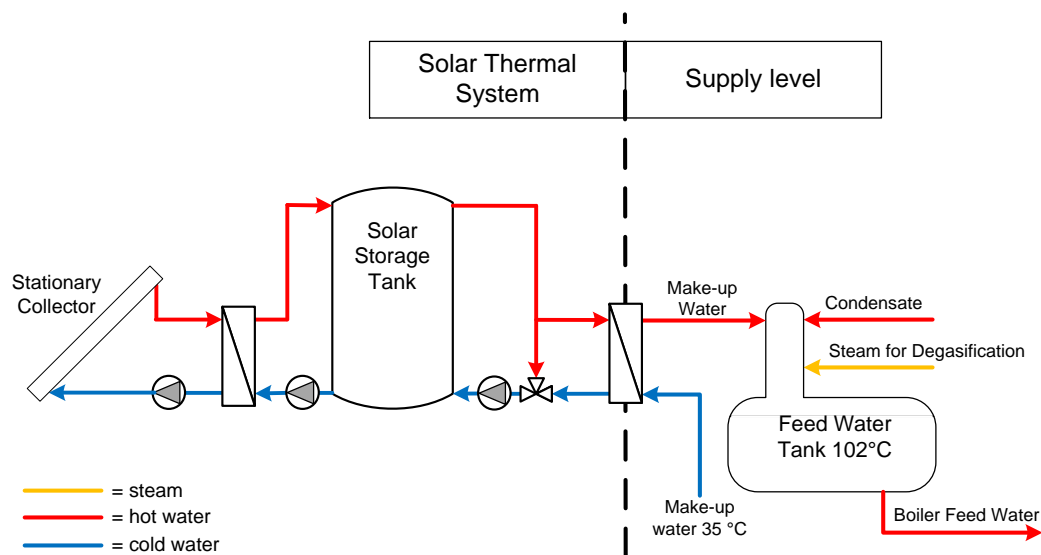
Figure 3.17. pre heating of make-up water, solar thermal system with a storage

As shown in Figure 3.17, the solar thermal system is composed of three hydraulic circuits: in the collector loop a pump makes the water flow in the stationary collectors and then in a heat exchanger, where heat is transferred into the storage charging cycle, before coming back to the pump. At the other side of the heat exchanger water flows from the bottom to the top of the storage with the same mass flow of the collector loop, taking the solar heat into the storage.

On the discharging side of the storage, a mass flow is pumped when the upper storage temperature is hot enough to deliver the needed minimum temperature to pre-heat the make-up water through a heat exchanger. As in 3.4.1, a heat exchanger by-pass is used to regulate the mass flow in the heat exchanger, in order to avoid the make-up water temperature to get too high.

The presence of a storage allows exploiting better the solar irradiation and prevent stagnation, which could damage the collector. On the other hand the system is more expensive and the temperature difference between make-up water and collector is higher, because of the presence of two heat exchangers.

3.4.3 Description of the components

WEATHER:

The weather type is similar to the load type.

It reads in an external .txt file containing time variant weather data and makes it available in ColSim, as it happens with the load type. The weather files used in this model have been generated with Meteonorm 7; they provide information about the ambient temperature and the horizontal irradiation (global, diffuse and direct) in a chosen location during a year, with a resolution of one hour.

COLLECTOR:

For this configuration the use of stationary collectors is possible, since the temperature difference between fluid and environment is always under 100°C. In the ColSim type at first solar energy gains are calculated, as shown in equation (3.14):

$$Q_{\text{sun}} = \eta_0 * A * \left(K_{\tau\alpha,\text{dir}} * G_{bt} + K_{\tau\alpha,\text{diff}} * G_{dt} \right) \tag{3.14}$$

Q_{sun} is the energy absorbed by the collector, before subtracting the thermal losses. η_0 is the optical efficiency is calculated with a null incidence angle,

$K_{\tau\alpha,\text{dir}}$ and $K_{\tau\alpha,\text{ diff}}$ are the incidence angle modifiers, G_{bt} and G_{dt} are the beam and diffuse radiation on the tilted surface.

$K_{\tau\alpha,\text{dir}}$ and $K_{\tau\alpha,\text{ diff}}$ are written in tables generated with a ray tracing program. Knowing the angle θ, it is possible to find the correct $K_{\tau\alpha,\text{dir}}$ and $K_{\tau\alpha,\text{ diff}}$ (this approach is typical for concentrating collector, the most used in ColSim).

G_{bt} and G_{dt} are calculated within the collector code, since the weather file usually provides radiation data for horizontal surfaces. To calculate radiation on a tilted surface the collector slope and orientation, given as parameters, are needed.

Then the thermal losses are calculated, as shown in equation (3.15):

$$Q_{\text{loss}} = [\, a_0 * (T_{\text{mean}} - T_{\text{amb}}) + a_1 * (T_{\text{mean}} - T_{\text{amb}})^2] * A_c \qquad (3.15)$$

a_0 and a_1, as well as η_0, are parameters to characterize the collector.

It is possible to calculate the thermal energy gain of the collector as $Q_{\text{sun}} - Q_{\text{loss}}$; this term is then divided for the number of nodes in which the collector is discretized and is used as Q_{gain} in the Plug Flow model shown in Figure 3.3.

The collector chosen for the simulation is the flat-plate double covered Solid Gluatmugl HAT collector, characterized by the parameters shown in **Fehler! Ungültiger Eigenverweis auf Textmarke.** and Figure 3.18.

Table 3.1. parameters of the used flat plate collector

	$\eta\,0$	a1	a2
flat plate collector	0,811	2,71	0,01
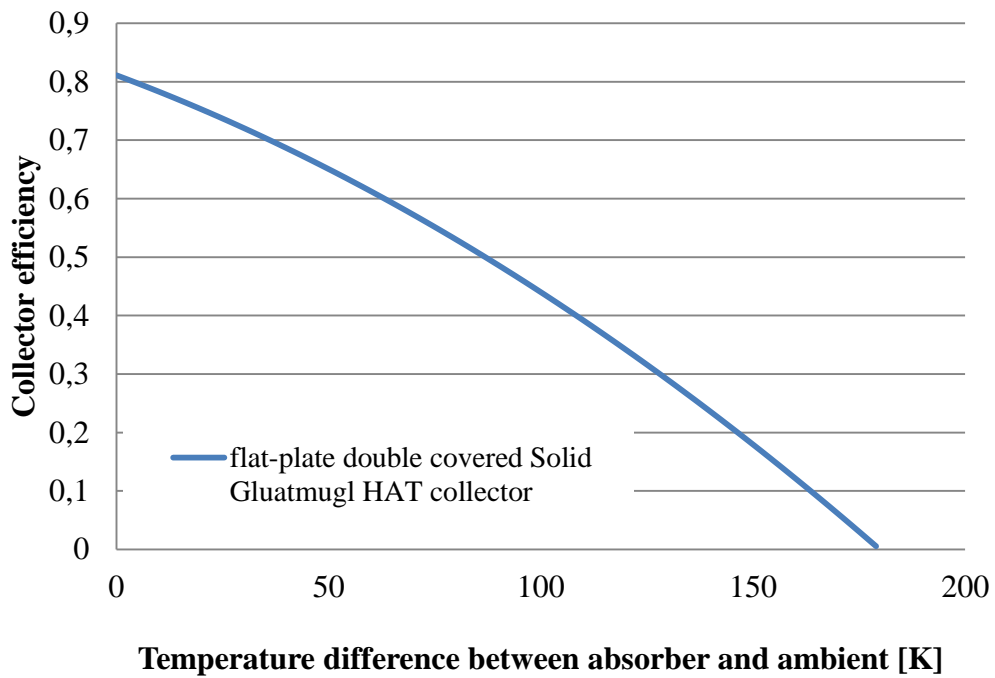
Figure 3.18. efficiency curve of the used collector

Another option would have been to use evacuated tube collectors; within the frame of this thesis this option won't be investigated.

Other parameters of the collector type that have to be chosen are collector slope and absorber area. Several simulations with different collector slope will find out what is the optimal collector slope that maximizes the solar energy. The absorber area will be also varied, in order to compare solar thermal systems of different size.

PUMP:

The collector pump generates the mass flow of the collector loop. The maximal mass flow is set to 30 [l/(h*m²)] [11].
The pump is switched on if the following conditions are respected: the solar radiation has to be positive; the outlet temperature of the collector exceeds of ΔT_{on} a reference temperature:

$$T_{\text{out,collector}} \geq T_{\text{reference}} + \Delta T_{\text{on}} \tag{3.16}$$

where $T_{\text{reference}}$ can be either the integration temperature of the make-up water in the configuration without storage, or the top tank temperature in the configuration with a storage. The storage temperature can't exceed a limit, determined by the constructor. In this case the storage can reach a maximum temperature of 95°C, a common limit for not pressurized storage (it is possible to have higher limit with pressurized storage, which on the other hand are more expensive and therefore usually not selected for this integration).
It has been chosen $\Delta T_{\text{on}} = 20$ °C in order to avoid the collector pump to be switched on and off intermittently.

The pump is switched off if one of the conditions above is not respected, or when the reference temperature defined above of exceed the collector outlet temperature of $\Delta T_{\text{on}} = 0$ °C:

$$T_{\text{out,collector}} \leq T_{\text{reference}} - \Delta T_{\text{off}} \tag{3.17}$$

Moreover, for the configuration without the storage this pump is switched off when the laundry processes require no energy, while in the configuration with the storage it can work also when there is energy demand from the processes until the storage is fully charged.

In the configuration without the storage the collector mass flow changes as the make-up water mass flow changes (partial load), in order to have better heat exchanger performance. In reality this solution is expensive, because it would require a pump regulated by an inverter.

The configuration with the storage needs two more pumps in the system. one for the storage charging, by pumping cold water from the bottom of the storage and feeding it to the heat exchanger between storage and collector field.
The second pump discharges the storage by taking hot water from the top of the storage and sends it to a heat exchanger in order to feed heat to the make-up water. The mass flow of this pump is the same of the make-up water; the pump is switched on when the top tank temperature exceeds of ΔT_{on} the make-up water temperature, which is always 35°C, and is switched off when the tank temperature is too low, as it happens with the collector pump.

BY-PASS:

The make-up water temperature is controlled to be lower than 100°C, otherwise there could be steam in the pipes, damaging the components due to too high pressure.

For that reason has been installed a by-pass that reduce the hot water mass flow that supplies heat to the make-up water if the make-up water temperature is getting too high. The by-pass is composed of a diverter which splits the mass flows and a mixer that joins them after the heat exchanger. The diverter is regulated by a controller that calculates the maximum amount of hot water necessary to bring the make-up water to 100°C; if the hot water mass flow exceeds this limit it is split by the diverter, by-passing the heat exchanger, as shown in Figure 3.19.
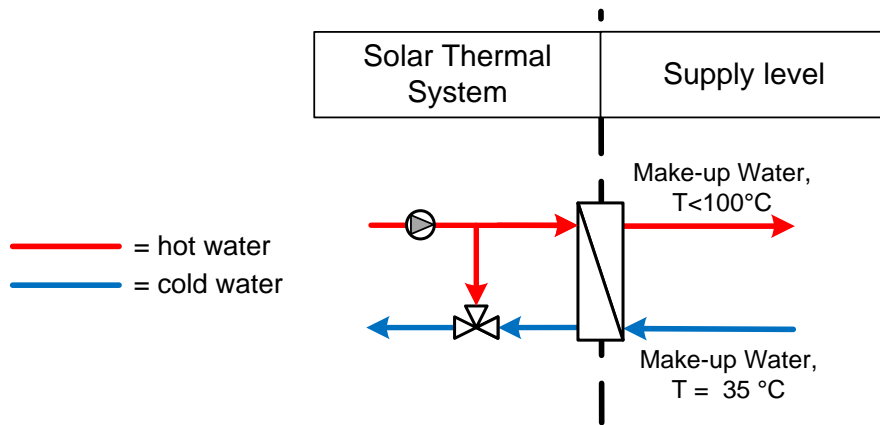
Figure 3.19. model of by pass

Another option would be to use of fresh water station, showed in Figure 3.20: it splits the cold water mass flow coming from the heat exchanger in order to regulate the temperature of the hot water flowing to the heat exchanger.
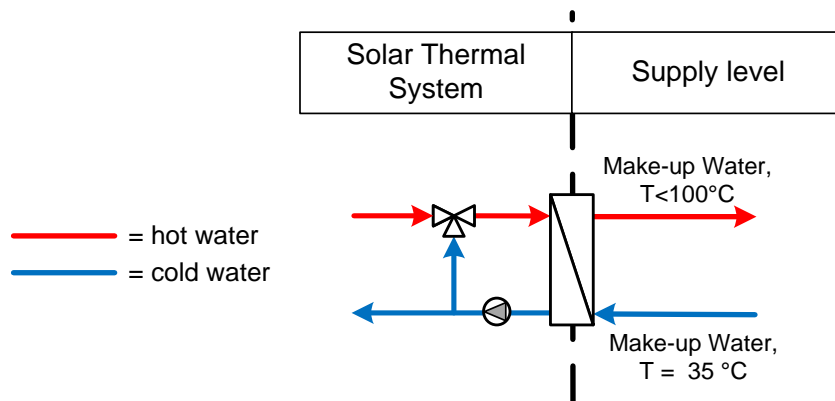
Figure 3.20. fresh water station

In such a system is the return temperature of the water stays constant, while using a by-pass it increases. This could be a problem in a stratified storage, where it has to be kept a temperature difference between the top and the bottom. Nevertheless this component is not required if the storage is not pressurized, since the maximal storage temperature is lower than the maximal make-up water temperature.

STORAGE:

The storage type is the same used in the steam network model, described in chapter 3.3.2.
The solar storage used in this configuration is not pressurized, because usually in the practise pressurized storage are too expensive for such a use. Therefore the temperature has to be kept under 95 °C.
A pre dimensioning of the storage is based on [7], choosing a volume of 50 l/m²$_{collector}$. Moreover the impact of the storage volume on the system performance will be discussed with an energetic analysis based on several simulations with different storage volume.
The heat loss coefficient $(U*A)_s$ of the storage is calculated as a function of the storage volume according to [11]:

$$(UA)_S = 0{,}16 * \sqrt{V_S} \tag{3.18}$$

where V_S is the storage volume [m³].

3.5 Modelling of solar heating of boiler feed water in ColSim

The third system configuration modeled in ColSim is a solar thermal system that pre-heats the boiler feed water before it enters the boiler.
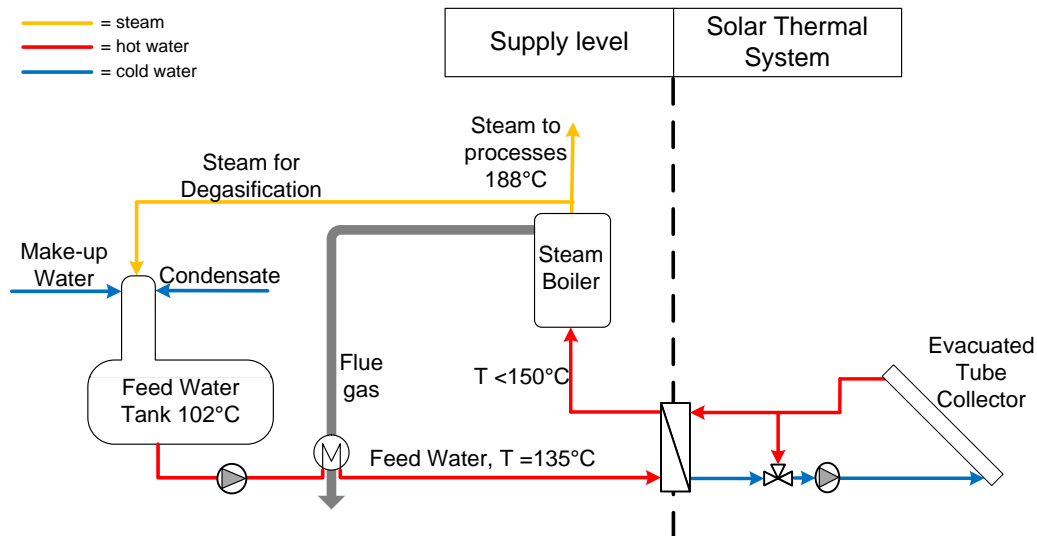
Figure 3.21. pre heating of boiler feed water after an economiser

As described in chapter 3.3, the boiler feed water flows from the feed water tank, where it is kept at 102°C and 1,2 bar, to the boiler, where it becomes steam at 188°C and 12 bar.

It is possible to pre heat this water between tank and boiler up to 150°C, since the pump can increase the pressure up to 5 bar. Higher temperature could decrease the performance of the boiler and therefore must be avoided.

There is an economizer that uses the flue gas from the boiler to pre heat the feed water, reaching around 135°C. This reduces the temperature gap for solar heating to 15 °C. Therefore this is not a very attractive integration point for solar process heat, since only a small temperature range supplied by the collectors can be used. Moreover the temperature level is quite high, so more expensive collectors are required to heat the fluid efficiently up to 150°C. In order to do that the collector must resist a pressure of 8-10 bar, in order to keep the water liquid with temperatures superior to 150°C, necessary for the heat exchange.

The model of this configuration is very similar to the one of the make-up water integration without storage, with the only difference that the heat exchanger is placed on the boiler feed water lines instead of on the make-up water lines. No storage is used, since it would be necessary to install an expensive pressurized storage. On the other hand this configuration without a storage is not feasible if there are discontinuous mass flows, as discussed in chapter 3.4.1 for the make-up water integration.

Also the components are the same of the previous model, using just evacuated tube collectors since with these temperatures flat-plate collectors would have a too low efficiency.

3.6 Modelling of direct steam generation in ColSim

The fourth configuration modelled in ColSim is the integration of the steam network presented in the chapter 3.3 with a solar thermal system that generates steam. It follows a description of the model, its components, control strategy and parameters.

3.6.1 Description of the model

As stated in chapter 2.3.2, steam generation has a share of around 90% of the total energy required by the steam network; for this reason this integration is the one with the highest quantitative potential, having the possibility to deliver far more energy than the others.

Direct steam generation means that the boiler feed water at 102°C enters in a collector field already at 12 bar and there evaporates; another possibility is to have a liquid in the collector field, for example thermo oil, and use it afterwards to evaporate the water in a heat exchanger. Within the frame of this thesis just direct steam generation will be investigated.

Since this integration has to produce steam at 188°C, concentrating collectors are required.
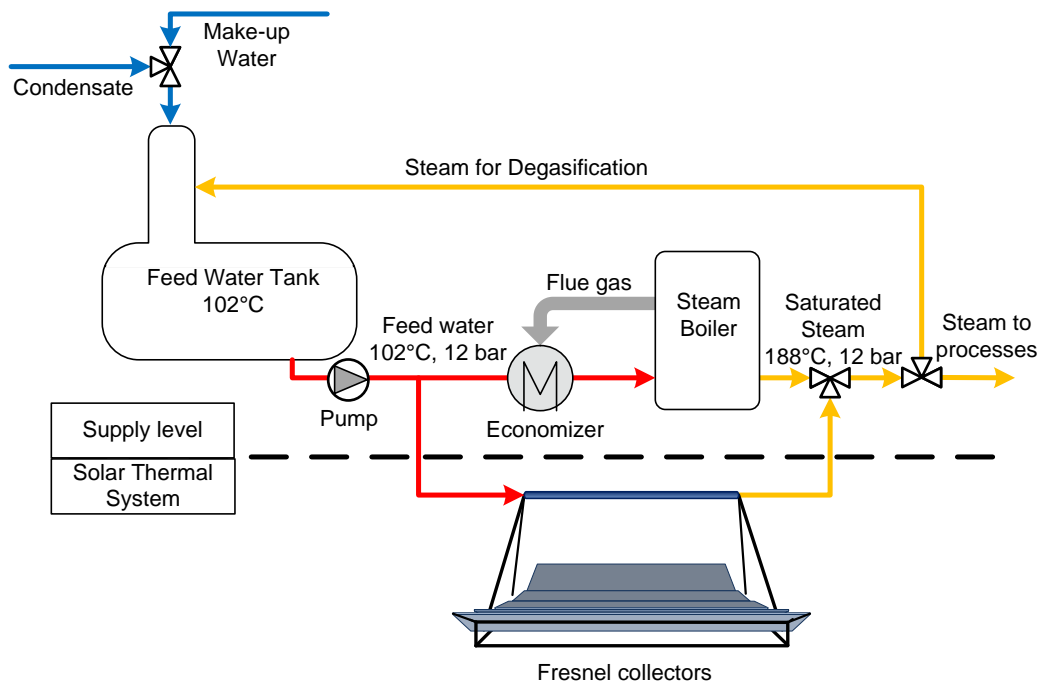
Figure 3.22. direct steam generation with Fresnel collectors

As shown in Figure 3.22, the solar integration point for steam generation is in parallel with the steam generation with the existent boiler. The total pumped mass flow remains unvaried, since it depends on the load demand, but it is split before the economizer sending to the solar field the amount of water that can be evaporated depending on available irradiation. After the boiler and the collector field, the two steam mass flows are mixed and sent to the processes.

It has to be remarked that such a model simplifies many aspect of direct steam generation: there is no drum that avoids water to flows in the steam line, pressure drops are neglected, transient state are not considered and is possible to varies freely the mass flow in the solar field, while in reality it should be kept constant or regulated very carefully . These simplifications are due to limit of ColSim.

3.6.2   Description of the components

COLLECTOR:

For this configuration is necessary to use linear concentrating collectors, in order to evaporate at 188 °C.

The type used in ColSim to model such collectors is different from the one utilized for stationary collectors, presented in chapter 3.4.3. The solar energy absorbed by the collector is calculated as in equation (3.19):

$$Q_{sun} = \eta_0 * A * K_{\tau\alpha} * G_{bt} \tag{3.19}$$

Where G_{bt} is the direct irradiation on the collector aperture area.
Energy losses have to be subtracted to the absorbed energy to find the solar energy gain. In linear focussed collector fields the so-called end losses must be considered: end losses are energy losses related to the irradiation of solar rays reflected by the end of the mirror line, missing the absorber.
Heat losses are calculated as in equation (3.15); the solar energy gain is then calculated subtracting the end losses and heat losses to the absorbed energy.

This type allows also setting a target temperature and steaming quality reached by the fluid at the outlet.
Since the outlet and inlet conditions of the fluid are known, as well as the gained energy, it is possible to calculate the steam mass flow that can be generated by the solar field. This information is used to control the diverter that splits the feed water. In that way in the solar field enters the amount of water that can be evaporated at 188°C and 12 bar and the boiler and solar field produce together the exact amount of steam needed.
If the solar energy gained is more than the energy required by the steam network, the mass flow that can be generated by the solar field is bigger than the entire feed water mass flow. In order to avoid superheating the mirrors are defocused, limiting the maximal power of the solar field.

The collector selected for the simulation is the Linear focusing Fresnel collector Industrial Solar LF11, characterized by the parameters shown in Table 3.2.

Table 3.2. parameters of the used concentrating collector

	η 0	a1	a2
Fresnel collector	0,635	0	0,00043

This collector has a lower optical efficiency than the stationary collectors; on the other hand it has much lower thermal losses, so that it is suitable for high temperature applications.
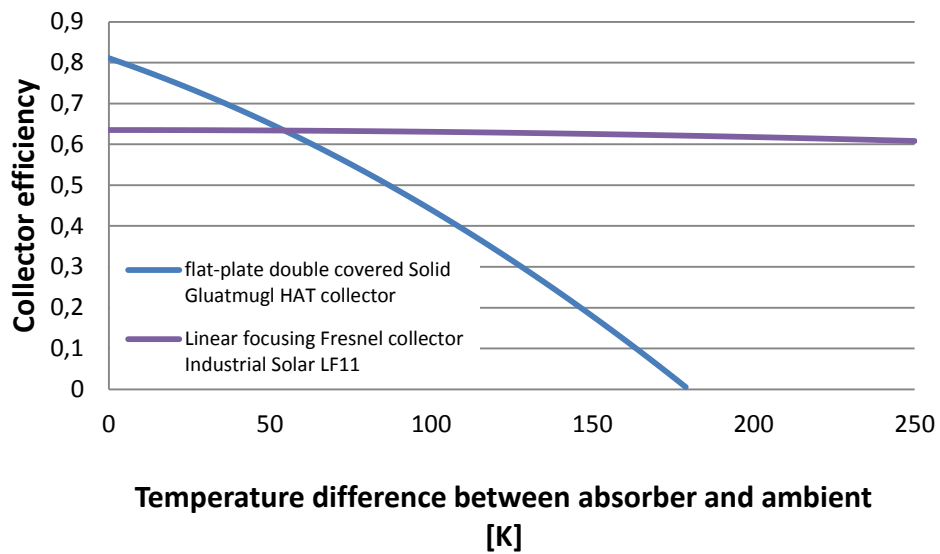
Figure 3.23. efficiency curve of Fresnel collector compared with flat-plate collector

As shown in Figure 3.24, each module of the collector is wide 7,5 meters and long 4,06 m; according to [29], the aperture surface of the primary collectors of one module is 22 m² and the minimum number of modules for a row is 8, so that the minimum aperture surface of a row is 176 m². This area has to be reduced to 169 m² since the usable length of the receiver is 96,2% of its total length [30].
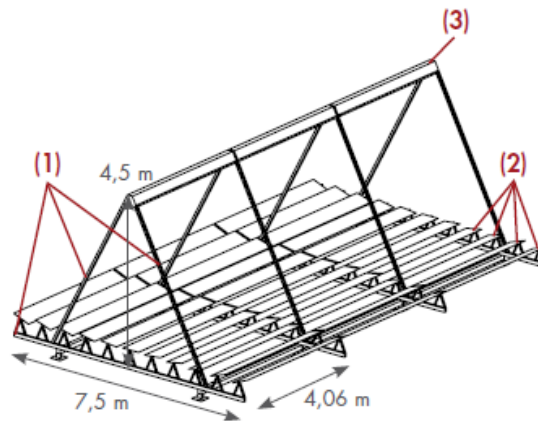
Figure 3.24. Industrial Solar linear Fresnel collector LF-11
1: support, 2: primary reflector, 3: receiver [29]

Since the collectors are usually placed on the top of the roof, that as geometrical constraints, the minimum number of modules has been chosen; on the other hand the shorter the rows the lower the efficiency of the collectors, because

every row has constant end losses due to missed absorption of the radiation reflected by the last mirrors, while the energy gained increase with the length of the row so that long row has in percentage lower end losses.

Several simulations with different number of collector rows are performed in order to compare solar thermal plants of different size.

3.7   General parameters

All the models developed in ColSim have some common features, described in this chapter.

3.7.1   Time Step

ColSim has been developed to allow running simulations with a short time step, which means with a short temporal discretization that can realistically represent the behaviour of the controllers. On the other hand the shorter the time step the longer last the simulation. So a compromise must be found.

Moreover many types in ColSim neglect the dynamic behaviour of the real component: for example the boiler is modelled with a heater type, which can change instantaneously the fluid temperature and has no thermal inertia.
The use of short time steps, on the order of the second, is not useful for a model that uses such types.

In the developing of the models it has been done a choice on what level of detail should have been kept: one possibility is to use types describing realistically the dynamic of the components, having a spatial discretization and solving the differential equations of the Plug Flow model; such a model would require a short time step. The other possibility is to use simpler types, as described above, and longer time steps. This last option implies the loss of a realistic description of the transient state of the system, but on the other hand requires much lower simulation time.

In conclusion it has been choice the second option, with a time step of 60 seconds, because of the complexity of the model that require around 100 minutes to accomplish an annual simulation.

3.7.2   Number of Nodes

Types that use the Plug Flow model described in chapter 3.1 are discretized spatially in n nodes, where n is a parameter chosen by the user. The more the

nodes the more accurate is the description of the component but the longer is the simulation time; therefore the pursued strategy is to run several simulations, decreasing the number of nodes until the output of the type start to change so that the minimum number of nodes that can give an accurate representation has been found.

3.7.3 Locations

Each simulation has been performed both in Würzburg (Germany) and Sevilla (Spain), showed in Figure 3.25.
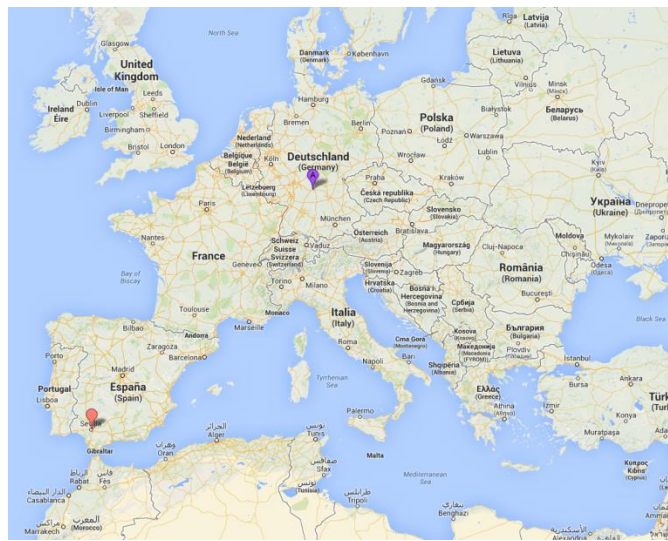
Figure 3.25. position of the selected sites

Würzburg has been chosen as representative German city, having a typical central European climate; the available irradiation during one year is shown in Figure 3.26.
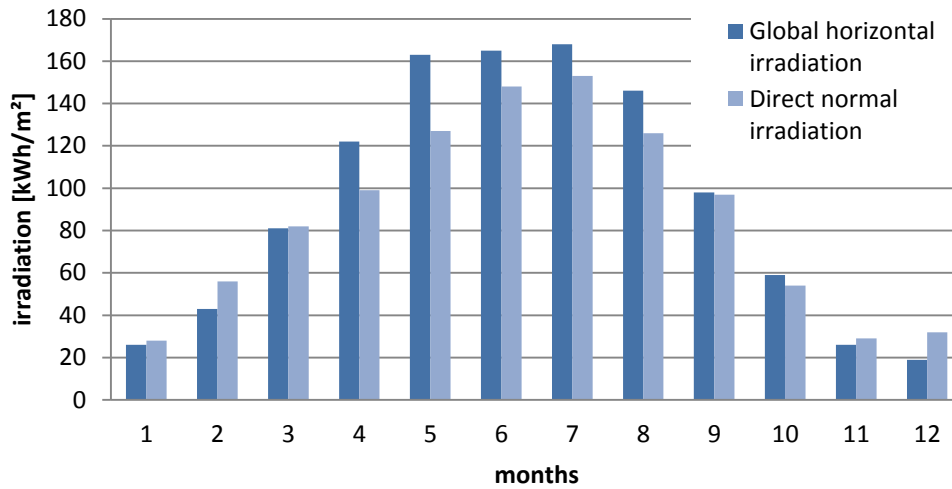
Figure 3.26. monthly irradiation in Würzburg [31]

Sevilla has been chosen as suitable location for steam generation, having direct normal irradiation uncommonly high for Europe. The available irradiation during one year is shown in Figure 3.27: the DNI is Sevilla appears to be more than double than the one in Würzburg.
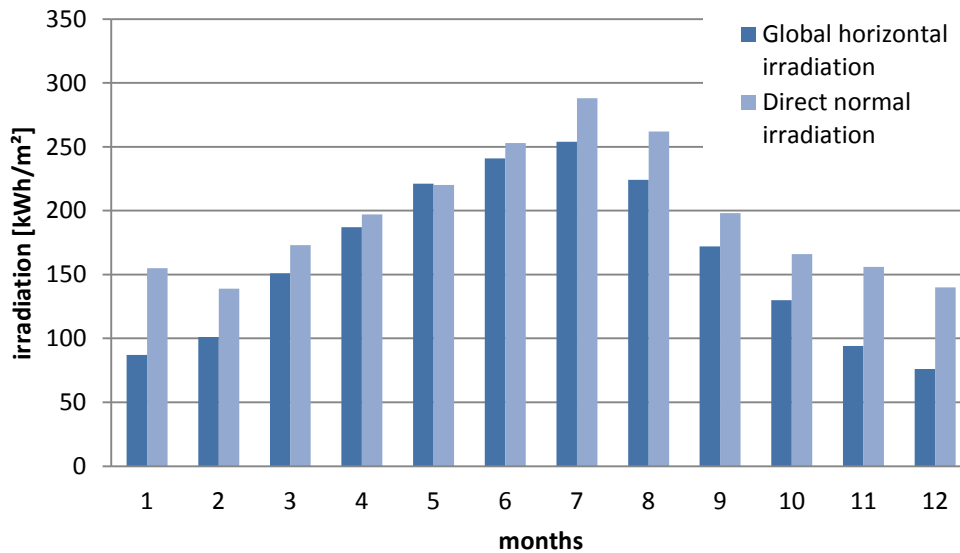
Figure 3.27. monthly irradiation in Sevilla [31]

3.8 Evaluation method

To optimize the configurations and compare the different integration points the results of annual simulations will be analyzed through energy and economic indicators.

3.8.1 Solar energy gained

The aim of the solar thermal integrations showed in chapter 3.4, 3.5 and 3.6 is to supply heat to the steam network described in chapter 3.3, reducing the amount of energy supplied by the boiler. Nevertheless the amount of solar energy gained is not a parameter that can alone determine if the installation of a solar thermal system is worthwhile or if the chosen configuration (i.e. collector aperture area, volume of the storage) is economically optimized, if costs related to the installation and operation of the solar thermal system are neglected. Therefore it will be used just to find the optimal collector slope, without changing the components installed and consequentially the investment costs.

3.8.2 Solar fraction

The solar fraction quantifies what percentage of the total heat demand is supplied with solar energy, as shown in equation (3.20).

$$SF = \frac{Q_{\text{solar energy gained}}}{Q_{\text{energy demand}}} \quad [\%] \tag{3.20}$$

This parameter gives an idea of the quantitative impact of a solar integration but is not an indicator of its economic convenience.

It can be used also a solar fraction on integration point, which quantifies what percentage of the heat that could be transferred in a specific integration point is supplied by solar energy. For example, for the make-up water pre heating the maximum temperature achievable is 100 °C; if the make-up water is always heated with solar energy to 100 °C, the solar fraction on this integration point would be 100 %.
This parameter gives an idea of how much the potential of the integration point is exploited but is not an indicator of its economic convenience.

3.8.3 System utilization

The system utilization quantifies what share of the available solar energy is gained by the solar thermal system, as shown in equation (3.21).

$$\text{system utilizaton} = \frac{Q_{\text{solar energy gained}}}{Q_{\text{solar avaialble}}} \quad [\%] \tag{3.21}$$

The higher the system utilization, the higher the amount of solar energy gained per square meter of collector aperture area.

3.8.4   Maximal cost of solar thermal system

A solar thermal system requires an initial investment to buy and install the components; moreover in the following years it requires maintenance and it consume electricity, but on the other hand it allows saving fuel and can be incentivized with subsidies for renewable energy. The sum of negative costs and positive benefits over one year is called cash flow CF.
To evaluate an investment, all the cash flows spread on the entire service life of the plant have to be discounted back to the present value as shown in equation (3.22), taking in account that a future cash flow have a lower present value due to interest, inflation and risk.

$$PV = \frac{CF_t}{(1 + i)^t} \tag{3.22}$$

where *PV* is the present value of the cash flow *CF* of the year *t* and *i* is the weighted average cost of capital.
The discounted cash flow can then be summed as showed in equation (3.23), obtaining the net present value of the investment at the year *N*:

$$NPV_N = \sum_{t=0}^{N} \frac{CF_t}{(1 + i)^t} \tag{3.23}$$

Usually an investment has a negative cash flow in the first year, due to the investment, and positive cash flow in the following years. Therefore the greater *N* the greater the *NPV* will be. If *N* is the service life of the plant, *NPV* is the total value of the investment. if it is positive the investment is supposed to give revenue, if it is negative will give losses and therefore is not recommended.

The payback period *PBP* is the time necessary to regain the initial investment, considering equation (3.23), it is the *N* at which $NPV_N = 0$.
The payback period is an interesting parameter because the longer the regain time the higher the risk of the investment; for that reason if the PBP of a plant is too long it is difficult to find investors.

In this case it has been set as a goal a *PBP* of 5 years, the maximum period of time that usually companies are disposed to wait [32] and it has been calculated in excel how high should be the plant costs per square meter of collector area to be repaid in such a *PBP*; within this thesis this cost will be called "maximal feasible cost of a solar thermal system" or $C_{mf.}$ [€/m²$_{collector}$]

This analysis has been done considering the following benefits and costs:

- Gas saved: Output of the simulation in [kWh/y]
- Cost of natural gas: 0,0569 [€/kWh] in Germany, 0,0456 [€/kWh] in Spain [33]
- Investment costs: result; initially given as hypothesis in [€]
- O&M costs: 1% * Investment costs [€/y] [34]
- Electricity consumed by the solar thermal plant: 2% * Gas spared [kWh/y] [34]
- Cost of natural gas: 0,1879 [€/kWh] in Germany, 0,1482 [€/kWh] in Spain [33]
- Interest rate: 8%

The cash flow of every year has been calculated as sum of positive profits (gas saved [€/y]) and negative costs (investment costs, O&M costs, electricity costs [€/y]).

No subsidy has been considered at first to state if this price is realistically achievable or what subsidies are required to make it competitive. Moreover no increase of price of natural gas or electricity has been considered because it is difficult to foresee their future trends; it is also interesting to see if the collector price is sustainable with the actual energy prices.

Table 3.3 show an example of economic analysis in Würzburg, with amount of gas spare every year = 5000 kWh/y. The goal is to reach a PBP = 5 years (NPV = 0 at the 5th year) and is reached changing the investment cost on the first year. This result, highlighted in yellow, is then divided by the collector area, obtaining the $C_{mf.}$ [€/m²$_{collector}$] that repays the solar thermal system in 5 years.

Table 3.3. example of economic analysis; gas and electricity german price, gas spared = 5000 kWh/y

year	C inv	o&m costs	el. costs	gas cost	CF	PV	NPV
[y]	[€]	[€/y]	[€/y]	[€/y]	[€/y]	[€/y]	[€/y]
1	-1114,97	-11,15	-14,78	284,50	-856,40	-856,40	-856,40
2	0,00	-11,15	-14,78	284,50	258,57	239,41	-616,99
3	0,00	-11,15	-14,78	284,50	258,57	221,68	-395,31
4	0,00	-11,15	-14,78	284,50	258,57	205,26	-190,05
5	0,00	-11,15	-14,78	284,50	258,57	190,05	0,00
6	0,00	-11,15	-14,78	284,50	258,57	175,98	175,98
7	0,00	-11,15	-14,78	284,50	258,57	162,94	338,92
8	0,00	-11,15	-14,78	284,50	258,57	150,87	489,79

Since this analysis is based on hypothesis on future natural gas and electricity costs as well as discount rate, is necessary a sensitivity analysis on these assumptions.

3.9 Summary of the integration points modelled

Table 3.4 shows a summary of the features of the integration points modelled.

Table 3.4. summary of the modelled integration points

	T range [°C]	fluid [-]	collector [-]	storage [-]
make-up water	35 - 102	water	flat plate	no
make-up water + storage	35 - 95	water	flat plate	yes
feed water	135 - 150	water	evacuated tube	no
steam generation	102 - 188	water, steam	linear Fresnel	no

Chapter 4

Results

This chapter describes the results of the simulations performed in ColSim with the models illustrated in chapter 3.

4.1 Aim of the simulations

The goal of this thesis is to evaluate the potential of solar thermal integrations in a steam network. To do that several simulations have been performed with the models of the different integration points described in chapter 3.4, 3.5 and 3.6. In particular collector slope (for stationary collectors), collector aperture area and volume of the solar storage have been varied.
The results have been analyzed with the indicators described in chapter 3.8 in order to find which are the most worthwhile configurations and if they are feasible under the economical assumption considered.

4.2 Validation of the models

The models described in chapter 3.3, 3.4, 3.5 and 3.6 have to be validated, to proof that the results of the simulation performed with these models are trustworthy.

4.2.1 Validation of the steam network model

As described in chapter 3.3, in the steam network model the temperatures of the processes and of the feed water tank are measured and sent to a PID controller in order to produce the required amount of steam.
It is therefore necessary to check if the control works properly, that means if the temperatures are reached quickly, without offsets and oscillations. In order to do that it is necessary to tune the PID controller. It is required an integral term to have a positive control signal, described in equation (3.13), also when the error signal described in equation (3.12) is null.
Particular attention has been given to the validation of the closed load, because the presence of a heat exchanger causes a time delay in the answer of the process and this make the tuning more difficult. In the open process and in the feed water tank the steam is instead mixed with water and therefore the temperatures are reached instantaneously.

Figure 4.1 shows the validation of the closed load. The steam mass flow, the process temperature and the condensate temperature are represented in a complete working day, from 06:00:00 to 16:00:00.
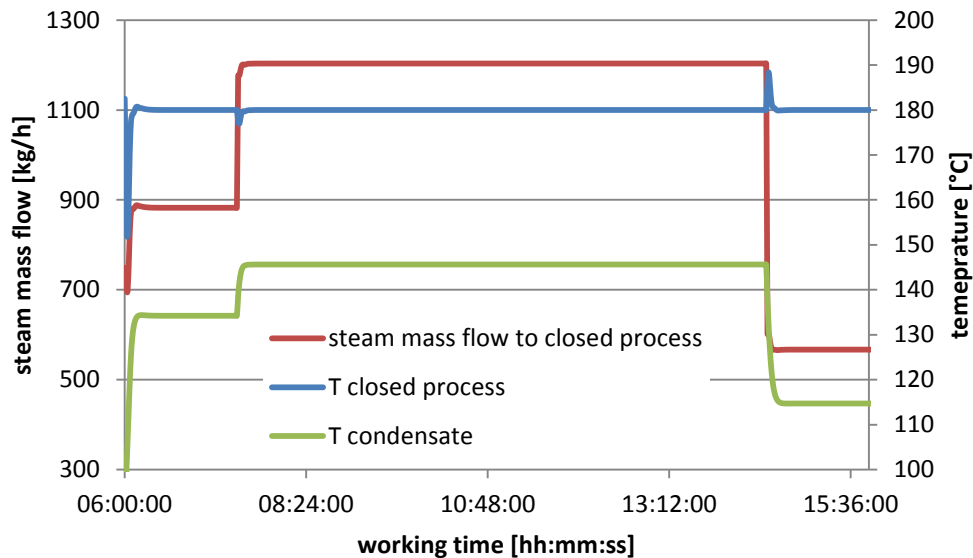
Figure 4.1. validation of the closed load: steam mass flow, process temperature and condensate temperature after the heat exchanger

The closed process temperature (180 °C) is reached and kept steady, as required. Oscillation are registered at the beginning, at 07:30:00 and at 14:30:00, when the load mass flow change and the generated steam mass flow has to be adapted to the new situation: at the beginning of the working day, when the load is switched on, 8 minutes are required to reach a steady temperature of 180°C; at 07:30:00 the load temperature decrease to 177°C and comes back to a constant value of 180°C in 3 minutes; at 14:30:00 the load temperature reaches 186°C and comes back to a constant value of 180°C in 4 minutes.

It is interesting to notice that the condensate outlet temperature changes when the heat required by the load varies, even if the steam mass flow is adapted. In particular the higher the load mass flow the higher the condensate temperature.
The reason of this trend is that in ColSim the overall heat transfer coefficient *U* and the heat exchanger surface *A* of the heat exchanger type are constant. The heat exchanger type transfers heat according to equation (3.11): this means that the amount of heat exchanged varies just as a function of the temperatures of the nodes.
On the other hand, if for example the mass flow decreases but the temperatures of the nodes remains initially the same (because of thermal inertia), there is less

mass of fluid for the same amount of heat exchanged and therefore the difference of specific enthalpy of each fluid increases.

After a transient state the node temperatures will get closer, reducing the amount of heat exchanged, according to the process heat demand.

The overall heat transfer coefficient of a real heat exchanger doesn't remain constant if there is a partial load, but decrease [35]:

$$U = \frac{1}{\frac{1}{h_i} + \frac{1}{h_o}} \qquad (4.1)$$

Where h_i and h_o are the internal and external heat transfer coefficients; h_i can be estimated with the following equations:

$$Re_D = \frac{4\dot{m}_D}{\pi D_i \mu} \qquad (4.2)$$

$$Nu_D = 0.023 * Re_D^{4/5} * Pr^{0.4} \qquad (4.3)$$

$$h_i = Nu_D * \frac{k}{D_i} \qquad (4.4)$$

Equation (4.2) is valid for flow in circular tubes and states that the Reynolds number Re_D is proportional to the mass flow; the Dittus-Boelter equation (4.3), valid for turbulent flow in circular tubes, and equation (4.4) show that if the mass flow and therefore Re_D decrease also the Nusselt number consequentially h_i and U decrease.

The fact that U is considered constant in ColSim is an assumption that simplifies the system but produce a deviation from reality. Nevertheless this has no effect on the main result of the simulation, which is the calculation of the amount of steam generated by the boiler: thanks to the flashing of the condensate, all the sensible heat over 100°C present in the condensate is supplied to the open process. This means that properties of the condensate before coming back to the feed water tank are always constant and therefore the generated steam mass flow doesn't depends on the condensate temperature at the outlet of the heat exchanger.

The open load and the tank have target temperatures of 70°C and 102°C respectively, which are reached by mixing steam with water. Theirs temperature trend are shown in Figure 4.2.
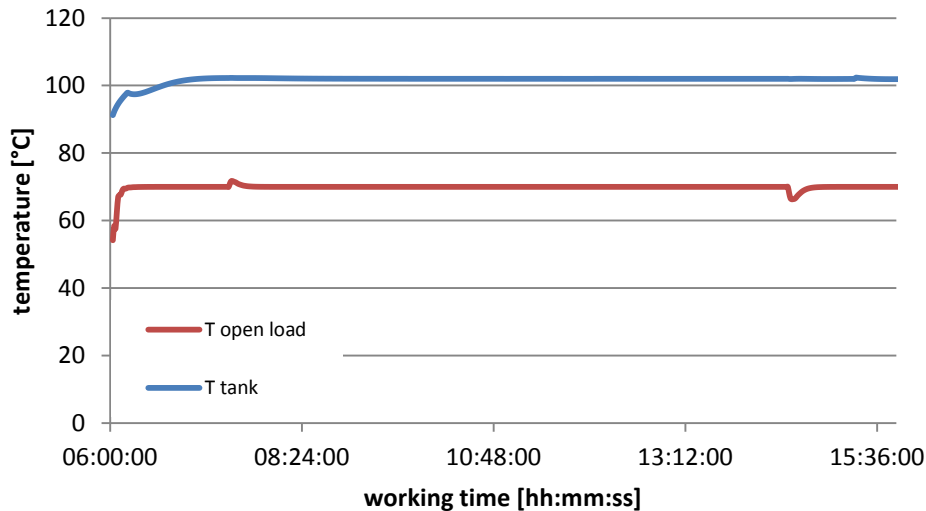
Figure 4.2. validation of the open load and feed water tank: measured temperatures

Table 4.1 gives an overview of the results described before; it is interesting to notice that the steam mass flow to the open load doesn't follow exactly the open load mass flow reduction when there is partial load. This is because there is less flash steam production from the condensate at lower temperature and therefore more steam in percentage is required from the boiler, according to what explained above.

Moreover it has to be remarked that the steam mass flow directed from the boiler to the open process is just 15% of the total generated steam. The open load receives actually a higher mass flow, corresponding to 20% of the generated steam, because of the introduction of flash steam.

Table 4.1. measured temperatures and steam mass flows

| load | FEED TANK | | CLOSED LOAD | | | OPEN LOAD | |
| | T | steam | T | steam | T cond | T | steam |
[%]	[°C]	[kg/h]	[°C]	[kg/h]	[°C]	[°C]	[kg/h]
75	101,98	50,49	180,00	882,56	134,24	70,00	193,62
100	102,00	62,01	180,00	1203,31	145,64	70,00	231,61
50	102,12	30,63	180,00	567,13	114,73	70,00	150,35

Other types used in this model such as throttles, heaters, diverters and mixers just change the fluid properties as required by the user, so that their output is not a variable but a parameter of the simulation. It has nevertheless been necessary to check if all these types work as required and follow their control strategy. In particular the parameters that have been checked are temperature, pressure and mass at the input and output of each type.

An additional validation of the model has been performed using energy balances.
A first balance has been done on the feed water tank: as shown in Figure 3.10, the tank has two inlet mass flows (cold water and steam) and hot water as the outlet. Moreover there are heat losses. An energy balance has been done adding these four energy fluxes calculated during one year, neglecting the variation of energy stored in the tank since it is ideally kept at constant temperature around 102°C .
As shown in Table 4.2, the annual energy balance on the feed water tank gives an error of 0,02%.

Table 4.2. annual energy balance on the feed water tank

inlet water [MJ]	steam [MJ]	outlet water [MJ]	heat losses [MJ]	energy balance [MJ]	error [%]
18106	6755	24641	215	-4,07	0,02%

A global energy balance checks if the heat incoming in the system, supplied by the boiler, is the same amount of energy outgoing because of the heat demand of the load, the heat losses in the header types and the heat wasted in the outlet mass flow from the processes.
As shown in Table 4.3, the global annual energy balance gives an error of 0,04%.

Table 4.3. annual global energy balance, steam network in Sevilla

boiler [MWh]	demand [MWh]	heat losses [MWh]	wasted heat [MWh]	energy balance [MWh]	error [%]
2271	2170	6	95	-1	0,04%

It has to be noticed that the wasted heat includes heat losses on the condensate line that cools the condensate to 90°C. These heat losses have been modeled with a cooler type but in reality they happen in pipes.

4.2.2 Validation of the water pre heating without a storage model

The stationary collector performances have been checked. In order to do that it has been utilized a simple model of a collector field located in Sevilla having 100 m² of collector aperture and a constant mass flow of 800 kg/h at constant inlet temperature of 20°C. This model is shown in Figure 4.3.
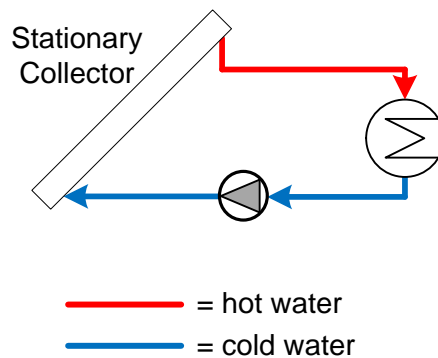
Figure 4.3. model for the validation of stationary collector

The $K_{\tau\alpha}$ is calculated by ColSim interpolating data from a table given by the producer.
In Figure 4.4 are shown the $K_{\tau\alpha}$ calculated by ColSim, in red, and the original data, in green given just for positive angle: they are correctly calculated.
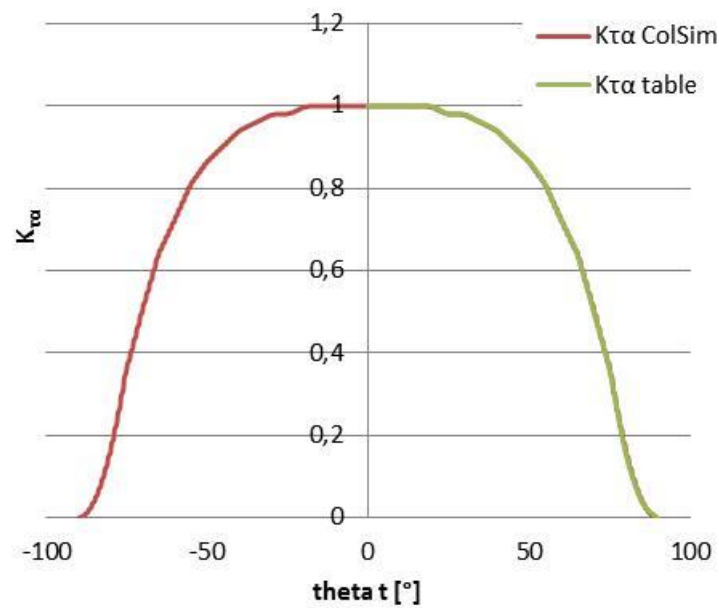
Figure 4.4. $K_{\tau\alpha}$ **as a function of theta transversal: comparison between the results in ColSim and the real data**

The energy fluxes of the collectors have been calculated in Excel according to equations (3.14) and (3.15), using as input the ambient and mean temperature given by the simulation in ColSim; the results have been compared with the output of the simulation in ColSim, has shown in Table 4.4, in order to validate the collector code

Table 4.4. comparison between the results of ColSim and excel calculations

	Q absorbed [kWh]	Q losses [kWh]
ColSim	1613	472
Excel	1613	472
error	0,00%	0,00%

The other types of this model are a pump, a heat exchanger and a header, in addition to the steam network validated in chapter 4.2.1: it has been checked temperature, pressure and mass flow in order to assure that they operate as

expected. In particular it has been checked that the make-up water temperature doesn't exceed 100 °C.

Moreover it has been validated the control strategy of the collector pump. In particular it has been checked that there is a mass flow in the collector if and only if solar energy can be used and transferred to the process.

As shown in Figure 4.5, the collector mass flow is positive between around 8:30 am (point A) and 16:00 pm (point B). As shown in Figure 4.6, point A is when the outlet collector temperature is 20°C higher than the make-up water temperature, so that heat can be supplied to the process (it has been set a high limit to avoid oscillating behaviour of the collector pump); point B is when there the make-up water mass flow stop and therefore also the collector mass flow has to be stopped; all the radiation out of this period is not exploited, reducing the collector utilization.

Moreover during the weekend the processes are not working, so that all the available solar energy is wasted.
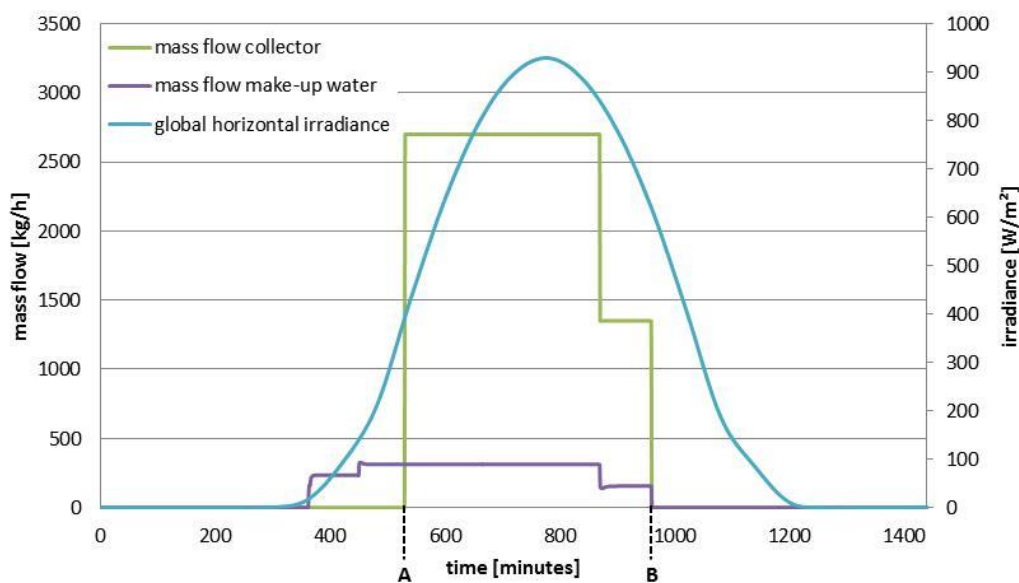
Figure 4.5. daily trend of collector mass flow, make-up water mass flow and available irradiance; simulation performed the 2nd of July in Sevilla, collector surface 40m²
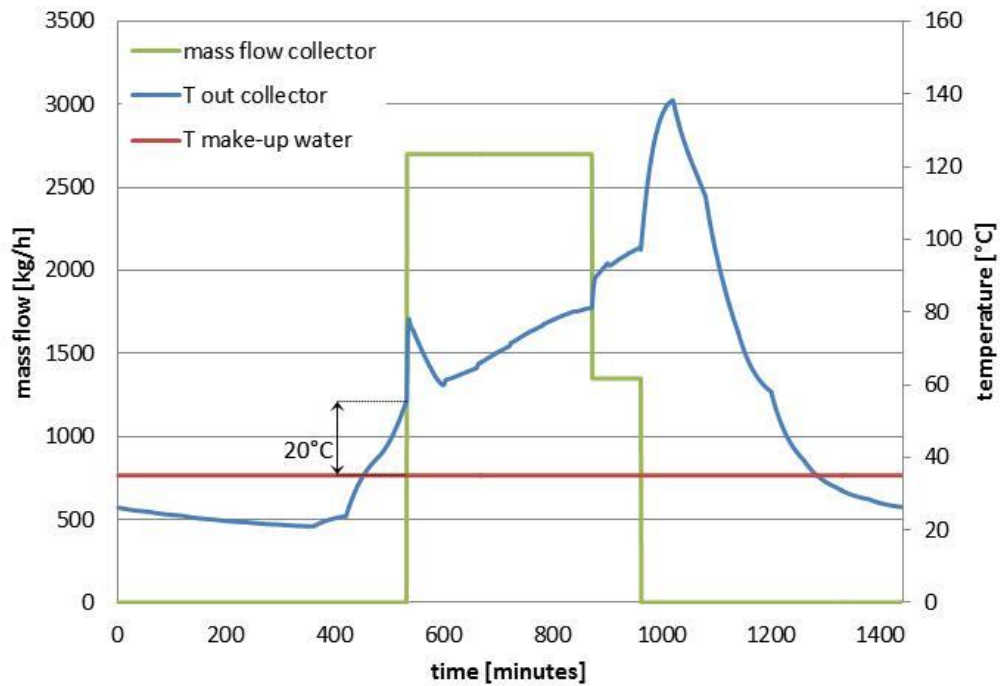
Figure 4.6. daily trend of collector outlet temperature, make-up water temperature and collector mass flow; simulation performed the 2nd of July in Sevilla, collector surface 40m²

At last energy balances have been performed.

As shown in Figure 3.16, the solar thermal system gains heat in the collector and then delivers it to the make-up water; moreover there are heat losses in the pipes. It has been performed an energy balance along one year, summing these three energy fluxes, as shown in Table 4.5.

As shown in Table 4.5, the annual energy balance on the collector loop gives an error of 0,09%.

Table 4.5. annual energy balance on collector loop in Sevilla, collector surface = 60 m²

collector gains [MWh]	heat supplied [MWh]	heat losses [MWh]	energy balance [MWh]	error [%]
21	21	0,2	0	0,09%

A global energy balance checks if the heat incoming in the system, supplied by the solar thermal system and the boiler, is the same amount of energy outgoing because of the heat demand of the load, the heat losses and the heat wasted in the outlet mass flow from the open load:

As shown in Table 4.6, the global annual energy balance gives an error of 0,05%.

Table 4.6. annual global energy balance, make-up water integration in Sevilla, collector surface = 60 m²

collector [MWh]	boiler [MWh]	demand [MWh]	heat losses [MWh]	wasted heat [MWh]	energy balance [MWh]	error [%]
21	2251	2170	6	95	1	0,05%

4.2.3   Validation of the water pre heating with a storage model

The collector type has been already validated in chapter 0. Other types of this model are pumps, heat exchangers, header and a storage, in addition to the steam network validated in chapter 4.2.1: it has been checked the mass flows, pressure and temperatures at the inlet and outlet of each type, in particular it has been proofed that the storage never gets hotter than 95 °C.

It has been validated the control strategy of the pumps. At first it has been checked that there collector pump works if and only if solar energy can be gained and transferred to the storage.

As shown in Figure 4.7 and Figure 4.8, the storage mean temperature slightly decreases during the night because of heat losses. At 6 pm, when a make-up water mass flow is available, the storage temperature is high enough to supply heat to the make-up water: the storage is discharged and its temperature drops. When the collector is hot enough it starts to charge the storage, so that the storage temperature increases. At the end of the day no more solar heat is available and the storage temperature decreases again due to heat losses.
The storage discharging mass flow and the make-up water mass flow are the same. This means that, thanks to the storage, the make-up water is pre-heated during all the working hours, longer than with the previous integration shown in Figure 4.5.
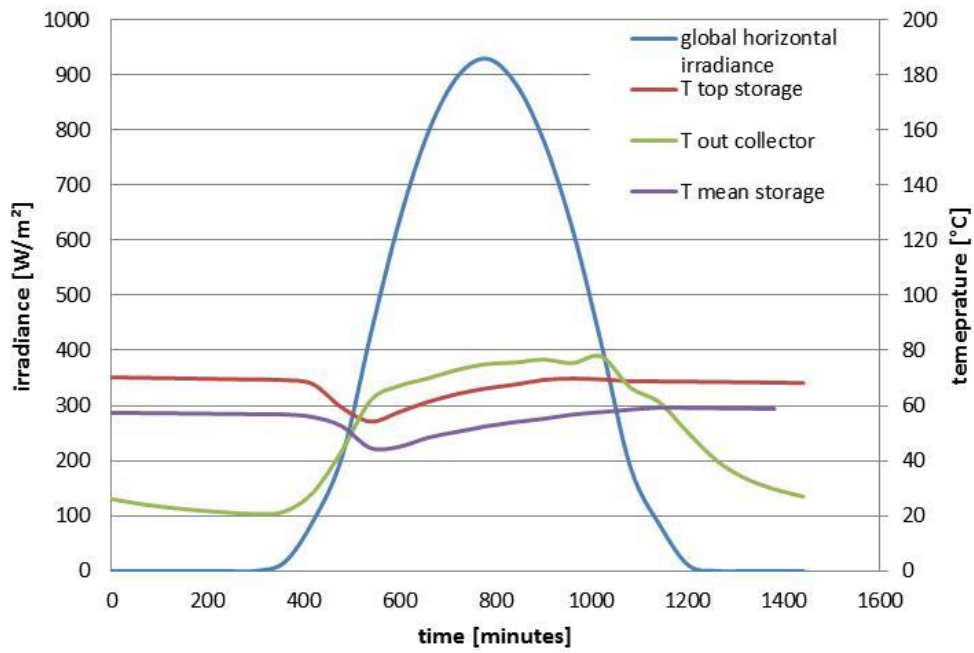
Figure 4.7. charging of the solar storage; simulation performed the 2nd of July in Sevilla, collector surface 20m², storage volume 50 m³/m² collector
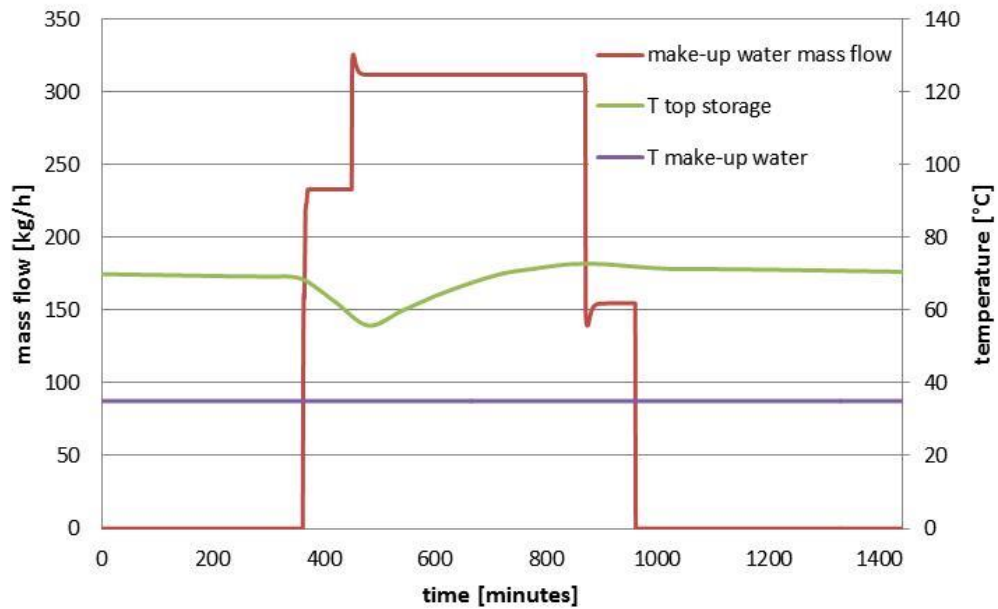
Figure 4.8. discharging of the solar storage; simulation performed the 2nd of July in Sevilla, collector surface 20m², storage volume 50 m³/m² collector

At last energy balances have been performed.
Collector loop: As shown in Figure 3.17, the solar thermal system gain heat in the collector and then delivers it to the storage; moreover there are heat losses in the pipes. It has been performed an energy balance along one year, summing these three energy fluxes, as shown in Table 4.11.

Table 4.7. annual energy balance on collector loop in Sevilla, collector surface = 50 m²

collector gains [MWh]	heat supplied [MWh]	heat losses [MWh]	energy balance [MWh]	error [%]
37	37	0,3	0	0,01%

As shown in Table 4.11, the annual energy balance on the collector loop gives an error of 0,01%.

Solar storage: as shown in Figure 3.17, the tank is charged by the collector and discharged by the make-up water using two heat exchangers. Moreover there are heat losses. An energy balance has been done adding these three energy fluxes calculated during one year, neglecting the variation of energy stored in the tank
As shown in Table 4.8, the annual energy balance on the feed water tank gives an error of 0,25%.

Table 4.8. annual energy balance on the solar storage, storage volume 50 m³/m² collector

charging heat [MJ]	discharging hea [MJ]	heat losses [MJ]	energy balance [MJ]	error [%]
36559	32737	3730	91	0,25%

A global energy balance checks if the heat incoming in the system, supplied by the solar thermal system and the boiler, is the same amount of energy outgoing because of the heat demand of the load, the heat losses and the heat wasted in the outlet mass flow from the open load: as shown in Table 4.9, the global annual energy balance gives an error of 0,00%.

Table 4.9. annual global energy balance, make-up water integration with storage in Sevilla, collector surface = 50 m²

collector [MWh]	boiler [MWh]	demand [MWh]	heat losses [MWh]	wasted heat [MWh]	energy balance [MWh]	error [%]
37	2239	2170	11	95	0,5	0,00

4.2.4   Validation of the direct steam generation model

The integration on direct steam generation consists of a diverter, a mixer and a linear Fresnel collector field, in addition to the steam network validated in chapter 4.2.1.

The linear concentrating collector type has been validated. The solar energy gained has been calculated in excel, knowing fluid enthalpies and mass flow (provided by ColSim), and has been compared with the results of the simulations performed in ColSim.

Table 4.10. comparison between the results of ColSim and excel calculations; simulation performed the 2nd of July in Sevilla, 10 rows of linear Fresnel collectors

	Q_{gained} [kWh]
ColSim	6127
Excel	6116
error	0,18%

It has been validated that the collector generates only saturated steam at 12 bar and 188°C.

In order to do that, the diverter must split the exact mass flow that can be evaporated with the solar energy gained in the time step (no mass or energy is stored in this collector model). Moreover, if the solar field could generate more steam than required by the processes, the primary reflectors are defocused and the collector mass flow is reduced to the amount required by the processes.

Figure 4.9 shows that the steam is always generated with the required properties. Figure 4.10 shows that as soon as DNI is available, saturated steam at 188°C is generated. The collector mass flow increases with the DNI. After 14:30 the steam network operates at partial load and therefore less energy is required: the

solar field is defocused in order to supply the exact amount of energy required for steam generation (the boiler doesn't provide energy at this moment). After 16:00 no solar energy is exploited because there is no heat demand.
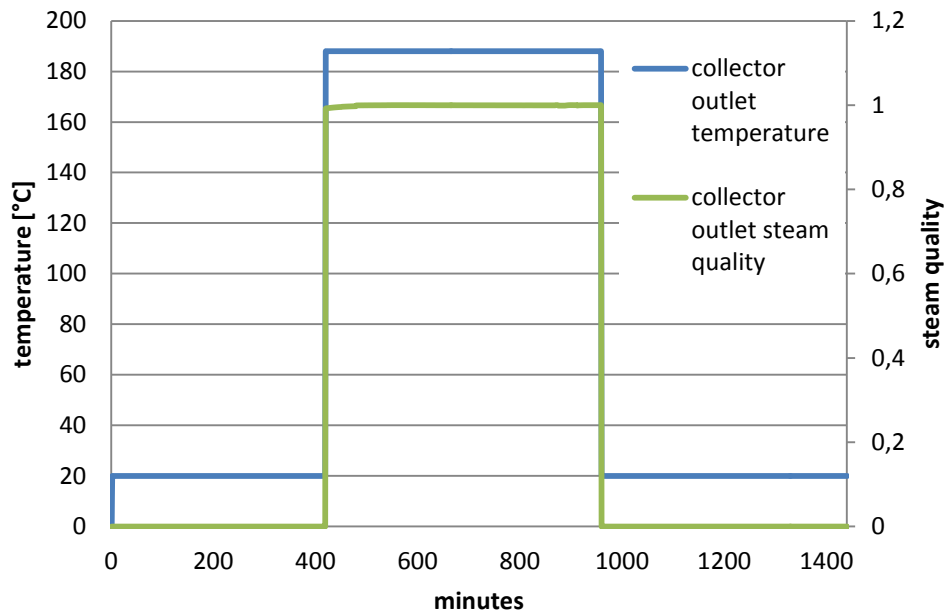
Figure 4.9. daily trend of collector outlet temperature and steam quality
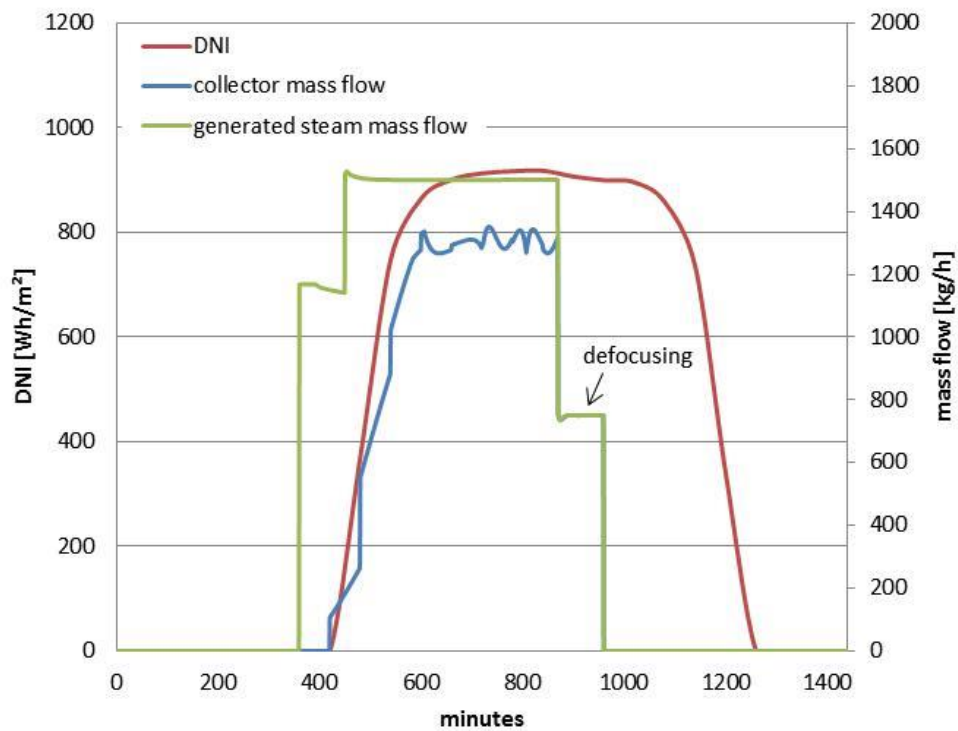
Figure 4.10. daily trend of DNI, collector mass flow and generated steam mass flow; simulation performed the 2nd of July in Sevilla, 10 rows of linear Fresnel collectors

As in the previous case, it has been done a global energy balance.

Table 4.11. annual global energy balance, direct steam generation in Sevilla

collector [MWh]	boiler [MWh]	demand [MWh]	heat losses [MWh]	wasted heat [MWh]	energy balance [MWh]	error [%]
673	1598	2267	6	95	-1	0,05%

As shown in Table 4.11, the global annual energy balance gives an error of 0,05%.

4.3 Results

In this chapter are shown the results of the simulations performed.

Collector slope, collector aperture area and solar storage volume have been varied, in order to evaluate different configurations. In particular:

- the collector slope has been changed with a resolution of 5° from from 15° to 40°
- the collector aperture area for flat plate collectors has been changed with a resolution of 5 m² from 5 m² to 50 m²
- the collector aperture area for linear Fresnel collectors has been changed with a resolution of 338 m², corresponding to 2 collector rows, from 2 rows to 16 rows
- the storage volume has been changed with a resolution of 15 l/m² from 50 l /m² to 95 l /m²

The simulations will show which configuration is the most efficient between the ones simulated.

4.3.1   Results of the pre heating of make-up water without storage model

At first the optimal collector slope was investigated. Then several simulations have been performed, changing the solar field area. As described in chapter 3.8.4, the solar energy gains have been used in an economic analysis in excel to calculate the solar thermal system cost C_{mf} that would give a PBP of 5 years with such a system, for each collector area: this means that every solar thermal system that cost less than this price will be repaid in less than the PBP, and can therefore be an attractive choice for investors.
All the simulations have been performed both in Sevilla and in Würzburg.

Simulations with collector slope from 15° to 40° have been performed in order to find the optimal slope angle for flat-plate collectors. The simulations have been performed with a collector area of 40 m², value chosen according to the pre-dimensioning indicated in [7].

The slope that maximizes the solar energy gain is 20 ° in Sevilla and 35° in Würzburg.

Figure 4.11 and Figure 4.12 show the performances of this configuration as a function of the collector area.

The solar fraction on the integration point increases along with the collector area, since more energy is gained. The solar energy gain per square meter of collector aperture has an optimum: this because the larger the areas the more frequent will stagnation happen, wasting solar energy and therefore reducing the efficiency of the solar thermal system. On the other hand too small collector

areas are also less efficient because the heat losses of the pipes that go from the solar field to the steam network are kept constant in the simulations and therefore are in percentage more relevant if the solar field is small.
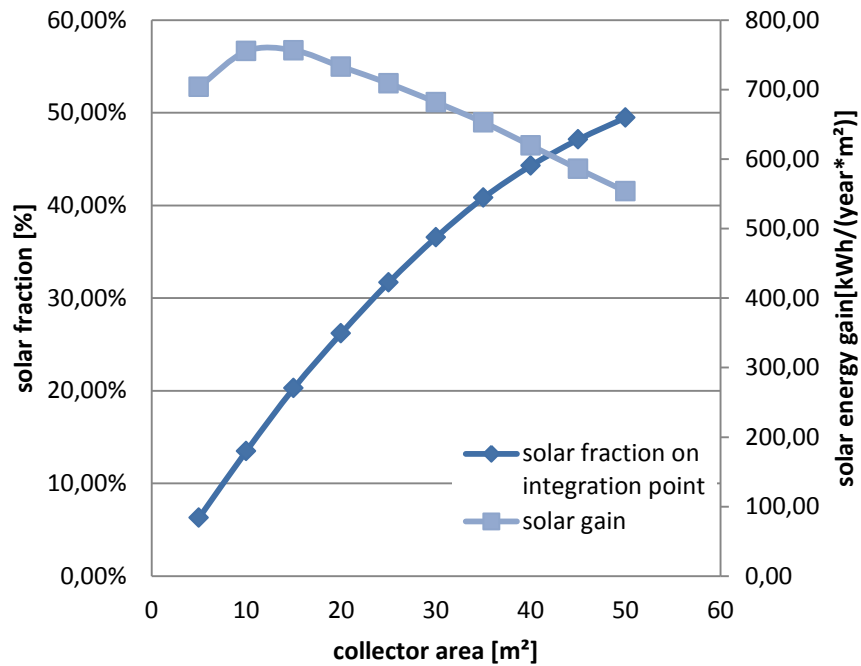
Figure 4.11. solar fraction and solar energy gains of make-up water pre heating with flat plate collectors in Sevilla
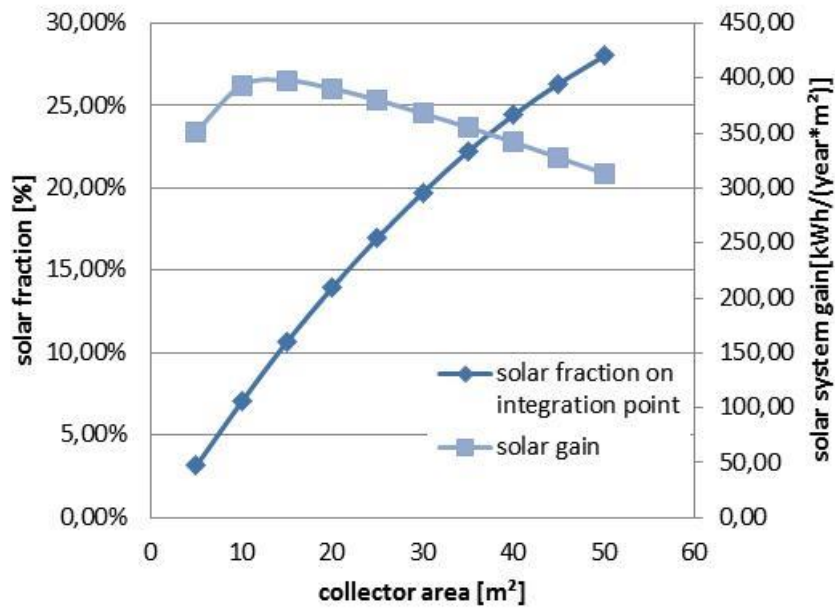
Figure 4.12. solar fraction and solar energy gains of make-up water pre heating with flat plate collectors in Würzburg

Table 4.12 and Table 4.13 shows the performance of the most efficient configuration (15 m²)

Table 4.12. performance of flat-plate collectors for water pre heating in Sevilla

collector aperture area [m²]	system utilization [%]	solar fraction [%]	solar fraction on integration point [%]	solar energy gains [kWh/year*m²]
15	33,46%	0,50%	20,27%	756

Table 4.13. performance of flat-plate collectors for water pre heating in Würzburg

collector aperture area [m²]	system utilization [%]	solar fraction [%]	solar fraction on integration point [%]	solar energy gains [kWh/year*m²]
15	30,93%	0,26%	10,67%	398

Figure 4.13 and Figure 4.14 show the cost that the solar thermal system should have to be repaid in 5 years, with the assumption described in chapter 3.8.4.
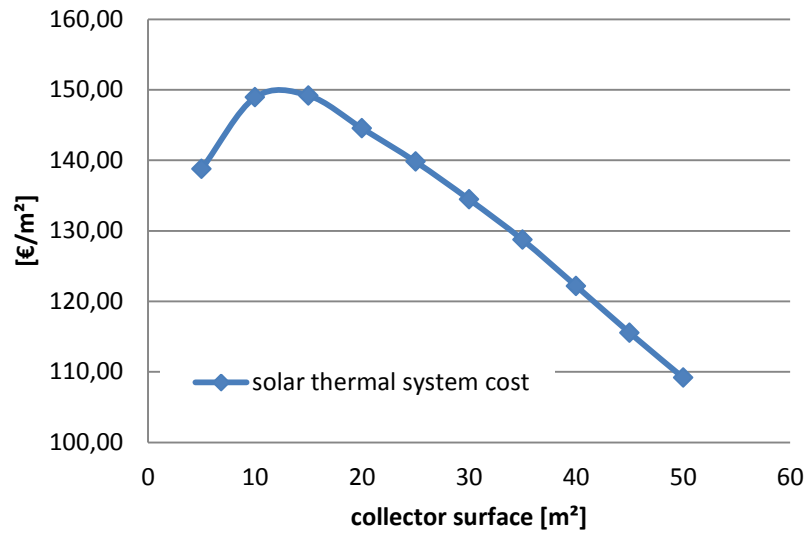
Figure 4.13. maximal feasible solar thermal system cost in Sevilla
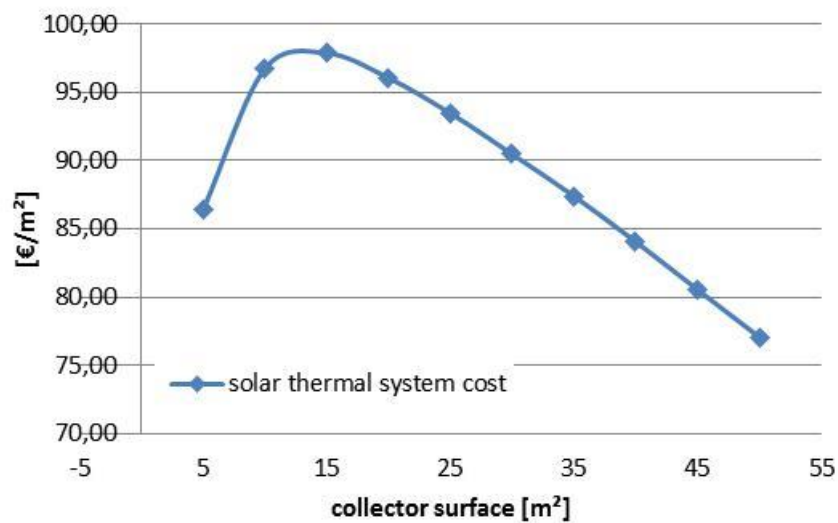
Figure 4.14. maximal feasible solar thermal system cost in Würzburg

The solar thermal system is affordable if it costs less than 150 [€/m²] in Sevilla and 98 [€/m²] in Würzburg.

4.3.2 Results of the pre heating of make-up water with storage model

A solar thermal system without a storage cannot exploit the solar irradiation available when there is no heat demand. It has been calculated the amount of irradiation post processing the simulation results in excel: in this integration point, with the load profile chosen, the not exploited irradiation amounts to 29,94 % of the annual incident global irradiation in Würzburg and to 30,82 % in Sevilla.
It is therefore interesting to calculate to what extent a storage can improve the performance of the solar thermal system modelled.

As in the previous case, at first it has been searched the optimal collector slope.
Then several simulations have been performed, changing the solar field area. All these simulations have been performed with a solar storage specific volume of 50 $[l/m^2_{collector\ area}]$.
As described in chapter 3.8.4, the solar energy gains have been used in an economic analysis performed in excel to calculate the solar thermal system cost C_{mf} that would give a PBP of 5 years with such a system, for each collector area: this means that every solar thermal system that cost less than this price will be repaid in less than the PBP, and can therefore be an attractive choice for investors.
Moreover, simulations with different storage specific volume have been performed in order to analyze on an energetic point of view the influence of the storage dimensions on the system performances.
All the simulations have been performed both in Sevilla and in Würzburg.

The slope that maximizes the solar energy gain is 30°in Sevilla and 35° in Würzburg.

Figure 4.15 and Figure 4.16 show the performances of this configuration as a function of the collector area.
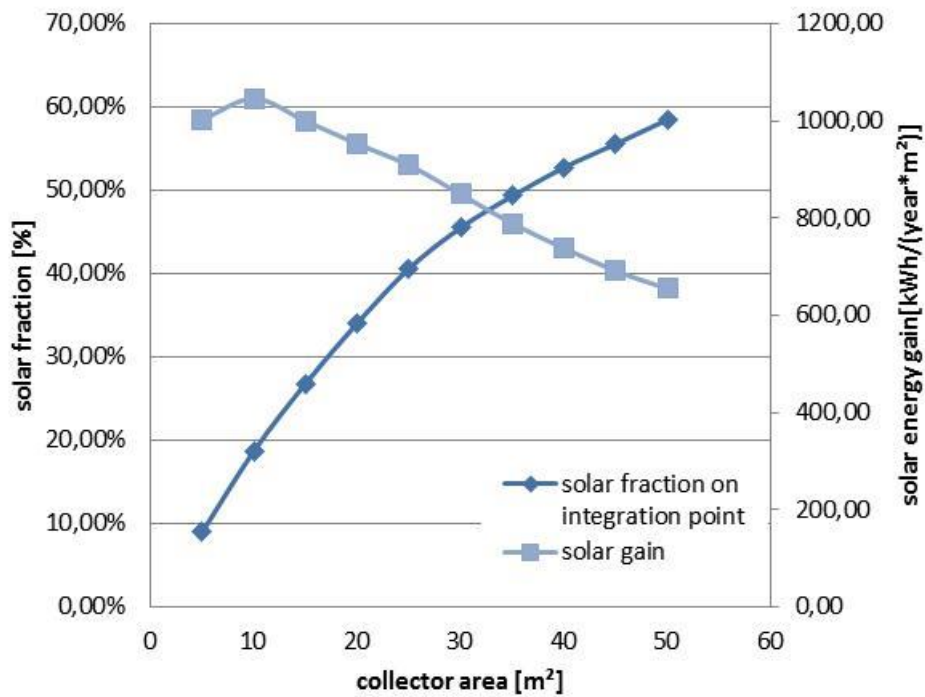
Figure 4.15. solar fraction on the integration point and solar energy gains of flat plate collectors with storage in Sevilla (storage volume = 50 l/m²)
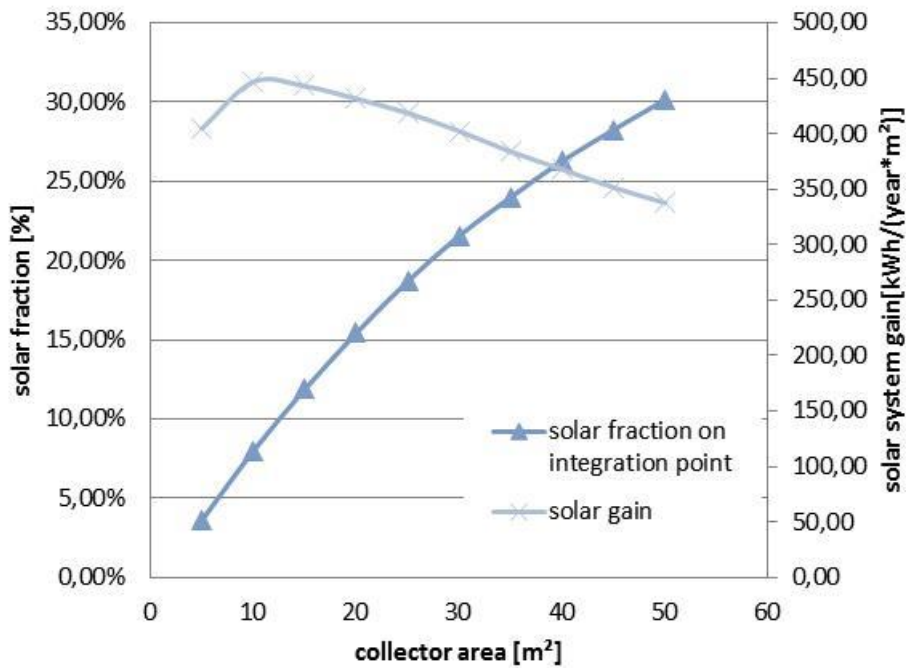
Figure 4.16. solar fraction on the integration point and solar energy gains of flat plate collectors with storage in Würzburg

Table 4.14 and Table 4.15 show the performance of the most efficient configuration (10 m²)

Table 4.14. performance of flat-plate collectors with storage in Sevilla

collector aperture area [m²]	system utilization [%]	solar fraction [%]	solar fraction on integration point [%]	solar system gains [kWh/year*m²]
10	46,26%	0,48%	18,69%	1045

Table 4.15. performance of solar thermal system with flat-plate collectors with storage in Würzburg

collector aperture area [m²]	system utilization [%]	solar fraction [%]	solar fraction on integration point [%]	solar thermal system gains [kWh/year*m²]
10	34,73%	0,20%	7,98%	446

Figure 4.17 and Figure 4.18 show the cost that the solar thermal system should have to be repaid in 5 years, with the assumption described in chapter 3.8.4.
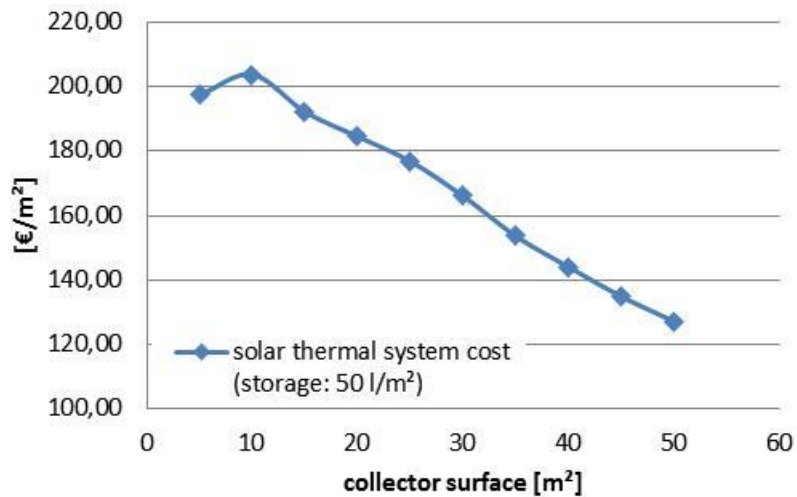
Figure 4.17. maximal feasible solar thermal system cost
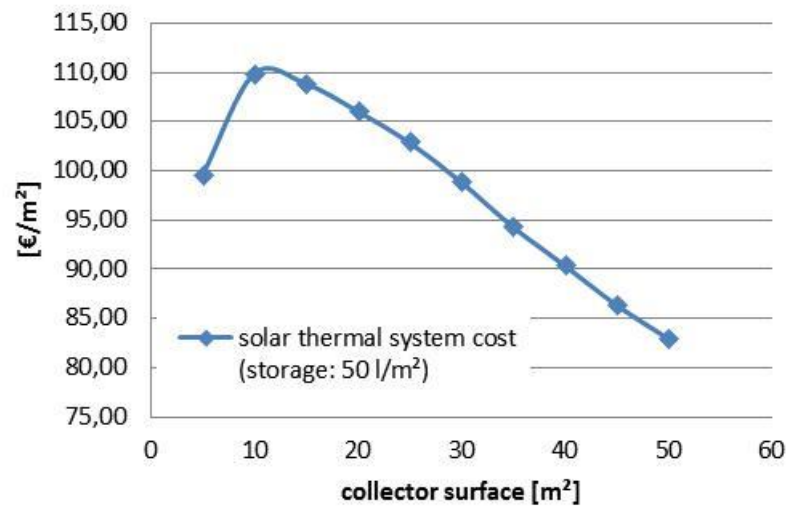
Figure 4.18. maximal feasible solar thermal system cost

The solar thermal system is affordable if it costs less than 207 [€/m²] in Sevilla and 110 [€/m²] in Würzburg.

Other simulations have been performed with different solar storage volumes.
The results of the economic analysis done with two different storage specific volume in Sevilla are shown in Figure 4.19.
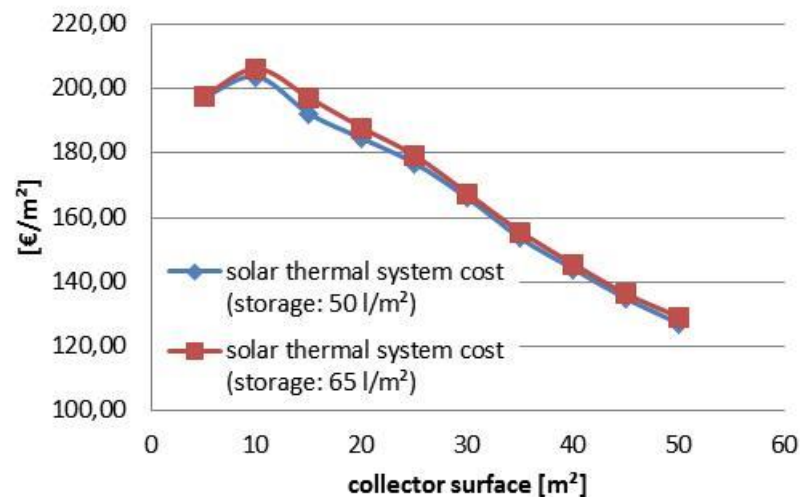
Figure 4.19. maximal feasible solar thermal system costs with two different storage specific volume

The two curves in Figure 4.19 are very similar. Therefore other simulations with different storage specific volumes have been performed only for the most efficient collector aperture area (10 m²).

Figure 4.20 shows the results of these simulations: the solar energy gains increase with the storage volume. However, their second derivative is negative. This means that the bigger the storage the lower will be the increase of solar energy gains. Further analysis of the convenience of larger storage volume will be discussed in chapter 5.
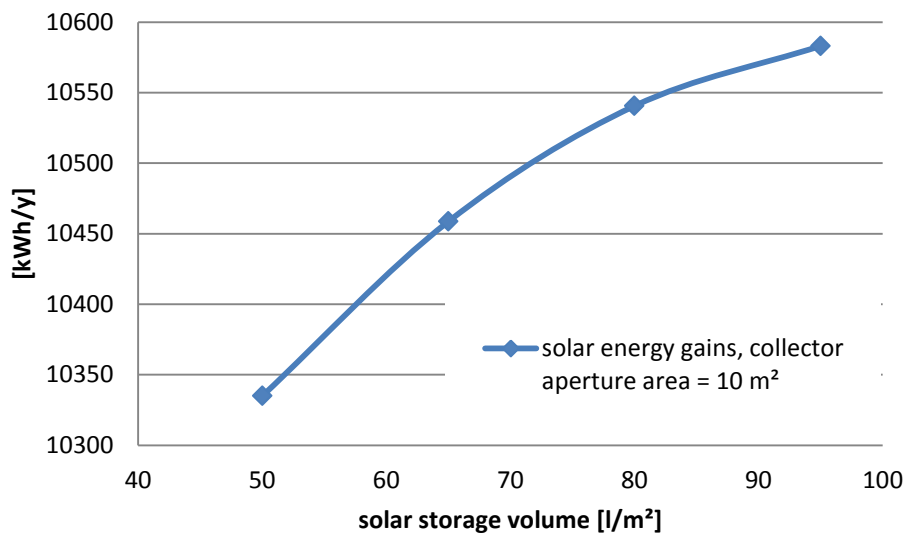
Figure 4.20. solar energy gains as a function of the solar storage specific volume

4.3.3   Results of the pre heating of boiler feed water model

As explained in chapter 2.3.2, the solar integration on boiler feed water is usually considered to be not convenient if an economizer is installed, as it is in the modelled steam network.

To proof this statement, a simulation has been performed in Sevilla choosing an evacuated tube CPC collector (Ritter XL Plasma) having aperture area of 60 m², according to the pre-dimensioning indicated in [7], without using a storage.

The collector has $\eta_0 = 0,688$, $a_1 = 0,583$, $a_2 = 0,003$.

The results have been then analyzed in excel, founding the collector cost C_{mf} that would give a PBP of 5 years:

Table 4.16. performance of evacuated tube collector for feed water pre heating in Sevilla

collector aperture area	system utilization	solar fraction	solar fraction on integration point	solar system gains	solar system cost (PBP = 5 y)
[m²]	[%]	[%]	[%]	[kWh/year*m²]	[€/m²]
60	4,07%	0,27%	9,18%	92	20

The solar system price per square meter is 20 €/m². Since this maximal cost is way below the market price, this configuration will not be investigated any further.

4.3.4   Results of the direct steam generation model

Several simulations with different number of collector rows have been performed, in Sevilla as well as in Würzburg.

Figure 4.21 and Figure 4.22 show the performances of this configuration as a function of the collector area. The solar energy gained per square meter of collector is almost constant for small collector areas and decreases for larger areas: the larger the area, the more frequent will defocusing happen, wasting solar energy and therefore reducing the efficiency of the solar thermal system. Too small collector areas are also less efficient because the losses of the pipes that go from the solar field to the steam network are kept constant in the simulations and therefore are in percentage more relevant if the solar field is small (this assumption could overestimate the heat losses of small system, making them less performing than in reality)
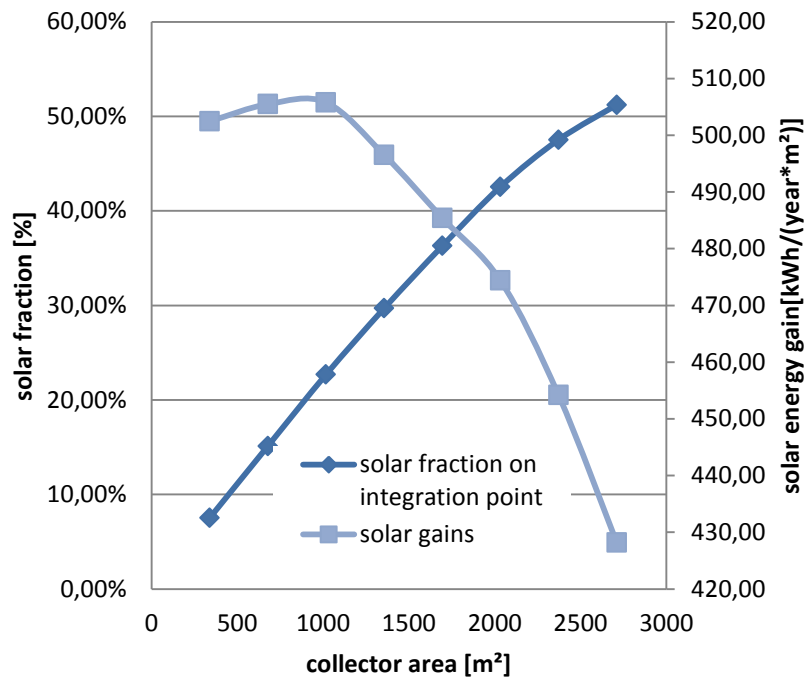
Figure 4.21. solar fraction and solar energy gains of Fresnel collectors in Sevilla
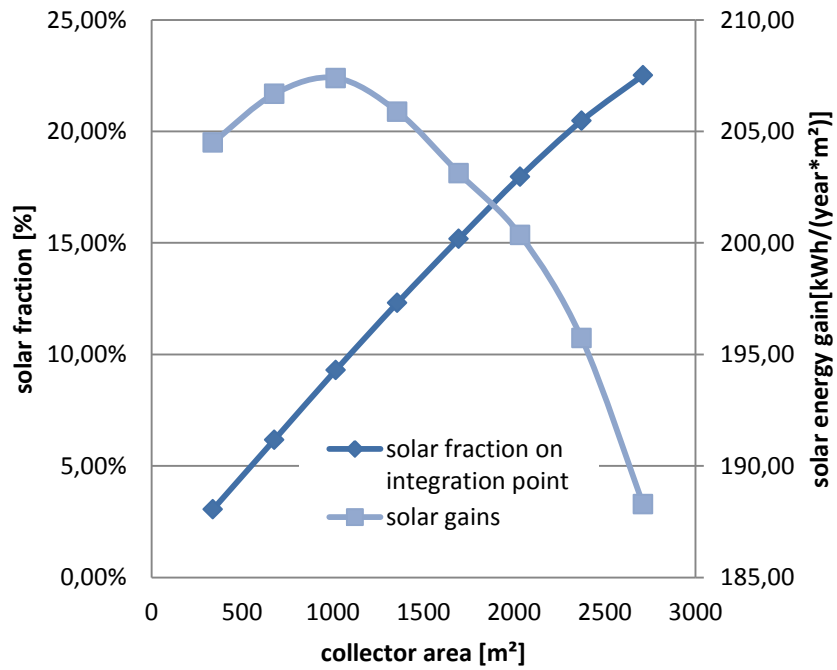
Figure 4.22. solar fraction and solar energy gains of Fresnel collectors in Würzburg

Table 4.17 and Table 4.18 show the performance of the most efficient configuration (1017 m²).

Table 4.17. performance of Fresnel collectors for direct steam generation in Sevilla

collector aperture area [m²]	system utilization [%]	solar fraction [%]	solar fraction on integration point [%]	solar system gains [kWh/year*m²]
1017	21,48%	22,64%	22,69%	505

Table 4.18. performance of Fresnel collectors for direct steam generation in Sevilla

collector aperture area [m²]	system utilization [%]	solar fraction [%]	solar fraction on integration point [%]	solar system gains [kWh/year*m²]
1017	20,12%	9,28%	9,30%	207

The system utilization is around 20% in Sevilla and 10% in Würzburg, which means that just around one fifth and one tenth of the available energy is exploited. This because the incidence angle is not null, and this dilutes the irradiation on the collector surface (the available irradiation considered in this case is the DNI) and creates optical losses calculated with the IAM that reduces the optical efficiency under the maximal 63,5% of this collector, particularly in the winter months when the sun is low and therefore the incidence angle is higher than in summer; moreover the collector can gain energy just when steam is required, that means that during the weekend and the not-working hour all the solar energy available is loss.
Thermal losses decrease the energy gains of less than 5%, much less than it happens with flat-plate collectors, as shown in Figure 3.23.

Figure 4.23 and Figure 4.24 show the cost that the solar thermal system should have to be repaid in 5 years, with the assumption described in chapter 3.8.4.
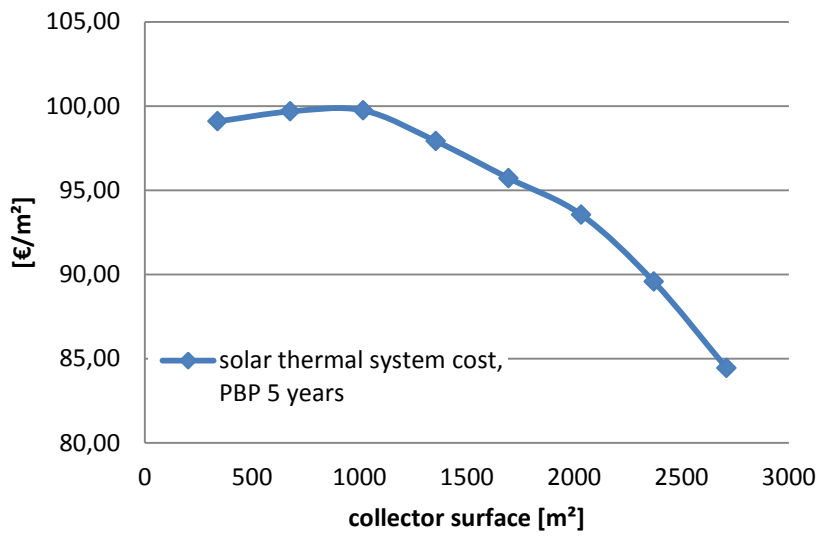
Figure 4.23. maximal feasible solar thermal system cost
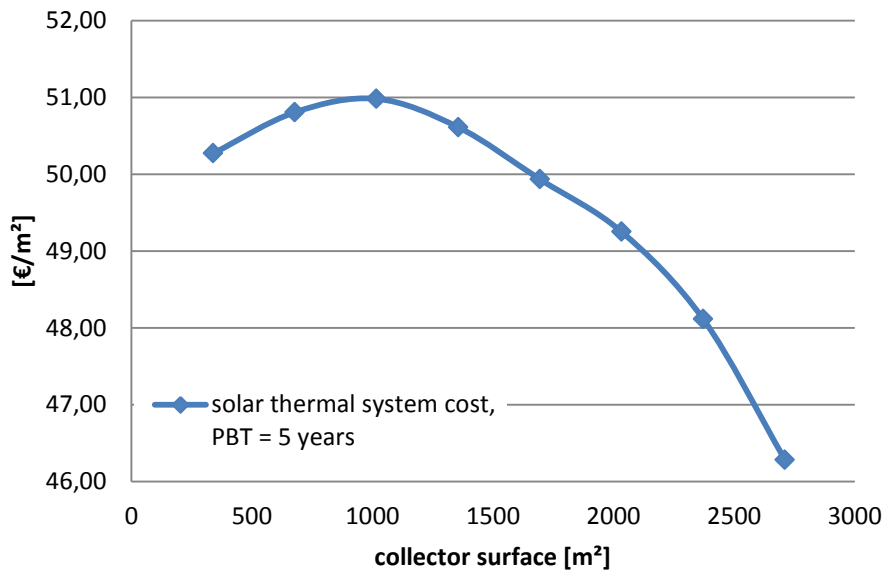
Figure 4.24. maximal feasible solar thermal system cost

The solar thermal system is affordable if it costs less than 100 [€/m²] in Sevilla and 51 [€/m²] in Würzburg.

4.4 Sensitivity analysis

It has been analyzed the influence of the assumptions described in chapter 3.8.4 on the economic analysis previously performed.

At first it has been checked how the maximal feasible cost of the solar thermal system varies if the parameters of the economic analysis are individually changed of ± 25%, in order to understand which has a stronger influence on the solar thermal system cost.
This analysis has been done on the most efficient configuration for pre heating of make-up water in Würzburg, characterized by a collector area of 15 m²: Figure 4.25 shows that the two parameters that have a stronger impact are the payback period and the natural gas price, causing a rise of respectively 18,48 % and 26,58 % of the maximal solar thermal system price if they increase of 25%. The other parameters analyzed are interest rate, o&m costs and electricity price: they vary less than 3% the solar thermal system costs.

Figure 4.25. variation of the maximal feasible cost of a solar thermal system. Case: pre heating of make-up water without storage in Würzburg, collector surface = 15 m²

It is interesting to look more in detail the effect of the variation of the gas price. In Table 4.19 and Table 4.20 shows the variation of the maximal feasible solar thermal system costs previously calculated if a different gas price is assumed; for each model has been chosen the most efficient configuration.

Table 4.19. maximal feasible solar thermal system cost [€/m²] in Sevilla as a function of the gas price

	gas price variation		
	-25%	standard	+25%
make-up water, no storage	109,56	148,91	188,78
make-up water, storage	151,48	203,80	261,00
direct steam generation	73,26	99,74	126,22

Table 4.20. maximal feasible solar thermal system cost [€/m²] in Würzburg as a function of the gas price

	gas price variation		
	-25%	standard	+25%
make-up water, no storage	71,84	97,85	123,85
make-up water, storage	80,65	109,84	139,04
direct steam generation	37,43	50,98	64,53

Moreover, it has been assumed no change of gas price. This hypothesis is unrealistic; on the other hand it is difficult to guess what the change rate will be in the next years, as shown by Figure 4.26, which describes the trend of the gas price for industrial consumers in Germany in the last years. The gas price is increased, even if there has been also a drop of the price in 2009 and 2012.
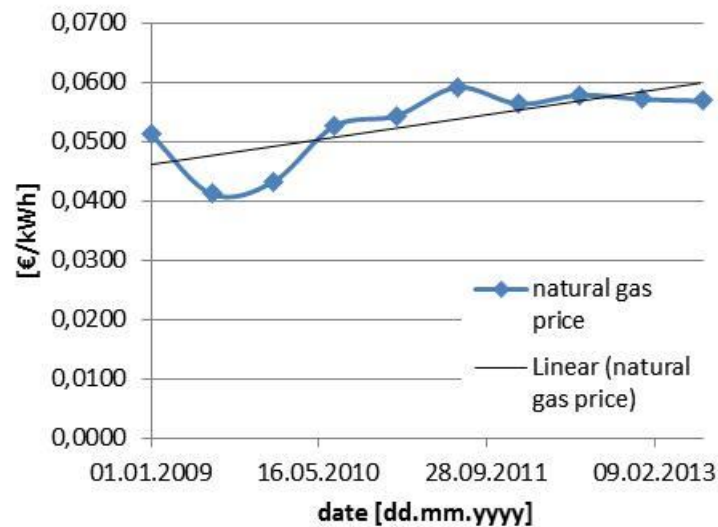
Figure 4.26. historical trend of gas price for industrial consumers in Germany (all taxes and levies included) [33]

It is interesting to check how the present analysis would change if an increase of gas price would be considered. This analysis has been done on the most efficient configuration for pre heating of make-up water in Würzburg, characterized by a collector area of 15 m².

Figure 4.27 shows the variation of the maximal feasible cost of a solar thermal system as a function of the increase of gas price. It appears clear that the increase of gas price has an effect on the economic analysis performed. The hypothesis of no increase is therefore conservative.
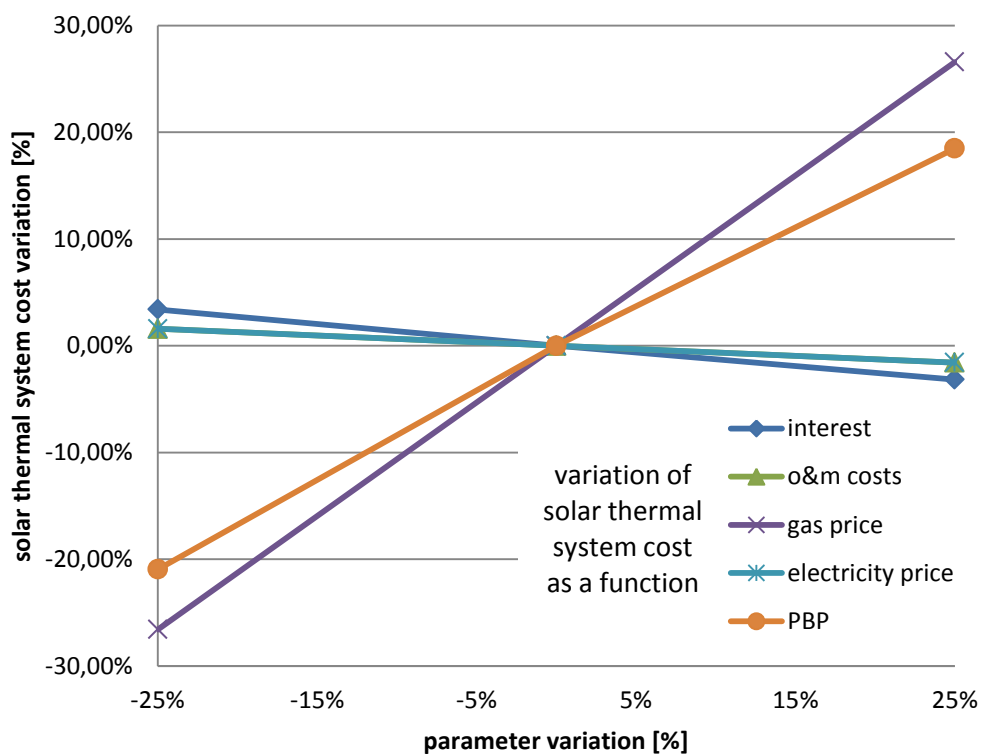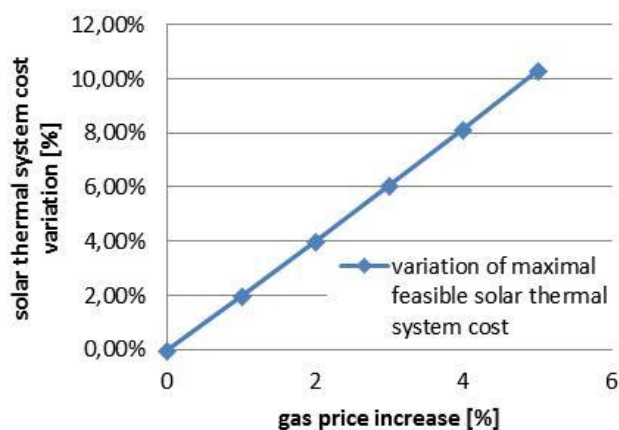

Figure 4.27. variation of the maximal feasible cost of a solar thermal system. Case: pre heating of make-up water without storage in Würzburg, collector surface = 15 m²

Chapter 5

Discussion

This chapter contains an evaluation of the results displayed in chapter 4.
The results of the simulations will be analyzed to compare the different integration points.
Moreover the maximal feasible cost of the solar thermal systems founded with the economic analysis performed in excel will be discussed, in order to evaluate the feasibility of the modelled configurations.

5.1   Evaluation of the different integration points

Figure 5.1 show the system utilization of make-up water pre heating, boiler feed water pre heating and direct steam generation in Sevilla.
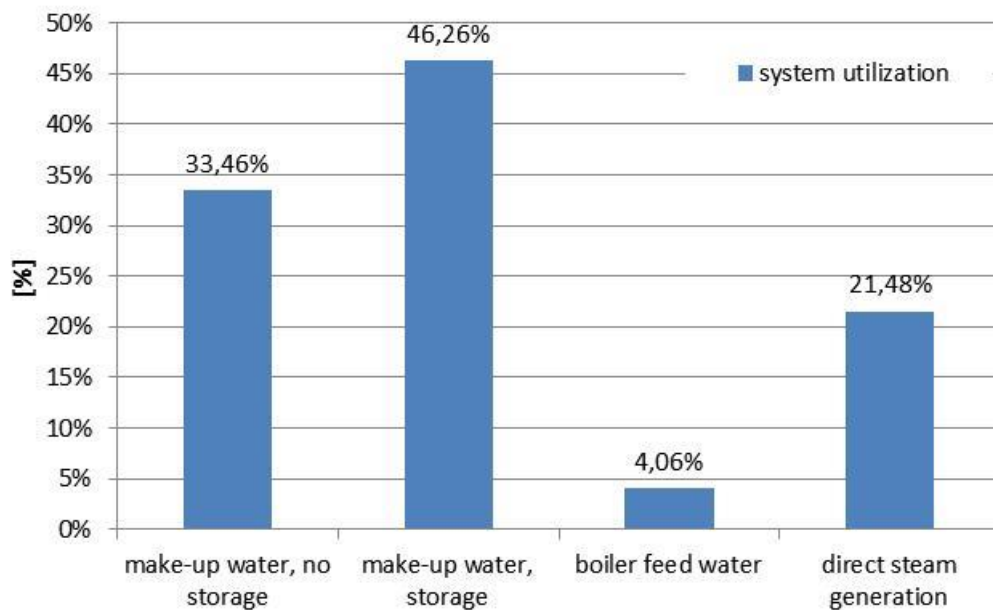
Figure 5.1. system utilization of different solar thermal systems in Sevilla (for each of them has been chosen the most efficient configuration)

Figure 5.2 compares the solar energy supplied to the steam network and the demand on integration point of direct steam generation and make up water pre heating with a storage
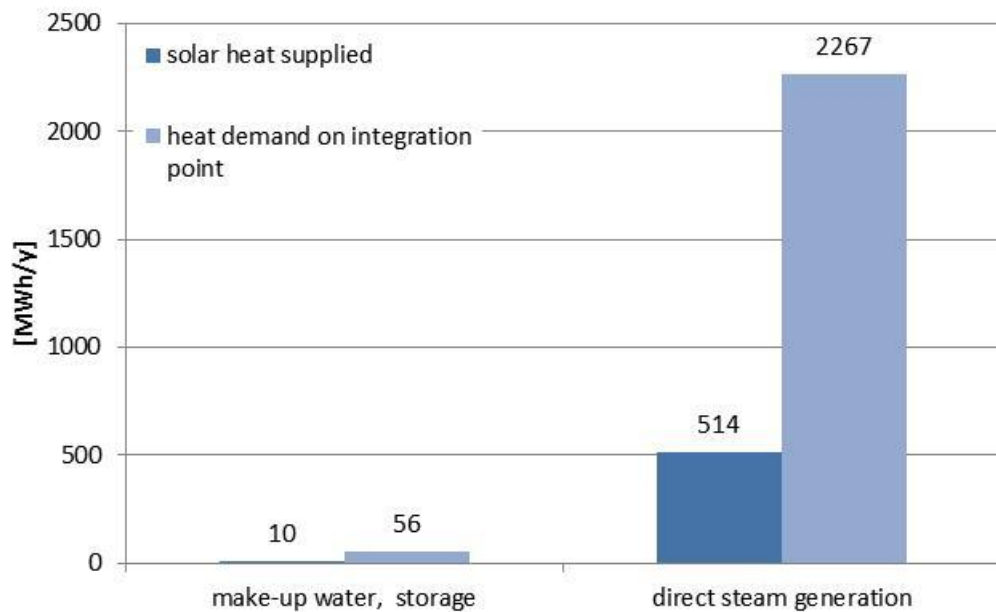
Figure 5.2. solar energy supplied and heat demand of different solar thermal systems in Sevilla (for each of them has been chosen the most efficient configuration)

The make-up water mass flow amounts to only 20% of the total mass flow going to the boiler, as shown in 4.2.1. Moreover the enthalpy difference in this integration point is much smaller than the enthalpy difference due to evaporation, as shown in Table 2.1.For these reasons the make-up water pre heating from 35 °C to 102 °C has a share of only 2,58 % of the total heat demand of the steam network. This value is also the upper limit of the solar fraction reachable. Therefore the solar thermal system required on this integration point is small in comparison with the integration on steam generation.

On the other hand the integration on make-up water allows obtaining high system utilization, which means the solar thermal system exploits efficiently the solar energy. Moreover the installation of a storage increases considerably the performance of the make-up water pre heating system (+38,25% of system utilization in Sevilla). This result was expected, since the storage allows exploiting solar energy also when there is no heat demand.

The performances of both the system modeled are considerably better in Sevilla than in Würzburg, because of the much higher amount of solar irradiation available. Moreover has to be remarked that the collector slope that maximizes the solar energy gains is higher in Würzburg, as expected since it is located northern than Sevilla. Other effects that influence the collector slope are the load profile and the presence of a storage.

The integration on boiler feed water has worse performance because of the presence of the economiser. Also this result was expected and therefore this integration has been no longer considered.

Direct steam generation has lower system utilization than the integration on make-up water because Fresnel collectors have worse optical efficiency than flat-plate collectors (that on the other hand cannot be used in this temperature range because of too high heat losses). Moreover this system has no storage, so that it doesn't exploit the radiation available when there is no heat demand.
On the other hand the integration on direct steam generation has a much larger solar field, which means it can supply much more energy to the steam network.
The performances of this system are considerably better in Sevilla than in Würzburg because of the higher DNI of south Spain in comparison with central Germany.

5.2 Economic evaluations

5.2.1 Reference costs of solar thermal systems

In order to evaluate the economic results shown in chapter 4, it is necessary to identify reference values of the cost of solar thermal systems.

At first water pre-heating systems have been analyzed.

Table 5.1 shows reference costs of solar thermal systems having flat-plate collectors. It emerges that small plants have higher specific costs.

Table 5.1. solar thermal system cost [€/m²] using flat-plate collector [36]

		collector aperture area [m²]		
		100	300	≥ 1000
solar thermal system cost	[€/m²]	715	450	375

Figure 5.3 shows the dependence of the cost of stationary collectors and water storages on their dimensions. Again the cost decreases with the plant size. However, over 50 m² of collector surface, corresponding to 2500 liter of storage volume assuming 50 $l/m^2_{collector}$, the costs show only minor dependence on the plant size. In particular flat-plate collector have a price between 200 €/m² and 300€/m², while buffer water storage cost around 1 €/l.
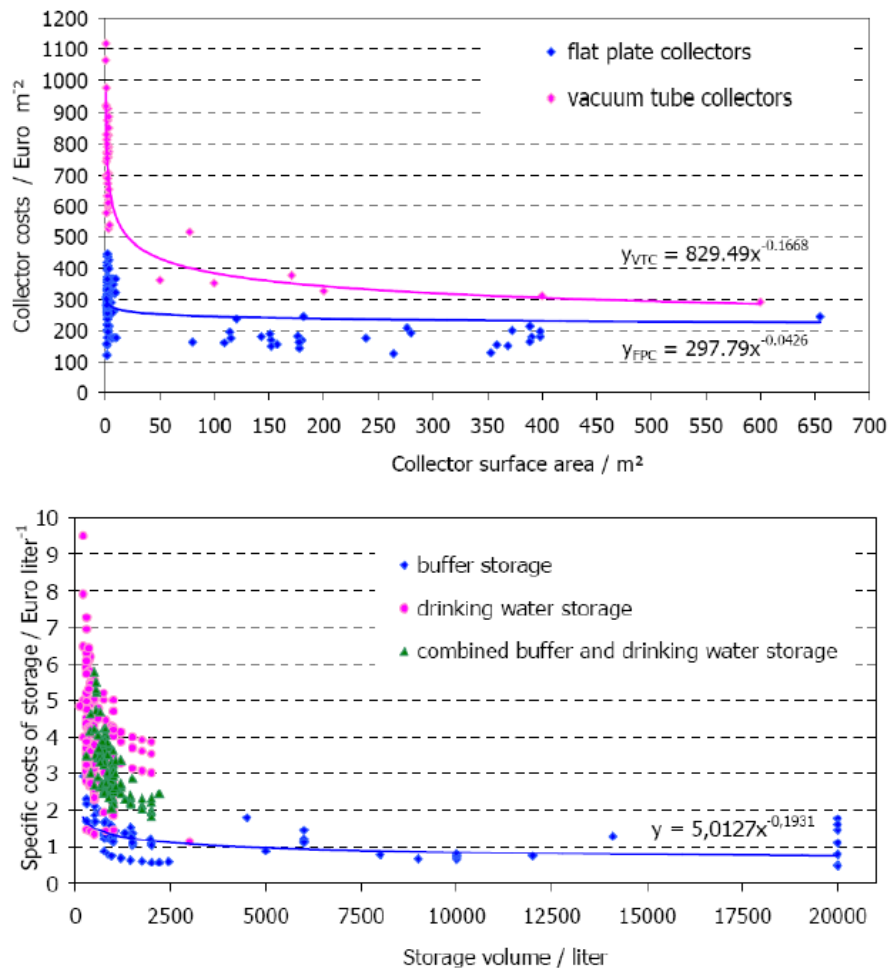
Figure 5.3. cost of solar collectors and storages as a function of their dimension [37]

Direct steam generation using linear concentrating collectors is not widespread and therefore is difficult to find a reference price of this kind of systems. Henning Fröhlich, in his master thesis written at ISE Fraunhofer about direct steam generation for process heat and cogeneration, uses a system price for direct steam generation with linear Fresnel collectors of 400 €/m², system costs included [38]. This price is given by the manufacturer.

The same cost for Fresnel collector is present other works on process heat with Fresnel collectors [39].

This price will be used in this thesis as a reference for solar thermal system for direct steam generation without storage with linear Fresnel collectors.

5.2.2   Subsidies

No subsidies for renewable energies have been considered in the economic analysis performed. The reason of this choice is that subsidies may change over time and from country to country, therefore considering current German or Spanish subsidies it would limit the meaning of the present analysis.

However, since subsidies for renewable energies exist in many countries, the comparison between the economic results of chapter 4 and the market prices of 5.2.1 must consider their benefit.

In Germany the subsidies for solar process heat amount to 50% of the investment [40]. In Spain many solar process heat plants realized in the last years have been subsidized with between 30% and 40% of the investment [41].

5.2.3   Economic feasibility of solar pre heating of make-up water

Chapter 4 showed the maximal system costs that would make an investment in the modeled plants interesting. Real plants are feasible if they cost less than the investigated specific system costs shown in Chapter 4.

As shown in Table 4.19, the configuration that could be repaid more quickly both in Sevilla and in Würzburg is pre-heating of make-up water with storage with 10 m² of collector aperture.

SEVILLA:

The C_{mf} of such a system is 203,80 €/m². Comparing this result with the reference value of 715 €/m² shown in Table 5.1, it emerges that typical plants of this size are more than 3,5 times more expensive and therefore the investment in this plant is not economically worthwhile.

Considering subsidies less than or equal to 50% of the investment, as they are described in chapter 5.2.2, the considered system would be competitive if it costs less than around 400 €/m².

According to Table 5.1, a plant of this size is too expensive also with subsidies. Large plants cost less than or equal to 400 €/m²; on the other hand, as shown in and Figure 4.17, larger solar thermal systems would be less efficient and therefore would be competitive only with a lower cost of the solar thermal systems.

The conclusion is that pre heating of make-up water with flat plate collectors is not an economically attractive choice for a middle sized laundry in Sevilla. This conclusion is valid within the assumption considered: if the fuel price change, the subsidies rise or a company is willing to expect a longer PBP than 5 years, the investment would be profitable.

However, an industry with a far larger heat demand than a middle sized laundry could scale the considered configuration in order to install a large collector field with a similar efficiency.
It emerges that, also within the economic assumptions considered and with current subsidies, such a plant would be economically worthwhile.
These evaluations are summarized in Figure 5.4.
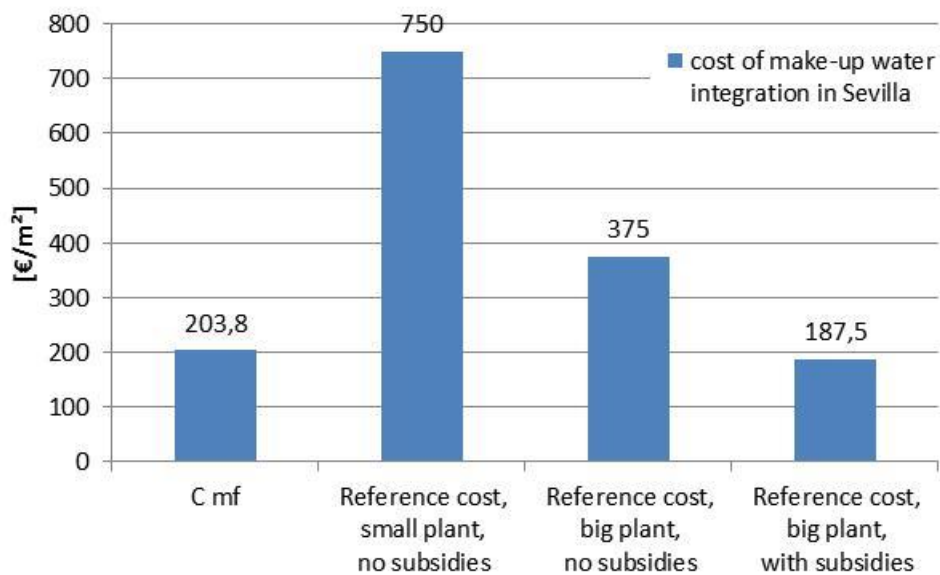
Figure 5.4. comparison between C $_{mf}$ and reference cost for make-up water integration in Sevilla

WÜRZBURG:

The results in Chapter 4 show that a flat plate collector system with storage for make-up water heating in Würzburg is only profitable if the specific system costs are less than 109,84 €/m². Comparing this result with the reference value of 715 €/m² Table 5.1, it emerges that typical plants of this size are more than 6,5 times more expensive and therefore this plant is not economically feasible.

Considering subsidies less than or equal to 50% of the investment, as they are described in chapter 5.2.2, the considered system would be competitive if the costs are below 200 €/m².
According to Table 5.1, a plant of this size is too expensive also with subsidies.

The conclusion is that pre heating of make-up water with flat plate collectors is not an economically attractive choice for a middle sized laundry in Würzburg.

This conclusion is valid within the assumption considered. It can be interesting to find for what gas price such a plant would become worthwhile: it has been considered an industry with a larger energy demand than a middle sized laundry (as it has been done previously for Sevilla). It has been then chosen a solar thermal system cost of 200 €/m², valid for a large solar thermal system subsidized with 50% of the investment. The economic analysis tool in excel consents to calculate that to repay this configuration in 5 years the gas price should be 0,1 €/kWh, while the current gas price in Germany is 0,06 €/kWh. These evaluations are summarized in Figure 5.5.
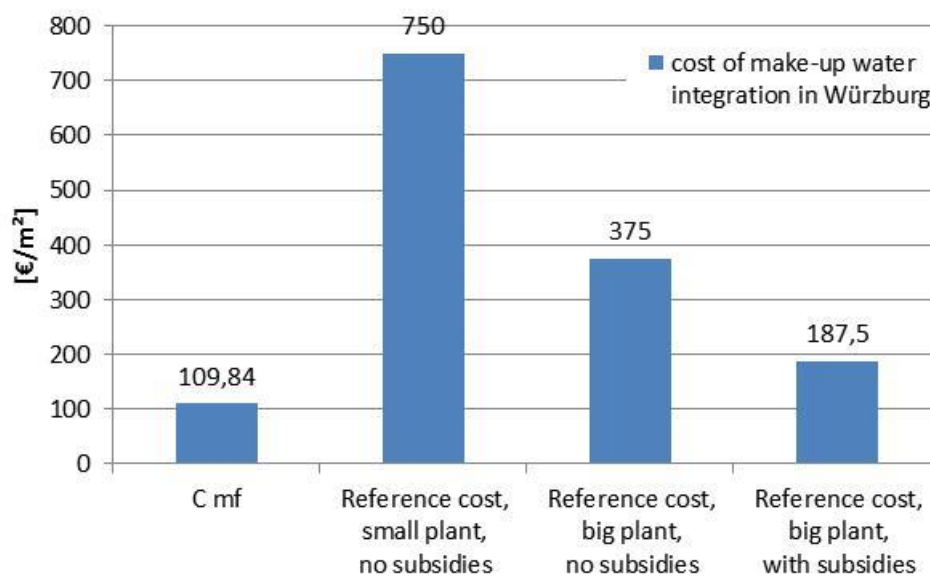
Figure 5.5. comparison between C $_{mf}$ and reference cost for make-up water integration in Würzburg

CONSIDERATION ABOUT THE STORAGE VOLUME:

As shown in chapter 4.3.2, an increase of solar storage volume at constant collector area reduces the energy consumption of the boiler. Nevertheless the bigger the storage the lower the increase becomes. Therefore there is a point at which the increase of storage volume and the consequent increase of solar energy gains can't pay back the additional cost of the storage itself. This is the optimal volume of the storage, because larger storages are too expensive and smaller storages exploit too few energy.

In order to calculate this volume it would be necessary to know the cost of solar storages. As shown in Figure 5.3, the specific cost of buffer storage of little dimension, such as the one used in the model, it is strongly dependent on the size of the tank.

Literature research about the cost of the components is not a topic included in this thesis, therefore no optimization of the storage volume have been done within this thesis.

5.2.4 Economic feasibility of solar direct steam generation

In chapter 4 have been shown the maximal system costs that would make an investment in the modeled plants interesting. Both in Sevilla and in Würzburg the optimal direct steam generation system has 1017 m² of collector aperture for the simulated system model.

SEVILLA:

The C_{mf} of such a system is 99,74 €/m². The reference cost for Fresnel collectors described in chapter 5.2.1 is 400 €/m². It emerges that typical plants are more than 4 times more expensive and therefore this plant is not economically worthwhile.

Considering subsidies less than or equal to 50% of the investment, as they are described in chapter 5.2.2, the considered system would be competitive if it costs less than around 200 €/m²: such a plant is too expensive also with subsidies.

The conclusion is that direct steam generation with linear Fresnel collectors is not an economically attractive choice for a middle sized laundry in Sevilla.
It must be reminded that the modeled system has no storage and therefore it can't exploit a large part of the available radiation, as shown in Figure 4.10. Therefore this plant is more suitable for industrial processes with a continuous energy demand.

As shown by the sensitivity analysis described in chapter 4.4, the gas price has a strong impact on economic evaluations. Therefore it can be interesting to find for what gas price such a plant would become feasible.
For this scenario solar thermal system costs of 200 €/m² were assumed, valid for a linear Fresnel collector solar thermal system subsidized with 50% of the investment. The economic analysis tool in excel consents to calculate that to repay this configuration in 5 years the gas price should be 0,09 €/kWh; the current gas price in Spain is 0,05 €/kWh.
These evaluations are summarized in Figure 5.6.
.

Figure 5.6. comparison between C mf and reference cost for direct steam generation in Sevilla

WÜRZBURG:

In Würzburg a direct steam system has a C_{mf} of 50,98 €/m². Comparing this result with the reference cost for Fresnel collectors described in chapter 5.2.1, it emerges that typical plants are around 8 times more expensive and therefore this plant is not economically worthwhile.
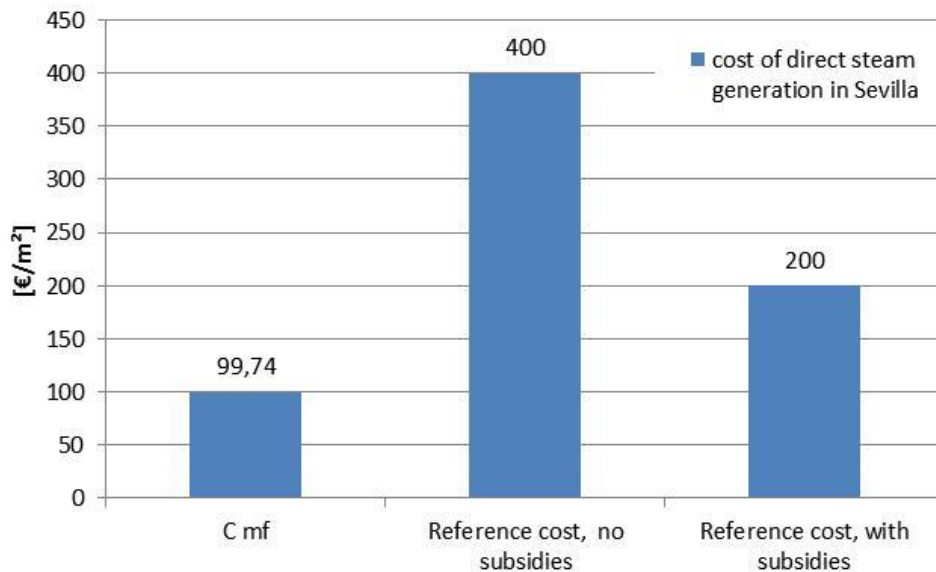
Considering subsidies less than or equal to 50% of the investment, as they are described in chapter 5.2.2, the considered system would be competitive if it costs less than around 200 €/m²: such a plant is not economic also with subsidies.

The conclusion is that direct steam generation with linear Fresnel collectors is not an economically attractive choice for a middle sized laundry in Würzburg.
The main problem is that Würzburg, like all central Europe, has not high enough DNI values and therefore is not a good location for direct steam generation. Moreover the modeled system has no storage and therefore it can't exploit a large part of the available radiation, as shown in Figure 4.10.

It can be interesting to find for what gas price such a plant would become worthwhile: it has been chosen a solar thermal system cost of 200 €/m², valid for a linear Fresnel collector solar thermal system subsidized with 50% of the investment. The economic analysis tool in excel consents to calculate that to

repay this configuration in 5 years the gas price should be 0,21 €/kWh, while the current gas price in Germany is 0,06 €/kWh.

These evaluations are summarized in Figure 5.7.
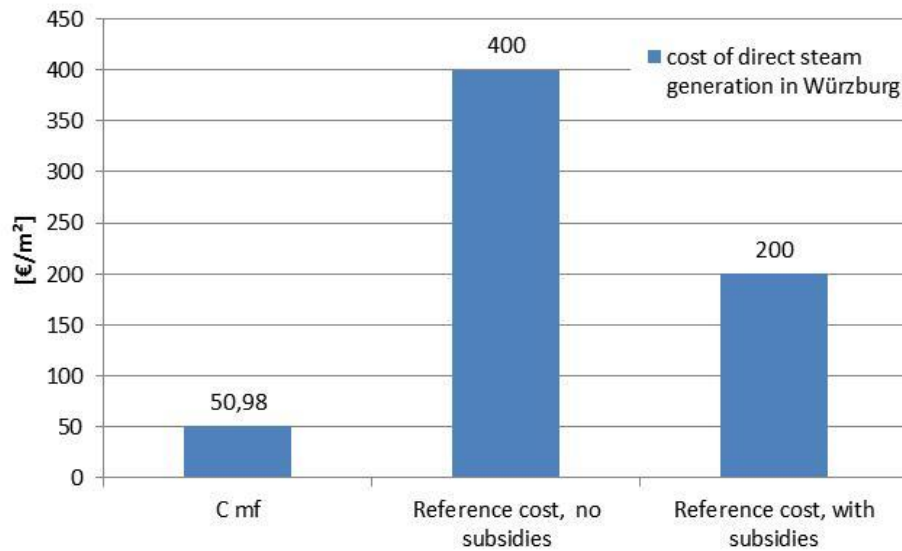
Figure 5.7. comparison between C $_{mf}$ and reference cost for direct steam generation in Würzburg

Figure 5.8 provides a validation of these evaluations: the use of Fresnel collectors for process heat application is suitable for locations with high DNI and high cost of fossil fuel. The price of natural gas is too low in both the location chosen to make solar thermal competitive; moreover Würzburg has too low DNI (1000 kWh/m²*y [31]), while Sevilla (DNI = 2300 kWh/m²*y [31]) is an interesting location for more expensive fuels.
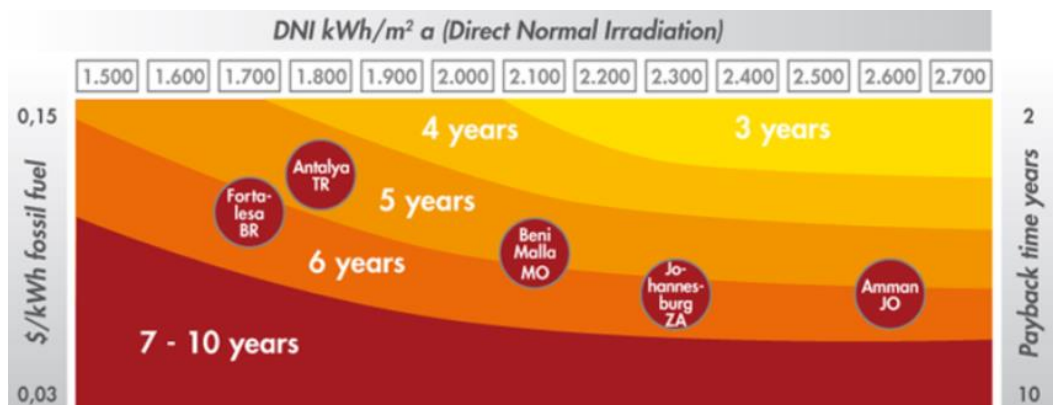
Figure 5.8. PBP as a function of DNI and fossil fuel cost; some real solar thermal system for process heat using linear Fresnel collectors are shown [42]

5.3 Reliability

The results and evaluations exposed are valid only under several assumptions and simplifications.

MODELLING AND SIMULATING:

As explained in chapter 3.7.1, the most of the types available simplify the behaviour of the real components changing the properties of the fluid instantaneously. The modeled steam network has mostly stationary conditions. Therefore the development of new types capable of describing more accurately the transient state has been considered too time costly, without bringing major advantages.

The modeling of the heat demand of the processes has been done in two steps: at first the model of a middle sized energy efficient laundry proposed by Michael Schmid has been adopted. This limits the validity of the results to industrial processes having heat demand, load profile, pressure and temperature level similar to a middle sized laundry.
The laundry model has been then modified: standard instead of advanced efficiency measures have been considered and some simplifications have been done to fit the requirement of ColSim. In particular the mass flow at the outlet of the open process has been recirculated as make-up water, while in the reality these two mass flows differ from each other: the make-up water in the steam network model has a mass flow profile like in Figure 3.5 instead as in Figure 3.6. This assumption can have relevant effect on the integrations of a solar thermal system. The real mass flow makes more convenient the installation of a storage, since the modeled mass flow is continuous between 6:00 and 16:00 while the real make-up water mass flow is intermittent.
Nevertheless this assumption was not avoidable because in ColSim every hydraulic circuit ha to be closed.

In the validation of the steam network model has been done an energy balance. As explained in chapter 4.2.1, it has been done a distinction between heat losses that take place in header types and wasted heat that is taken by cooler types after the processes. In reality the wasted heat on the condensate line should be considered as a heat loss, since it is heat lost in pipes. This means that the heat losses in the energy balance are underestimated, while the wasted heat is overestimated.

Eventually, a complete analysis of the integration of a solar thermal system in a steam network should include further configuration with different components,

such as evacuated tube collectors and pressurized storages. The results obtained are therefore valid just for the investigated configurations, leaving open the possibility to find more worthwhile systems not considered within this thesis because of the limited time.

ECONOMIC EVALUATION:

The economic analysis performed is based on the assumption described in chapter 3.8.4. These assumptions have been subjected to a sensitivity analysis in chapter 4.4: it emerges that the two parameters that can have a deciding impact on the economic feasibility of a solar thermal plants are the payback period and the fuel price.

It has been considered a payback period of 5 years as longest period of time that a company could wait to repay the investment. Notwithstanding a company could invest also if the payback period is longer than 5 years, for example valuing the ambient benefits of solar thermal energy. The limit of 5 years used in the analysis performed has to be seen as value for which this investment would become economically interesting for the most of the industrial companies.

It has been chosen gas as fuel because it is the most common scenario. However there are steam networks that burn more expensive fuels: for example laundries without a connection to the gas net can use heating oil transported by trucks.
Moreover the fuel price is subjected to frequent variations that are scarcely predictable. Therefore it has been considered no increase of gas price in the economic analysis performed.
Both these considerations limit the evaluations on the feasibility of the solar thermal system considered to gas fuelled plant with current gas price. It is nevertheless possible to consider higher but realistic fuel price that could make the investigated configurations worthwhile.

Chapter 6

Conclusions and future developments

6.1 Conclusion

Purpose of this master thesis is the modeling of an industrial steam network and of its possible integrations with solar thermal systems; all the modeling work has been conduct with the software ColSim developed at Fraunhofer ISE.
These models have been then used to perform annual simulations in order to evaluate the current economic feasibility of the chosen configurations.

At first it has then been build a simulation model of an industrial steam network. On the basis of this steam network model, four solar thermal integrations have been developed: pre heating of make-up water with and without a solar storage, pre heating of boiler feed water and direct steam generation.
Annual simulations have been performed choosing as locations Sevilla and Würzburg. The results have been analyzed with energy indicators such as solar energy gains, solar fraction and efficiency of the system. At a later stage they have been post processed in excel: an economic analysis has been performed in order to evaluate whether the modeled solar thermal integrations are economically worthwhile for industrial company, using as main criterion a payback period of 5 years. A sensitivity analysis has been performed in order to understand how the economic evaluations depend on assumed parameters like gas price, payback period and interest rate.
The results of this economic analysis have been eventually compared with reference costs of solar thermal systems, to discuss their economic feasibility.

It emerges that the chosen configurations are currently not a profitable investment for middle sized industrial laundries.
Regarding make-up water pre-heating, it emerges that it exploits solar energy more efficiently than direct steam generation.
On the other hand it requires small amount of heat in comparison with steam generation (2,58% of the total heat demand), because the enthalpy difference in this integration point is small and the make-up water mass flow is only 20% of the total mass flow. For this reason the solar thermal systems are small and their specific costs are high.
Industrial processes that produce larger make-up water mass flows than middle sized industrial laundry could install larger solar thermal plant with lower

specific costs. In particular in Sevilla such a configuration would be already economically feasible with current subsidies for solar process heat.

Moreover, the presence of a storage increases considerably the solar energy gains. The choice of the storage volume depends on storage specific cost and has not been investigated within this thesis.

Regarding boiler feed water pre-heating, the system is not worthwhile if an economizer is present. Since economizers are already standard energy recovery system installed in the most of the steam networks, this integration is not feasible.

Regarding direct steam generation, it has a large potential in terms of reachable solar fraction of the whole steam network. On the other hand it exploits solar energy less efficiently than a make-up water pre heating system and therefore it requires longer period of time to be repaid.

Such a system is not suitable for industrial processes with a discontinuous heat demand like middle sized laundries. The main problem is that a large part of the available solar energy is not exploited, since no storage is installed. Moreover, for Würzburg the DNI is to low; therefore this integration is not recommended for central Europe.

It could be instead an interesting option in Sevilla if the heat demand would be more continuous all over the day.

6.2 Future developments

The developed models could be improved in several ways:

- New types that describe the dynamic behaviour of many components can be developed, in order to improve the level of detail of the model.

- In the steam network model, it could be developed a model of a mixed process, which puts together features of the closed and of the open processes.

- In the modeled integration points, other configurations could be investigated, for example using evacuated tube collectors instead of flat-plate collectors for make-up water pre heating.

- Other integration points could be investigated, in particular integration on process level, supplying heat directly to the industrial processes instead of to the steam network.

- Other industrial branches with different heat demand can be investigated, in order to find which load profile better match with the modelled integrations.

- The economic analysis can be improved with a thorough research of components and system price.
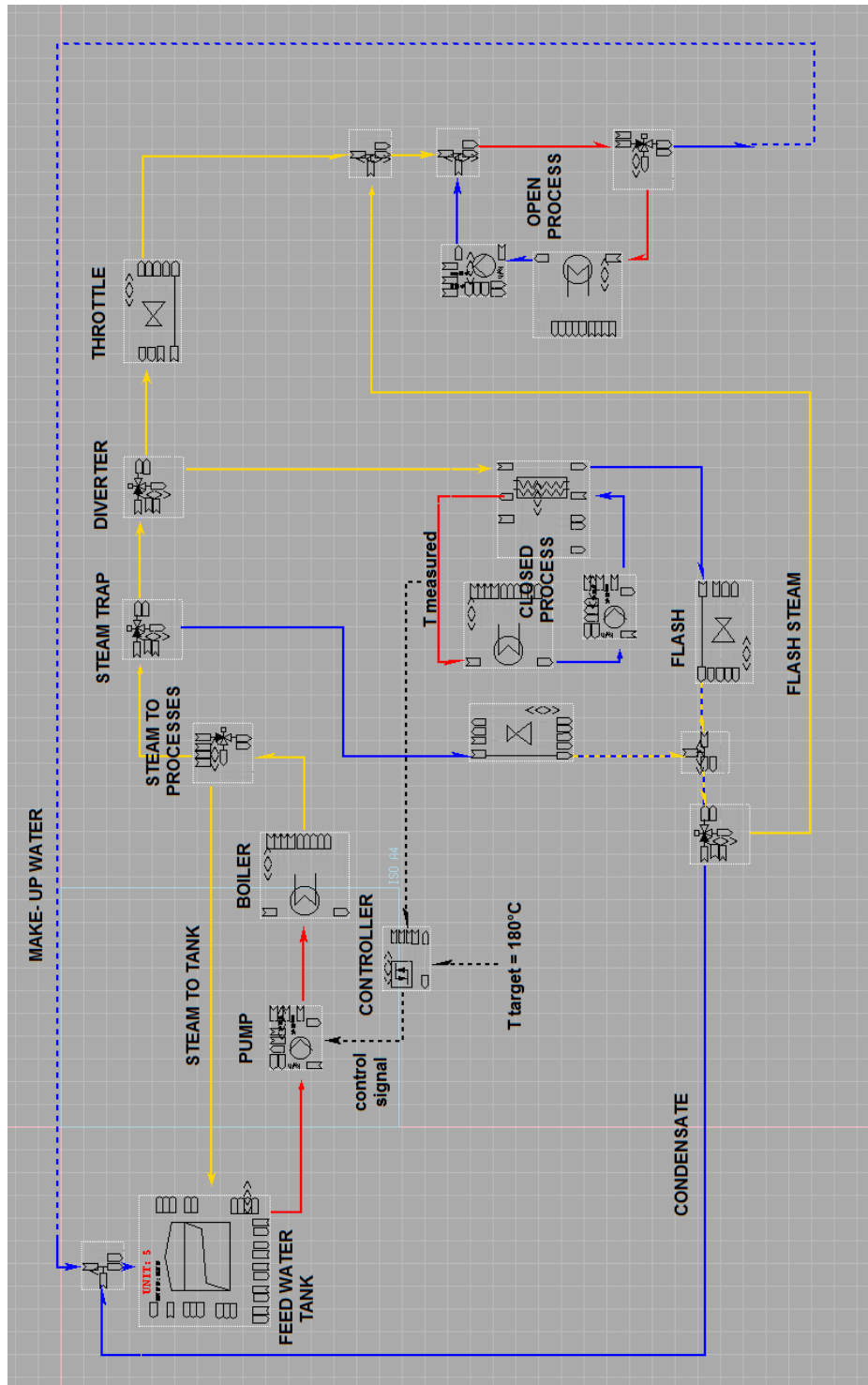
Appendix

Figure 1. hydraulic circuits of the steam network model in ColSim; it is shown also the control strategy of the closed load

Nomenclature

Symbol	Unit	Description
G	[W/m²]	Irradiance
H	[J/m²]	Irradiation
θ	[°]	Angle of incidence
θ_z	[°]	Zenith angle
h	[°]	Solar altitude angle
γ_s	[°]	Solar azimuth angle
β	[°]	Slope
γ	[°]	Surface azimuth angle
α	[-]	Absorptance
ρ	[-]	Reflectance
τ	[-]	Transmittance
$\tau\alpha$	[-]	Transmittance-absorptance product
$K_{\tau\alpha}$	[-]	Incidence angle modifier
η	[-]	Efficiency
$\dot{q}_u$	[W/m²]	Useful gain
$\dot{q}_l$	[W/m²]	Heat losses
η_0	[-]	Optical efficiency
a_1	[-]	Heat losses coefficient
a_2	[-]	Heat losses coefficient
ΔT	[K]	Temperature difference
A_c	[m²]	Absorber area
U	[W/m²*K]	Overall heat transfer coefficient
Δh	[kJ/kg]	Enthalpy difference
h	[s]	Time step

Symbol	Unit	Description
$\dot{m}$	[kg/s]	Mass flow
m_{plug}	[kg]	Mass of a Plug in ColSim
ΔQ_{plug}	[J]	Enthalpy of a Plug in ColSim
ctrl	[-]	Control signal
e	[-]	Error signal
K_p	[-]	Proportional coefficient
K_i	[-]	Integral coefficient
K_d	[-]	Derivative coefficient
T	[°C], [K]	Temperature
P	[bar]	Pressure
V_S	[m³]	Storage volume
SF	[%]	Solar Fraction
CF	[€]	Cash flow
PV	[€]	Present value
NPV	[€]	Net present value
PBP	[y]	Payback period
Re	[-]	Reynolds number
Nu	[-]	Nusselt number
Pr	[-]	Prandtl number
h	[W/(m²*K)]	Heat transfer coefficient
k	[W/(m*K)]	Thermal conducivity
D	[m]	Diameter
C_{mf}	[€/m²]	Maximal feasible cost of a solar thermal system

Symbol	Description
ISE	Institut für Solare Energiesysteme
EU	European Union
US	United States of America
PID	proportional-integral-derivative
n	Node (ColSim)
O&M	Operation and maintenance
DNI	Direct Normal Irradiation
T	Tilted surface
N	Normal surface
t	transversal
l	longitudinal
h	Time step (ColSim)
cp	Closed process
op	Open process
tank	Feed water tank
tot	total
amb	ambient
loss	Heat losses
i	internal
o	external
oe	Oil equivalent

Bibliography

1.	eurostat, *Energy, transport and environment indicators*. 2013.
2.	BMU *Entwicklung der erneuerbaren Energien in Deutschland im Jahr 2012, Stand: Juli 2013*. 2013. 5, 17.
3.	Emanuele Taibi, D.G., Morgan Bazilianc, *The potential for renewable energy in industrial applications.* Renewable and Sustainable Energy Reviews, 2012.
4.	European_Commission. *http://ec.europa.eu/clima/policies/package/index_en.htm*.
5.	Claudia Vannoni, R.B., Serena Drigo, *Potential for Solar Heat in Industrial Processes.* IEA SHC Task 33, 2008.
6.	U.S. Department of Energy, A.M.O., *Improving Steam System Performance: A Sourcebook for Industry, 2nd edition*, 2012.
7.	Stefan Heß, A.O., *Solar Process Heat Generation: Guide to Solar Thermal System Design for Selected Industrial Processes*, 2012, O.Ö. Energiesparverband.
8.	Schmid, M., *Identifikation und Bewertung von Systemkonzepten zur Integration solarer Prozesswärme in Wäschereien*, 2014, Universität Kassel.
9.	John A. Duffie, W.A.B., *Solar Engineering of Thermal Processes, 3rd edition*. 2006: John Wiley & Sons.
10.	Robert Stieglitz, V.H., *Thermische Solarenergie*, ed. S. Vieweg. 2012.
11.	DGS, *Leitfaden Solarthermische Anlagen*, 2012.
12.	Y. Tian, C.Y.Z., *A review of solar collectors and thermal energy storage in solar thermal applications.* Applied Energy, 2013.
13.	Werner Weiss, M.R., *Process Heat Collectors*, in *State of the Art within Task 33/IV*2008.
14.	Kalogirou, S.A., *Solar thermal collectors and applications.* Progress in Energy and Combustion Science, 2004.
15.	ECOHEATCOOL, *The European Heat Market*, 2006.
16.	Franz Mauthner, W.W., *Solar Heat Worldwide, Markets and Contribution to the Energy Supply 2011*, 2013, SHC.
17.	Martin J. Atkins, M.R.W.W., Andrew S. Morrison, *Integration of solar thermal for improved energy efficiency in low-temperature-pinch industrial processes.* Energy, 2009.
18.	Cédric Philibert, I, *Barriers to technology diffusion: the case of solar thermal technologies*, 2006.
19.	Spirax-Sarco, *The Steam and Condensate Loop*. 2011.
20.	CarbonTrust, *Steam and high temperature hot water boilers*, 2012.
21.	Viessmann *Planungshandbuch Dampfkessel*. 2011.
22.	Spirax-Sarco. *http://www.spiraxsarco.com/resources/steam-engineering-tutorials.asp*.
23.	Beeh, M., *Branchenbericht Übersicht über die Wäschereibranche*, 2013.
24.	S. Mekhilef, R.S., A. Safari *A review on solar energy use in industries.* Renewable and Sustainable Energy Reviews, 2011.
25.	Bastian Schmitt, C.L., Klaus Vajen, *Investigation of selected solar process heat applications regarding their technical requirements for system integration.*
26.	SHC *Task 49/IV IEA: Draft Integration Guideline, still work in progress*. 2013.
27.	FluidProp 2014.
28.	Flesch, J., *Development of a Simulation Model for a Solar Thermal Central Receiver System*, 2013, Technische Universität Berlin.

29.   IndustrialSolar, *Industrial Solar linear Fresnel collector LF-11, Technical Data*
30.   SchottSolar, *SCHOTT PTR®70 Receiver.*
31.   meteonorm7, 2012.
32.   Hess, S., et al., *Ergebnisse des IEE-Projekts SO-PRO: Auslegung von Solaranlagen für vier ausgewählte industrielle Prozesse*, in *Thermische Solarenergie / 22. Symposium, May 9-11*2012, OTTI e.V.: Kloster Banz, Bad Staffelstein, Germany. p. 76-77.
33.   eurostat. *http://epp.eurostat.ec.europa.eu/portal/page/portal/eurostat/home*. 2014.
34.   VDI-Gesellschaft, *VDI-Richtlinie 6002 - Blatt 1: Solare Trinkwassererwärmung - Allgemeine Grundlagen, Systemtechnik und Anwendung im Wohnungsbau*, 2004. p. 63-66.
35.   Incropera, D., Bergman, Lavine, *Fundamentals of Heat and Mass Transfer.* 2006.
36.   Fichtner_GmbH, *Industrielle Wärmekosten im Vergleich.* 2013.
37.   Wiemken, E., et al., *Bestimmung der Kollektorfläche von Solarthermieanlagen nach dem Erneuerbare-Energien-Wärmegesetz*, 2008, Fraunhofer-Institut für Solare Energiesysteme ISE.
38.   Fröhlich, H., *Modellierung, Simulation und Bewertung von solaren Prozesswärme-Systemen*, in *Karlsruher Institut für Technologie (KIT)*2014.
39.   Haagen, M., *The Potential of Fresnel Reflectors for process Heat Generation in the MENA Region*, 2012.
40.   Ausfuhrkontroll, B.f.W.u., *Merkblatt "Solare Prozesswärme" zum Antrag auf Förderung einer thermischen Solaranlage zur Prozesswärmeerzeugung.* 2013.
41.   Puente, F., *Solar Process Heat in Spain, markets and examples.* SOPRO, 2011.
42.   Zahler, C., *Fresnel collectors for industrial process heat applications, solar cooling and polygeneration.* ISES Webinar, 2014.